

UNCLASSIFIED

AD NUMBER
AD474551
NEW LIMITATION CHANGE
TO Approved for public release, distribution unlimited
FROM Distribution authorized to U.S. Gov't. agencies and their contractors; Critical Technology; OCT 1965. Other requests shall be referred to Air Force Materials Lab., Wright-Patterson AFB, OH 45433.
AUTHORITY
AFML ltr, 29 Mar 1972

THIS PAGE IS UNCLASSIFIED

AFML-TR-65-48  
Part II

474551

RESEARCH FOR SOLUBILITY OF INTERSTITIALS IN COLUMBIUM

II. A Study of Columbiu-Rich Alloys  
in the Ternary Systems Cb-Hf-O,  
Cb-Hf-N and Cb-Hf-C

A. TAYLOR

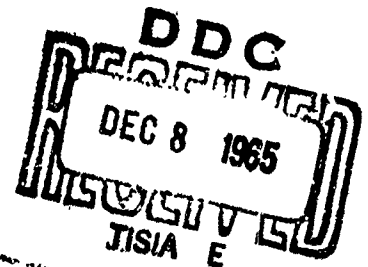
WESTINGHOUSE RESEARCH LABORATORIES

TECHNICAL REPORT AFML-TR-65-48, Part II

OCTOBER 1965

This document is subject to special export controls and each transmittal to foreign governments or foreign nationals may be made only with prior approval of the Metals and Ceramics Division (MAM), Air Force Materials Laboratory, Wright-Patterson AFB, Ohio.

AIR FORCE MATERIALS LABORATORY  
RESEARCH AND TECHNOLOGY DIVISION  
AIR FORCE SYSTEMS COMMAND  
WRIGHT-PATTERSON AIR FORCE BASE, OHIO



## NOTICES

When Government drawings, specifications, or other data are used for any purpose other than in connection with a definitely related Government procurement operation, the United States Government thereby incurs no responsibility nor any obligation whatsoever; and the fact that the Government may have formulated, furnished, or in any way supplied the said drawings, specifications, or other data, is not to be regarded by implication or otherwise as in any manner licensing the holder or any other person or corporation, or conveying any rights or permission to manufacture, use, or sell any patented invention that may in any way be related thereto.

Copies of this report should not be returned to the Research and Technology Division unless return is required by security considerations, contractual obligations, or notice on a specific document.

RESEARCH FOR SOLUBILITY OF INTERSTITIALS IN COLUMBIUM

II A Study of Columbium-Rich Alloys  
in the Ternary Systems Cb-Hf-O,  
Cb-Hf-N and Cb-Hf-C

A. TAYLOR

This document is subject to special export controls and each transmittal to foreign governments or foreign nationals may be made only with prior approval of the Metals and Ceramics Division (MAM), Air Force Materials Laboratory, Wright-Patterson AFB, Ohio.

## FOREWORD

This report was prepared by the Westinghouse Research Laboratories, Pittsburgh, Pennsylvania 15235, under Air Force Contract No. AF 33(657)-11157. The contract was initiated under Project No. 7351, "Metallic Materials", Task No. 735101, "Refractory Metals". The work was administered under the direction of the Air Force Materials Laboratory, Research and Technology Division, Wright-Patterson Air Force Base, Ohio, L.D. Parsons, project engineer, and directed by Dr. A. Taylor, Advisory Physicist in the Solid State Sciences Directorate, Westinghouse Research Laboratories.

This report covers the second stages of an investigation into Cb-rich alloys in the nine ternary systems Cb-(W,Mo,Hf)-O, Cb-(W,Mo,Hf)-N, and Cb-(W,Mo,Hf)-C with a view to determining the amounts of O<sub>2</sub>, N<sub>2</sub> and C which can be interstitially retained. The period covered is from 15 April 1963 to 1 June 1964.

Manuscript released by the Author October 1965 for publication as an RTD Technical Report.

This technical report has been reviewed and is approved.

*I. Perlmutter*

I. PERLMUTTER  
Chief, Physical Metallurgy Branch  
Metals and Ceramics Division  
Air Force Materials Laboratory

### ABSTRACT

The solubility of oxygen, nitrogen and carbon in columbium-rich columbium-hafnium alloys has been studied by means of x-ray diffraction, micrographic and thermal techniques using both a dynamic leak method and a Sieverts apparatus.

At pressures above  $10^{-14}$  torr  $O_2$ , Cb is in thermodynamic equilibrium with oxide vapor and can take up to 6 at. %  $O_2$  into solid solution at  $1775^\circ C$ . Above this temperature oxidation is "catastrophic" and the volatile oxides  $Cb_2O$ ,  $CbO$  and  $Cb_2O_5$  form on the surface. The "degassing" of Cb at  $2200^\circ C$  and above at  $10^{-6}$  torr is, in effect, brought about by the volatilization of the oxide and not by the de-adsorption of gaseous oxygen. The  $\alpha$ -Cb solid solution of the Cb-Hf-O system at  $1500^\circ C$  contains 9.0 at. %  $O_2$  at 2 at. % Hf, falling to 4.75 at. % for Cb and 0.2 at. % for an alloy containing 12 at. % Hf, the phase being characterized by the formation of  $HfO_2$  "clusters" or "molecules" within the body centered cubic  $\alpha$ -Cb matrix.

The ternary system Cb-Hf-N shows that although Cb can accommodate 9.48 at. % N interstitially at  $2200^\circ C$  and  $3 \times 10^{-1}$  torr  $N_2$ , the amount retained on quenching drops to about 1 at. %, the precise amount depending on the quenching rate. The addition of only 2 at. % of Hf immediately reduces the amount of  $N_2$  which can be accommodated at high temperatures to less than 0.5 at. %, the  $\alpha$ -Cb phase being in equilibrium with HfN. In the Cb-Hf-C system, the  $\alpha$ -Cb primary solid solution retains, at most, 0.55 at. % C at  $2000^\circ C$ , the carbide in equilibrium with the  $\alpha$ -Cb phase being essentially face centered cubic (Cb,Hf)C, and not  $Cb_2C$  as might have been expected.

TABLE OF CONTENTS

	<u>Page</u>
1. Introduction . . . . .	1
2. Materials and Sample Preparation . . . . .	2
2.1 Production of Cb-Hf Alloys . . . . .	5
2.2 Production of Cb and Cb-Hf Wires . . . . .	9
2.2.1 Columbium Wire . . . . .	10
2.2.2 Columbium-Hafnium and Columbium-Hafnium- Carbon Alloy Wires . . . . .	11
3. Oxidation of Cb and Cb-Hf Alloy Wires . . . . .	12
3.1 General Introduction - Some Previous Work . . . . .	12
3.2 The System Cb-O . . . . .	13
3.3 Experimental. . . . .	13
3.3.1 Oxidation by the Dynamic Leak Method . . . . .	17
3.4 The Lattice Parameter of Pure Columbium . . . . .	19
3.5 Lattice Parameters of $\alpha$ -Cb-O Solid Solutions . . . . .	20
3.6 Solid Solubility Limits of O <sub>2</sub> in Cb . . . . .	23
3.7 Pressure Temperature Relationship in the Cb-O System . . . . .	25
3.8 Interpretation of the log p versus 1/T curves . . . . .	27
3.9 The System Cb-Hf. . . . .	32
3.9.1 Lattice Parameters of Cb-Hf Binary Alloys . . . . .	33
3.10 Lattice Parameters and Phases in Cb-Hf-O Alloys . . . . .	34
4. Nitriding of Cb and Cb-Hf Alloys . . . . .	40
4.1 General Introduction - Previous Work . . . . .	40
4.2 Lattice Parameters of the $\alpha$ -Cb(N) Primary Solid Solution. . . . .	43
4.3 Determination of Nitrogen Solubility by the Dynamic Leak and Sieverts Methods . . . . .	46
4.4 Discussion of the Nitriding Results . . . . .	50
4.5 Nitrogen Retained on Quenching . . . . .	52
5. Columbium-Rich Columbium-Hafnium-Carbon Alloys . . . . .	58
5.1 General Introduction - Previous Work . . . . .	58
5.2 The Cb-Hf System . . . . .	59
5.3 The System Cb-C . . . . .	59
5.4 The System Hf-C . . . . .	59
5.5 The System Cb-Hf-C . . . . .	60

TABLE OF CONTENTS (cont'd)

	<u>Page</u>
5.6 The System Cb-C -- Present Investigation . . . . .	60
5.6.1 Discussion of the Results . . . . .	62
5.6.2 The System Cb-Hf-C -- Present Investigation . . . . .	63
5.6.3 The (Cb,Hf)C Phase Field. . . . .	65
5.6.4 The Cb <sub>2</sub> C Phase-Field . . . . .	67
5.6.5 The α-Cb Phase-Field . . . . .	67
Appendix I: X-Ray Diffraction Techniques . . . . .	71
Appendix II: Metallography of Cb-Hf-C Alloys . . . . .	74
References . . . . .	75

## ILLUSTRATIONS

<u>Fig.</u>		<u>Page</u>
1	Tungsten tube high temperature furnace.	79
2	Transverse section of Cb wire in copper sheath after swaging.	80
3	Structural relationships between the oxides of columbium (Terao).	81
4	Hypothetical plot of $\log p(O_2)$ versus $1/T$ .	82
5	Vacuum bell-jar and associated equipment for oxidizing Cb-alloy wires.	83
6	Sieverts apparatus.	84
7	Lattice parameters versus $O_2$ content of $\alpha$ -Cb-O solid solutions.	85
8	Comparison of lattice parameter-composition curves.	86
9	Solid-solubility limit of oxygen in $\alpha$ -Cb-O phase field.	87
10	Longitudinal section of 11 mil diameter Cb wire melted at $1775^\circ C$ in 0.5 torr $O_2$ + 760 torr He, showing localized swelling and eutectic structure.	88
11	Transverse section of Cb wire shown in Fig. 10 close to swelling.	88
12	Plots of $\log$ (pressure) versus $1/T$ for Cb-O system.	89
13	Typical plot of watts input versus surface brightness temperature for columbium wire oxidized by the dynamic leak method at a constant oxygen pressure of $10^{-3}$ torr.	90

ILLUSTRATIONS (cont'd)

<u>Fig.</u>		<u>Page</u>
14	Oxidized specimens of zone-refined Cb-wire using dynamic leak method.	91
	A. Oxidized 2 hr. at 1500°C, $10^{-5}$ torr $O_2$ . Single phase $\alpha$ -Cb.	
	B. Oxidized 15 min. at 1725°C, $7 \times 10^{-4}$ torr $O_2$ . $\alpha$ -Cb + CbO (on surface).	
	C. Oxidized 1 hr. at 1000°C, $5 \times 10^{-3}$ torr $O_2$ . $\alpha$ -Cb + CbO + CbO <sub>2</sub> (on surface).	
15	Partial Cb-O system.	92
16	Tentative Cb-Hf constitution diagram (Taylor & Doyle)	93
17	Lattice parameters of $\alpha$ -Cb Cb-Hf alloys	94
18	Cb-Hf-O. 1500°C isothermal	95
19	Cb-Hf-O. 1000°C isothermal.	96
20	Room temperature lattice parameters of Cb-Hf $\alpha$ -phase alloys containing 0, 1, 2, 4, 6 and 7 atomic percent oxygen and showing minima at 2:1 oxygen to hafnium ratio.	97
21	Resistance of Hf/Cb = 2.8/97.2 (atomic) alloys, 10.2 mils in diameter, 12" long, at 1500°C.	98
22	Phases in the Cb-N system.	99
23	Lattice parameters of $\alpha$ -Cb-N alloys	100
24	Lattice parameter of $\alpha$ -Cb-O and $\alpha$ -Cb-N interstitial solid solutions.	101

ILLUSTRATIONS (cont'd)

<u>Fig.</u>		<u>Page</u>
25	Longitudinal section of 11 mil columbium wire nitrided for 10 min. at 1680°C and $5 \times 10^{-4}$ torr $N_2$ . 200X. 1.75 at. % $N_2$ , 0.09 at. % $O_2$ .	102
26	Transverse section of 11 mil columbium wire nitrided for 10 min. at 1680°C and $5 \times 10^{-4}$ torr $N_2$ . 200X. 1.75 at. % $N_2$ , 0.09 at. % $O_2$ .	102
27	Longitudinal section of 11 mil columbium wire nitrided 10 min. at 1680°C and $5 \times 10^{-3}$ torr $N_2$ . 200X. 5.10 at. % $N_2$ , 0.09 at. % $O_2$ .	103
28	Transverse section of 11 mil columbium wire nitrided 10 min. at 1680°C and $5 \times 10^{-3}$ torr $N_2$ . 200X. 5.10 at. % $N_2$ , 0.09 at. % $O_2$ .	103
29	Temperature versus watts input during isobaric nitriding of Cb wire at 1.1 torr $N_2$ .	104
30	Isothermal equilibrium for the $\alpha$ -Cb-N terminal solid solution.	105
31	Constant composition equilibrium for the $\alpha$ -Cb-N terminal solid solution.	106
32	Maximum solubility of nitrogen in columbium.	107
33	$\alpha$ -Cb + 9.48 at. % $N_2$ , @ 2200°C in Sieverts apparatus. 11 mil wire. $\alpha$ -Cb + precipitated $Cb_2N$ . Longitudinal section, X500.	108

ILLUSTRATIONS (cont d)

<u>Fig.</u>		<u>Page</u>
34	$\alpha$ -Cb + 2.04 at % N <sub>2</sub> , Q. 2200°C in Sieverts apparatus. 14.5 mil wire, $\alpha$ -Cb + precipitated Cb <sub>2</sub> N. Transverse section. X500	108
35	Variation in N <sub>2</sub> pressure on nitriding Cb <sub>90.4</sub> Hf <sub>9.6</sub> wire at 1500°C.	109
36	90.4 Cb + 9.6 Hf nitrided to 15 at. % N <sub>2</sub> . 3 hrs. at 1500°C and radiation quenched. 11 mil wire. $\alpha$ -Cb + Cb <sub>2</sub> N + HfN. X500.	110
37	Tentative Cb-Hf-N phase diagram. 1500°C isothermal	111
38	Phase-fields in the system Cb-C (1600-1700°C) (G. Brauer et al.).	112
39	5.0 at % C, Cb-C alloy L.A. 24 hrs. at 1600°C in 1 x 10 <sup>-6</sup> torr and quenched.	113
40	1.0 at. % C, Cb-C alloy. L.A. 20 hrs. at 1600°C in 1 x 10 <sup>-6</sup> torr and quenched.	113
41	11 mil dia. "Aquadag" coated zone-refined columbium wire after heating for 16 hours at about 1700°C in 1 x 10 <sup>-6</sup> torr and quenched.	114
42	Tentative Cb-Hf-C phase diagram. 2000°C isothermal	115
43	Lattice parameters of CbC-HfC alloys.	116
44	Photomicrograph of 94 Cb 5 Hf 1 C, 24 hours at 2000°C and quenched. $\alpha$ -Cb + (Cb,Hf)C. 200X.	117

ILLUSTRATIONS (cont'd)

<u>Fig.</u>		<u>Page</u>
45	Photomicrograph of 94 Cb 5 Hf 1 C, 10 min. at 2200°C and quenched. $\alpha$ -Cb phase only. 200X.	117
46	Photomicrograph of 89 Cb 10 Hf 1 C, 24 hours at 2000°C and quenched. $\alpha$ -Cb + (Cb,Hf)C. 200X.	118
47	Photomicrograph of 89 Cb 10 Hf 1 C wire after coating with "Aquadag", annealing at 2000°C, and quenching. $\alpha$ -Cb + (Cb,Hf)C. 200X.	118
48	Typical Debye-Scherrer patterns of Cb-Hf-(O,N,C) alloys.	119 120

LIST OF TABLES

<u>Table</u>		<u>Page</u>
1	Sight-glass Correction.	7
2	Lattice Parameters of Analyzed $\alpha$ -Cb-O Solid Solutions.	21
3	Summary of Results on Cb-Hf-O Alloys.	36- 33
4	Phases in the System Cb-N.	42
5	Summary of X-ray and Microscopical Results Obtained with Nitrided 11 mil Diameter Cb Wire, Radiation Quenched.	45
6	Summary of Results on Cb-Hf-N Alloys Nitrided at 1500°C and Quenched.	57
7	Summary of Results on Cb-Hf-C Alloys.	66

## 1. Introduction

It is known that the presence of interstitial elements have a serious effect on the physico-mechanical properties of the element columbium and thus reduce its potential as a high-strength refractory material. There is, however, the possibility that the reaction of these interstitials with substitutional alloy additions could produce dispersed phases which would act as high-temperature strengtheners. However, little is known about the effects of substitutional alloying additions on the solid-solubility of interstitials in columbium, and vice-versa, and it was felt that if the effects of alloying elements in Groups IV-A and VI-A on the solution of interstitials in columbium were known, such knowledge would be valuable in interpreting and predicting the mechanical behavior of columbium-base alloys.

The proposed investigation was a study of columbium-base alloys consisting essentially of the binary systems Cb-W, Cb-Hf, and Cb-Mo, to which additions of the elements  $O_2$ ,  $N_2$ , and C were to be made, thus giving rise, in effect, to a study of the Cb-corner of the nine ternary systems, written concisely, as Cb-(W,Mo,Hf)-O, Cb-(W,Mo,Hf)-N, and Cb-(W,Mo,Hf)-C, the intention being to determine the amounts of  $O_2$ ,  $N_2$  and C which can be retained interstitially in the presence of substitutionally incorporated W, Mo, and Hf.

The initial phase of this study was an investigation of the Cb-corner of the three ternary systems Cb-W-O, Cb-W-N, and Cb-W-C. This in turn, involved a study of alloys in the binary systems Cb-W, Cb-O, Cb-N

and Cb-C, the last three binaries being of fundamental importance in the systems to be subsequently investigated, namely those based on Cb-Hf and Cb-Mo. The ternary systems based on Cb-W have already been dealt with in Technical Report AFML-TR-65-58 dated March 1965.

The second phase of the work, dealing with the systems Cb-Hf-O, Cb-Hf-N, and Cb-Hf-C are dealt with in the present report which contains the results of additional studies on the Cb-O and Cb-N systems required to substantiate the work carried out during the first year of the program. This new work necessitated the construction of a Sieverts apparatus which will be described below.

## 2. Materials and Sample Preparation

Owing to the relatively high reactivity of columbium, it readily forms oxides, nitrides and carbides which are frequently to be seen in the microstructures of Cb-base alloys. However, the amounts of these phases are usually small, and their dispersion throughout the matrix often leads to their presence being overlooked in conventional x-ray diffraction patterns owing to the diffracted spectra being below the visibility limit. In the present work, where only small amounts of oxygen, nitrogen and carbon can go into solid solution in the Cb-matrix, their presence in the initial alloying elements, in this case Cb and Hf, could lead to erroneous lattice parameter relationships, while the observation of a second phase in the microstructures could give a false idea of the solid-solubility limits.

For these reasons, it was decided to employ alloying elements of the highest possible purity and to zone-refine the columbium and degas the resulting alloys to bring the impurity level down to a few parts per million. These alloys would then be drawn to wire of diameter 10-12 mils, approximately, which would be suitable for doping with nitrogen or oxygen for subsequent x-ray and micrographic studies, whereas the carbon-containing alloys would be made by direct synthesis prior to the wire drawing stage. Once the main features of the systems to be studied were fully understood, it was found that the use of zone-refined material was unnecessary provided the samples were properly degassed prior to heat treatment, and provided that the doping gases were of the highest possible purity.

#### Columbium

Columbium wire was produced from two batches of material:

- (a) Zone-refined Cb-rod from Materials Research Corporation.

Maximum total impurities stated to be 25 ppm. Maximum  $O_2$  content, 9 ppm.

- (b) Cb powder from Kennametal, Inc. Particle size, 35 mesh,  $O_2$  content 200 ppm, C = 0.06 wt. %,  $N_2$  = 0.03, Ta = 0.10, Ti, Fe, Si, less than 0.01 wt. %.

The Kennametal columbium was zone-refined at our Bloomfield Lamp Works and used for producing 11 mil Cb-wire.

### Hafnium

The hafnium (Foote Mineral Co.) was in the form of crystal bar prepared by the Van Arkel iodide decomposition method. A typical analysis of the material in ppm was as follows: N 20, C 40, Al 50, Cu 20, Ti 35, W 20, Fe 150, Zr 23,000 (2.3%), Cl 300.

### Carbon

Ultra-high purity spectroscopic carbon (99.999% C, by Ultra-Carbon) was employed for making ternary Cb-Hf-C alloys for phase identification purposes and for doping Cb-rich alloys prior to wire-drawing.

### Oxygen

Whereas the previously reported work using the dynamic-leak method employed ordinary cylinder oxygen at low pressure, only oxygen of the very highest purity commercially available was employed with the Sieverts apparatus. Baker oxygen was used, having an analyzed maximum impurity content as follows, in ppm: N<sub>2</sub> 10, H<sub>2</sub> 1, A 20, CO<sub>2</sub> 10, CH<sub>4</sub> 15, Xe 1, Kr 10, H<sub>2</sub>O 10.

### Nitrogen

In the earlier dynamic leak method, ordinary cylinder nitrogen was employed with a purifying train of hot copper turnings. In the present work with the Sieverts apparatus, nitrogen of the highest possible purity (by Baker) was employed, the maximum impurity levels in ppm being as follows: O<sub>2</sub> 2, A 60, CH<sub>4</sub> 1, H<sub>2</sub> 1, CO 1, CO<sub>2</sub> 1, H<sub>2</sub>O 1, hydrocarbons 1.

## 2.1 Production of Cb-Hf Alloys

A conventional zone-refining furnace using the floating-zone melting technique was employed for producing pure Cb-rods from the Kennametal columbium for subsequent drawing-down into wire. In general, rods 8 inches long and 0.25 inch square section were prepared from the 35 mesh powder by compressing in a die and vacuum pre-sintering at 1200°C. The rods were then mounted vertically in the zone-refining furnace in a vacuum of  $10^{-5}$  -  $10^{-6}$  torr and subjected to local heating by means of electron bombardment.<sup>(1,2)</sup> By means of a magnetic drive which eliminated the need for sliding seals, the specimen could be moved smoothly and vertically in the vacuum chamber through the circular electron gun. By this means, pure columbium rods ranging from 0.2 to 0.25 inches in diameter and up to 6 inches in length could be produced for subsequent wire drawing.

Experience with Cb-W alloys showed that the process was unsuitable for making homogeneous alloys, there being a considerable loss of Cb by volatilization together with segregation of Cb toward one end of the bar. For these reasons, the Cb-Hf series of alloys were made by melting compressed mixtures of Cb 35 mesh powder with crystal-bar Hf turnings in a Kroll-type argon arc furnace, after which, the alloy buttons, which weighed about 10 grams, were re-melted in a high frequency levitation-melting furnace where they were degassed at a pressure of about  $10^{-6}$  torr and vacuum cast into 1/8 inch diameter rods for a subsequent homogenizing treatment for 1 day at 2000°C and drawing down into wire. The same procedure was employed for the series of Cb-Hf-C alloys examined, containing low levels of carbon, namely 0.5 and 1.0 atomic percent C.

Binary and ternary alloys containing around 33.3 and 50 atomic percent C were made by a solid state diffusion technique in which fine powder mixtures of the alloying elements were compressed into 1/2 inch diameter slugs at a pressure of 2500 psi and then heated in a pure graphite crucible for 24 hours at 2500°C. X-ray diffraction patterns were then taken of samples powdered by grinding in a tungsten carbide mortar, and, on account of the slight diffuseness of the Debye-Scherrer lines which indicated lack of perfect homogeneity, the slugs were re-ground and compressed, and given an additional solid-state diffusion homogenizing anneal for 3 days at 2000°C in a vacuum of  $10^{-5}$  -  $10^{-6}$  torr.

The homogenizing and equilibrating anneals of the various alloy slugs and rods were carried out in a tungsten tube furnace for various times and temperatures at a pressure of  $10^{-5}$  -  $10^{-6}$  torr. The general layout is shown in Fig. 1.

The heating element consists of a vertical tungsten tube 9-1/2 inches long and 1-1/4 inches in diameter, the wall thickness being 0.020 inch. The tube is surrounded by three concentric tantalum radiation shields resting on a tantalum support which also serves as the lower electrical connection to the tungsten tube. This connector is, in turn, supported by two hollow water-cooled stainless steel conductors connected in parallel and capable of carrying a current of 3000 amperes. The upper connection to the tungsten tube is likewise supported on water-cooled steel conductors arranged at 90° to the lower ones, the final connection being made via a laminated flexible cantilever consisting of several

layers of tantalum strip of thickness 0.005 inches. This arrangement provides sufficient flexibility for the expansion of the furnace tube on heating.

The specimen itself is suspended on a fine tungsten wire, the latter hanging from the center of a thin tungsten wire bridge which may be shorted across a power transformer and fused to enable the specimen to fall through the furnace tube and be instantaneously quenched in a bath of molten tin or rapidly cooled on a copper block.

The specimen may be observed during heat treatment via a 1/8 inch diameter spy-hole drilled in the wall of the tube, or from above. Since radiation through the hole conforms closely to black body conditions, the hole is used for temperature measurements by means of an optical pyrometer calibrated by the Bureau of Standards, the sighting of the instrument being made on the rear inner wall of the heater element, corrections being applied for the transmittance of the double quartz windows in the viewing port. In order to ensure that condensed metal on the viewing port does not seriously affect the temperature reading, the innermost window is made rotatable to ensure a perfectly clean surface for each observation. Finally, to ensure freedom from contamination by carbonaceous products from conventional pump oils, the furnace was evacuated by means of a mercury vapor pump fitted with a suitable baffle and liquid nitrogen trap. Corrections for the transmittance of the ports are given in Table 1.<sup>(3)</sup>

Table 1  
SIGHT-GLASS CORRECTION

$T_{\text{obs}}$ (°C)	Correction to be added (°C)	
	One pyrex or quartz window	Double quartz window
1,500	14	26
1,600	15	29
1,700	17	32
1,800	19	36
1,900	20	39
2,000	22	43
2,100	24	47
2,200	26	50
2,300	29	54
2,400	31	59
2,500	33	63
2,600	36	68
2,700	38	72
2,800	41	77
2,900	43	82
3,000	46	88

## 2.2 Production of Cb and Cb-Hf Wires

The choice of employing Cb and Cb-Hf alloys in the form of wires for oxidizing, nitriding and carburizing experiments was made on the basis of the following considerations:

- (a) Thin wires (10-12 mil diameter) can be readily oxidized or nitrided by directly heating the wires in the appropriate atmosphere by the passage of an electric current. The pressure of the gas and the temperature of the wire can be controlled. Carburizing can be carried out in vacuum with the wires painted with colloidal graphite, if required, or in an atmosphere of methane.
- (b) Any phase changes or solid-solubility effects can be followed by means of electrical resistivity measurements at temperature, or by plotting power-input as a function of temperature.
- (c) A near-quench can be obtained with thin wires by switching off the heating current, thus preserving the high temperature phases if the cooling rate is rapid enough.
- (d) Wire-form specimens are suitable for x-ray diffraction analysis by the Debye-Scherrer powder method and lattice parameter values can be accurately determined (see Appendix I).
- (e) Wire-form specimens can be fully degassed by heating to 2200°C in a vacuum of  $10^{-5}$  -  $10^{-6}$  torr until the  $O_2$  and  $N_2$  content is only a few parts per million. On the other hand, fine powders for x-ray diffraction work cannot be degassed so readily and

will tend to pick-up impurities and gas from their containers on account of their relatively large surface area/volume ratio.

- (f) Wire specimens can be readily subjected to microscopical examination and microhardness measurements.

### 2.2.1 Columbium Wire

No great difficulties were encountered in the production of Cb wire from a zone-refined material. A rod of Materials Research Corporation Cb, 1/4 inch in diameter and about 2 inches long was encapsulated in an OFHC copper tube of external diameter 5/8 inch. The tube and its contents were swaged at room temperature to 0.10 inch diameter and the copper was then removed by etching in nitric acid. Remarkably enough, the cross-section of the encapsulated wire (approximately 40 mil diameter) became roughly hexagonal during the swaging operation as shown by the photomicrograph in Fig. 2, although the copper sheath was circular in section. This phenomenon is presumably due to the original zone-refined rod being a single crystal, the soft copper polycrystalline matrix yielding to permit the columbium crystal to take up a preferred orientation.

After gently filing away the more ragged edges, the Cb wire was passed through a clean swaging die of diameter 0.036 inch to produce a more circular cross-section, after which the wire was etched for 2 minutes in a solution containing 50 H<sub>2</sub>O, 14 H<sub>2</sub>SO<sub>4</sub>, 5 HNO<sub>3</sub> and 20 HF, about 2 mils being removed from the surface by this treatment. The wire was then drawn through clean dies, while submerged in acetone, to a diameter of 0.020 inch

at which stage it was given a recovery anneal in vacuum for 5 minutes at 1200°C and then drawn to its final diameter of 0.0115 inch.

### 2.2.2 Columbium-Hafnium and Columbium-Hafnium-Carbon Alloy Wires

The following procedure was employed for producing the Cb-Hf and Cb-Hf-C (1.0 at. % C) alloy wires.

- (a) Grind-off burrs and surface blemishes, wash in acetone.
- (b) Insert into closely-fitting mild steel or stainless steel tube, indent ends of tube to prevent movement of sample.
- (c) Swage at room temperature in an automatically fed Torrington 111 swaging machine with 1/64" reduction in diameter per pass until inside diameter of tube is about 90/1000".
- (d) Remove tube by filing-through until the sample is revealed, and then strip off mechanically.
- (e) File and sand surface of the wire to remove blemishes.
- (f) Cold swage without encapsulation to about 20/1000" diameter using reductions of 10/1000" per pass.
- (g) Continue to swage using 2/1000" reduction per pass until diameter of wire is about 13/1000 - 14/1000".
- (h) Pickle wire in HF acid solution to remove any surface impurities.
- (i) Draw down to final size at room temperature (11/1000") in 1-2 passes using short-blade diamond dies and acetone as a lubricant.

This procedure yields good quality wire of uniform cross section and excellent surface finish.

### 3. Oxidation of Cb and Cb-Hf Alloy Wires

#### 3.1 General Introduction - Some Previous Work

A number of studies have been made on the temperature dependence of the solid-solubility of oxygen in columbium and of the oxides which form on the surface. In addition, studies have been carried out, notably by Bryant<sup>(4)</sup> on the influence of additions of molybdenum, rhenium and ruthenium to columbium on the solid solubility of oxygen in the metal.

Based on sintered alloys heated in the temperature range 1600 to 1700°C, Brauer<sup>(5)</sup> concluded that the solid-solubility limit of oxygen in columbium lay below 4.7 at. %, whereas Seybolt<sup>(6)</sup> using a Sieverts apparatus to meter the amount of oxygen added, found values ranging between 1.4 and 5.5 at. % oxygen in the temperature range 775 to 1100°C. According to Elliott<sup>(7)</sup> the solid-solubility of O<sub>2</sub> rises from 1.4 at. % at 500°C to about 3.9 at. % at 1800°C, whereas Bryant<sup>(4)</sup> using hardness as a criterion of oxygen content finds that the concentration ranges from 0.7 at. % O<sub>2</sub> at 700°C to 5.5 at. % at 1550°C. Finally, Gebhardt and Rothenbacher<sup>(8,9)</sup> using a combination of x-ray diffraction, micro-hardness and electrical resistivity measurements and micrographic studies have found that the concentration varies from 1.1 at. % O<sub>2</sub> at 750°C to 5.5 at. % O<sub>2</sub> at 1540°C. Apart from the work of Bryant<sup>(4)</sup> which shows that additions of molybdenum, rhenium and ruthenium to columbium all reduce the oxygen solubility and that zero solubility is reached when the electron/atom ratio of the alloy is about 5.75, no similar work has been done with tungsten and hafnium additions.

In addition to oxygen being taken into interstitial solid solution within the body centered cubic columbium structure, numerous oxides and sub-oxides can be formed depending on the temperature and the oxygen pressure. Among the more recent investigations, special mention should be made of the high-temperature x-ray diffraction studies on  $Cb_2O_5$  by Goldschmidt<sup>(10)</sup> and the electron and x-ray diffraction studies of Terao.<sup>(11)</sup> In brief,  $Cb(O)$  solid solution (body centered cubic),  $CbO_x$  (tetragonal),  $\delta$   $Cb-O$  (hexagonal),  $\gamma$   $Cb_2O_5$  (monoclinic) and  $\alpha$   $Cb_2O_5$  (monoclinic) are formed in air at either atmospheric or reduced pressure, whereas  $CbO_z$  (tetragonal),  $CbO$  (cubic, NaCl-type) and  $CbO_2$  (tetragonal) are formed only in air at reduced pressure. The relationships between the various oxides, which are structurally related, are shown schematically in Fig. 3.

### 3.2 The System Cb-O

A study of the Cb-corner of the Cb-Hf-O ternary system breaks down naturally into three stages as follows:

- (a) A study of the Cb-O binary system.
- (b) A study of the Cb-Hf binary system.
- (c) A study of the Cb-Hf-O ternary system.

### 3.3 Experimental

When columbium is exposed to an atmosphere of oxygen, the amount taken into interstitial solid solution within the body centered cubic

columbium lattice will be a function of the two variables, temperature and pressure. If true thermodynamic equilibrium is attained, lowering the pressure of the oxygen atmosphere or raising the temperature of the columbium should bring about a reduction of the oxygen in solid solution, while the reverse should occur as a result of raising the oxygen pressure or lowering the temperature. Similarly, if the condition of pressure and temperature are correctly adjusted, the body centered cubic  $\alpha$ -Cb phase will ultimately saturate with oxygen and the CbO phase will begin to form. Increasing the temperature at this point, or suitably reducing the oxygen pressure will cause the oxide to decompose to Cb + O until the oxidized columbium becomes single-phase  $\alpha$ -Cb solid solution again. Thus a determination of the solid-solubility limit of oxygen in columbium implies a determination of the equilibrium pressure of the oxygen liberated by the decomposing CbO phase at that particular temperature. A similar discussion also applies to the formation of CbO<sub>2</sub> from CbO, but the pressure involved is now that of the CbO<sub>2</sub> vapor which would decompose to form CbO.

At any given temperature, the oxygen pressure at which the  $\alpha$ -Cb primary solid solution becomes saturated with oxygen and the CbO phase begins to form is the same as the oxygen pressure which would be set up when the CbO phase is just beginning to decompose to form saturated  $\alpha$ -Cb solid solution and oxygen. Theoretically, at equilibrium, the pressure-temperature relationship should be capable of being expressed as a straight line plot of  $\log$  (oxygen pressure) versus  $1/\text{Temperature}$  ( $^{\circ}\text{K}$ ) as shown schematically in Fig. 4. Any alloy such as A lying on the high

temperature - low pressure side of the line should consist of  $\alpha$ -Cb primary solid solution. An alloy such as B, lying on the line would be, in effect, a saturated solid solution of oxygen in  $\alpha$ -Cb, and the CbO phase would be on the point of forming. An alloy such as C would first consist of CbO + saturated  $\alpha$ -Cb, but if oxygen is continually added to maintain the pressure constant as CbO forms, ultimately all the  $\alpha$ -Cb would be converted to CbO. In its turn, the CbO would oxidize to CbO<sub>2</sub> and finally to Cb<sub>2</sub>O<sub>5</sub>.

The compositions of any alloy exposed to a given equilibrium pressure of oxygen may be obtained by quenching the specimen from the high temperature and determining its oxygen content by chemical analysis, or, alternatively, by initially metering-in known quantities of oxygen, as will be described below. Thus it will be possible to ascribe compositions to the various points D, E, F, along the log p versus 1/T plot and hence effectively determine the oxygen solid-solubility limits of the  $\alpha$ -Cb phase as a function of oxygen pressure and temperature. A two phase alloy such as C at temperature T would consist of CbO plus saturated  $\alpha$ -Cb phase having a composition corresponding to G. It is also possible to draw lines of constant oxygen composition of the  $\alpha$ -Cb phase field, as a function of pressure and temperature, as indicated schematically by the line AE.

As we shall see later, in certain circumstances, the  $\alpha$ -Cb phase will not be in equilibrium with gaseous oxygen as such, but with vapors of the oxides CbO, CbO<sub>2</sub> and Cb<sub>2</sub>O<sub>5</sub>. In these cases, similar plots of log (oxide vapor pressure) versus 1/Temperature can be drawn. Failure to realize this can lead to complete misinterpretation of the results.

Two methods, which are fundamentally different in their approach were used to oxidize pure columbium and the columbium-hafnium series of alloys, although in all cases the specimens were in the form of wires which were about 12 inches long and 10-12 mils in diameter.

The first of these methods, which we may term the dynamic leak method and which was used in the early stages of the work, employs a large bell jar in which the oxygen atmosphere is maintained at the equilibrium pressure of the absorption process by leaking-in or pumping-off oxygen as required. The final composition of the oxidized wire is then obtained by quenching the sample, by simply switching-off the heating current, and then using chemical analysis, x-ray diffraction patterns and optical microscopy to establish the oxygen content, lattice parameters, and to identify phases present. The bell jar apparatus is shown in Fig. 5.

The second approach to the problem, which was made in the closing stages of the research, was to employ a Sieverts apparatus (Fig. 6) into which pre-determined amounts of oxygen (or nitrogen) could be metered and the wire sample heated until the pressure settled down to an equilibrium value. From the volume of the Sieverts apparatus and the change in pressure, it was possible to calculate the weight of oxygen absorbed and hence the composition of the wire at temperature without resorting to chemical analysis. However, x-ray diffraction and micrographic analyses were carried out on quenched specimens for purposes of phase identification and lattice parameter determinations.

### 3.3.1 Oxidation by the Dynamic Leak Method

As mentioned above, the apparatus used for the dynamic leak method of oxidizing columbium wire consists essentially of a large bell jar which can be evacuated by means of a 4 inch diameter oil diffusion pump fitted with a liquid nitrogen trap and capable of providing a vacuum of  $10^{-6}$  -  $10^{-7}$  torr using Dow Corning 705 silicone oil, the vacuum being measured by Philips and Alphatron gauges which were calibrated against a McLeod gauge.

The wire specimen, which is about 12 inches long and bent into the form of a hairpin, is suspended from both ends from two rigid copper supports which act as electrical leads for supplying the heating current, the brightness temperature of the wire being observed through the glass wall of the bell jar via a Leeds and Northrup optical pyrometer which was calibrated at the National Bureau of Standards. To prevent incorrect readings caused by any deposition of Cb vapor on the internal surface of the bell jar at temperatures in the region of  $2000^{\circ}\text{C}$  and above, an externally movable screen was placed inside the bell jar in the line of sight and only moved for sufficient time to take a reading.

Corrections were applied to the brightness temperature readings using the value  $\epsilon_{0.65\mu} = 0.374$  obtained by Whitney<sup>(12,13)</sup> for the emissivity of columbium, and  $\epsilon_{0.65\mu} = 0.70$  for the emissivity of columbium oxide ( $\text{CbO}_2$  or  $\text{Cb}_2\text{O}_5$ ), a correction also being applied for the transmittance of the bell jar from an experimentally determined curve.

After mounting the specimen, the bell jar was evacuated to the best value possible with the equipment ( $10^{-6}$  -  $10^{-7}$  torr) and the specimen given an initial thorough degassing treatment by heating it for about 10 minutes in the region of 2200-2300°C. This reduces the  $O_2$ ,  $N_2$  and C content of the wire to a few parts per million. (14)

Immediately after degassing as described above, the wire was cooled to room temperature and oxygen allowed to leak at a controlled rate into the bell jar, which was kept on the pumps, until the pressure stabilized at  $5 \times 10^{-5}$  or  $5 \times 10^{-4}$  torr  $O_2$  as required. The wire was then heated as rapidly as possible to the required temperature, adjusting the pressure of  $O_2$  to the predetermined value, and then quenched after a given time. The wire was then removed for x-ray, micrographic and chemical analysis.

This procedure was repeated with other columbium wires for various holding times and at temperatures ranging from 1000 to 2000°C, thus yielding specimens which were completely in the  $\alpha$ -Cb solid-solution range and those which consisted of the two phases, saturated  $\alpha$ -Cb and CbO.

In the case of pure columbium, the oxide formed on reaching the solid-solubility limit is on the surface of the wire only. As a result, once equilibrium has been set up between the oxide film on the surface and the saturated  $\alpha$ -Cb solid solution, the scale can be identified in situ by x-raying the sample, after which the scale is removed by dissolving it away in a mixture consisting, in parts by volume, of

50 H<sub>2</sub>O, 14 H<sub>2</sub>SO<sub>4</sub>, 5 HNO<sub>3</sub>, and 20 HF. The oxygen in solution in the α-Cb matrix is then determined by the conventional method of vacuum fusion analysis. Because the lattice parameter of columbium is greatly increased by oxygen in interstitial solid solution, it is possible, after chemically analyzing a number of calibration samples, to employ the lattice parameter as an accurate index of the oxygen content. It is, of course, also possible to employ other properties as an index of oxygen content, such as hardness or electrical resistivity,<sup>(8,9)</sup> for example, but chemical analysis coupled with x-ray diffraction methods is probably more satisfactory with the bell jar method in that the oxide phases can also be identified. It should be noted that subsequent work carried out with the Sieverts apparatus substantially confirmed the results obtained with the dynamic leak method, and assisted in their interpretation.

#### 3.4 The Lattice Parameter of Pure Columbium

Because the lattice parameters of Cb-rich Cb-Hf-O primary solid solutions were to be employed as one of the criteria of the precise value of the oxygen and hafnium solubility limits, the parameter value for high purity oxygen-free columbium becomes of the highest importance. All published values of the a-parameter of "pure" columbium are probably too high because of the oxygen content of the metal. Neubürger<sup>(15)</sup> gives a value  $a = 3.3007 \text{ \AA}$  (from kX) for the lattice parameter of "very pure Cb", whereas Edwards, Speiser and Johnston<sup>(16)</sup> give  $a = 3.3004 \text{ \AA}$  (from kX) for 99.8% Cb (containing 0.06 % Ta) at 18°C. Our own studies on the

Cb-Y system<sup>(17)</sup> indicate a progressive decrease in the lattice parameter of Cb as the yttrium content is increased, the a-parameter dropping from 3.3026 Å for "high purity" Union Carbide columbium to 3.2993 Å for an addition of 25 at. % Y, the drop in the parameter presumably being caused by the scavenging of oxygen by the added yttrium. The lowest value of a-parameter actually observed by Seybolt<sup>(6)</sup> during his work on the Cb-O system was  $3.3002 \pm 0.0002$  Å, and extrapolating back to zero oxygen a lattice parameter of 3.2999 Å is obtained. The same result is obtained by Gebhardt and Rothenbacher.<sup>(9)</sup> As we shall see in the next section, our own results lead to an extrapolated oxygen-free columbium lattice parameter which is appreciably lower, namely  $a = 3.2986 \pm 0.0001$  Å, the difference being due, in all probability, to our use of zone-refined material, although the same result was obtained from Kennametal columbium wire which was degassed in the Sieverts apparatus at 2200°C.

### 3.5 Lattice Parameters of $\alpha$ Cb-O Solid Solutions

Table 2 lists the lattice parameters of the  $\alpha$ -Cb phase of Cb-O alloys produced in the bell jar apparatus by the dynamic leak method.

A plot of the parameters as a function of the oxygen content yields the straight line shown in Fig. 7, the points off the line corresponding to  $\alpha$ Cb + CbO two-phase alloys and yielding the phase boundary lattice parameters. When extrapolated to zero oxygen content, the curve yields a "pure" columbium lattice parameter  $a = 3.2986 \pm 0.0001$  Å at 25°C.

Table 2  
Lattice Parameters of Analyzed Ocb-O Solid Solutions

Alloy No.	Treatment			Lattice Parameter $\lambda$	O <sub>2</sub> at. %
	Time	Temperature (°C)	Dynamic Oxygen Pressure, Torr		
1	As drawn			3.3004	0.47
2	5 min	2000°	$5 \times 10^{-7}$ air	3.2998	--
3	As (2) + 3 min	1085	$5 \times 10^{-4}$ O <sub>2</sub>	3.3114 Surface etched to remove scale	3.20
4	As (2) + 30 min	1085	$5 \times 10^{-4}$ O <sub>2</sub>	3.3114 Scale not removed	6.86
5	As (2) + 2-1/2 min	2158	$5 \times 10^{-4}$ O <sub>2</sub>	3.3209	5.60
6	As (2) + 180 min	2200	$1 \times 10^{-5}$ air	3.2994 + 0.0001	0.20
7	As (2) + 10 min	2200	0.5 O <sub>2</sub> + 760 He	3.3311	8.2**
8*	As (2)	1000		3.3094	4.0

\* Sieverts apparatus

\*\* By extrapolation of lattice parameter curve

The lattice parameters of the  $\alpha$ -Cb phase of the two-phase alloys for 1000°C and  $5 \times 10^{-5}$  torr  $O_2$  and 1085°C and  $5 \times 10^{-4}$  torr yields solid-solubility limits of 2.75 at. %  $O_2$  and 3.2 at. %  $O_2$  respectively. The result for 1000°C was also confirmed by a wire oxidized to 4 at. %  $O_2$  in the Sieverts apparatus.

Since the depth of penetration of the x-ray beam in the wire specimens is relatively small and the diffraction patterns and lattice parameters are more representative of the surface, tests were carried out to see whether the same results would be obtained from different depths within the x-ray samples. This was achieved by etching away successive layers. Thus an 11 mil diameter wire heated for 30 minutes at 1085°C and  $5 \times 10^{-4}$  torr  $O_2$  gave an  $\alpha$ -Cb pattern which was overlapped by lines of the surface oxide  $CbO$ , together with an  $\alpha$ -Cb phase parameter of  $a = 3.31(0) \text{ \AA}$ . On etching away the oxide film, a somewhat higher degree of accuracy in parameter determination could be obtained, and for etched-down diameters of 10.0, 6.4 and 3.0 mils respectively, the lattice parameters were 3.311(0), 3.311(4) and 3.311(6)  $\text{\AA}$ , an even higher accuracy being possible if the diffraction lines had not been somewhat "spotty" due to grain growth. These results indicate quite clearly that oxygen penetrates rapidly to the wire center and provides a relatively homogeneous cross-section from which reliable x-ray diffraction data can be obtained. Microstructures show no traces of oxide precipitation thus indicating that the rate of quenching is sufficiently rapid with 11 mil diameter wire to retain all the oxygen in interstitial solid solution.

It is of interest to compare the present lattice parameter results with those obtained by other workers. This is done in Fig. 8. Our own lattice parameter-composition curve is almost parallel to that of Gebhardt and Rothenbacher,<sup>(9)</sup> but starts at a lower Cb parameter value. This is almost certainly due to our use of zone-refined Cb as an initial material for the oxidizing experiments and the fact that Gebhardt and Rothenbacher used hardness values to determine the oxygen content in lieu of chemical analysis.

On the other hand, Seybolt's data extrapolate back to the same "pure" columbium parameter as Gebhardt and Rothenbacher but the rate of parameter increase with oxygen content is appreciably smaller. Since neither Seybolt<sup>(6)</sup> nor Gebhardt and Rothenbacher employed zone-refined columbium, it is not difficult to explain the high extrapolated columbium parameter, but the lower rate of parameter increase found by Seybolt is more difficult to account for, especially because the Sievert's method provides an accurate technique of metering the amount of oxygen added.

### 3.6 Solid-Solubility Limits of O<sub>2</sub> in Cb

Whereas the highest solubility of oxygen in columbium previously reported has been 4.4 atomic percent,<sup>(6,9)</sup> our highest analyzed oxygen content is 5.6 atomic percent, with  $a = 3.3209 \text{ \AA}$ . On the other hand, a sample of columbium wire heated for 10 minutes at 2200°C in a predominantly helium atmosphere consisting of 0.5 torr O<sub>2</sub> and 760 torr He was found to be single phase  $\alpha$ -Cb solid solution with a lattice parameter  $a = 3.3311 \text{ \AA}$ .

By extrapolating the lattice parameter-composition curve, this corresponds to an oxygen content of 8.2 atomic percent. Although we have not been able to repeat this result, it may be possible, under favorable conditions, to retain even more oxygen in interstitial solid solutions in columbium.

Various determinations of the oxygen solid-solubility limit in columbium are shown in Fig. 9. Our own results fall midway between those of Seybolt and of Gebhardt and Rothenbacher. The solid-solubility limit obtained by Elliott<sup>(7)</sup> indicates a much lower oxygen value in the region of 1800°C than those extrapolated from the results obtained by other workers and ourselves. In particular, our single phase  $\alpha$ -Cb alloys at 5.6 and 8.2 at. % O<sub>2</sub> at 2158° and 2200°C respectively would, according to Elliott, lie well within the  $\alpha$ -Cb - CbO (liquid) two-phase field. Further work is required at different pressures to settle this point satisfactorily.

Elliott reports the presence of a eutectic at 1915°C between  $\alpha$ -Cb containing about 4 at. % oxygen in solid solution and the cubic oxide CbO. We have heated a number of 11 mil diameter wire samples slowly in the bell jar apparatus in an atmosphere consisting of 0.5 torr O<sub>2</sub> and 760 torr purified He. In all cases  $\alpha$ -Cb - CbO complexes which formed melted at the surprisingly low temperature of 1775 ± 15°C. This will be discussed later.

The regions where local melting occurred were marked by the formation of spherical beads and the interruption of the heating current effectively quenched the beads from the liquid state producing a typical

eutectic structure as shown in Figs. 10 and 11. Only after melting and quenching was oxide observed within the grains and grain boundaries of the  $\alpha$ -Cb solid solution.

### 3.7 Pressure-Temperature Relationships in the Cb-O System

Based on the x-ray, micrographic and chemical analyses of Cb-O alloys produced in the bell jar apparatus using the dynamical leak method, it was possible to establish the amount of oxygen in solid solution in columbium at various oxygen pressures and wire temperatures, and from these to establish the maximum oxygen solid solubility under the various conditions of temperature and pressure. The results enabled a straight line curve to be established between  $\log$  (pressure of oxygen) versus  $1/\text{Temperature } (^{\circ}\text{K})$ , the line apparently representing the pressure at which the oxide  $\text{CbO}$  is in equilibrium with the  $\alpha$ -Cb primary solid solution.

This curve is represented by the line labelled  $\text{CbO}$  in Fig. 12. Any specimens made under the conditions of temperature and pressure to the left of the curve consist essentially of  $\alpha$ -Cb solid solution, the broken lines representing contours of equal oxygen concentration. Alloys immediately to the right of the  $\text{CbO}$  line are found to be two-phase, consisting of  $\alpha$ -Cb +  $\text{CbO}$ . A second line, labelled  $\text{CbO}_2$ , can be established, beyond which, under the dynamic flow conditions prevailing, the wire sample consists of the three phases  $\alpha$ -Cb +  $\text{CbO}$  +  $\text{CbO}_2$ . Yet another line must exist which marks the appearance of  $\text{Cb}_2\text{O}_5$ .

The location of the iso-compositional contours in the  $\alpha$ -Cb region of Fig. 12 could be located by making use of  $\alpha$ -Cb lattice parameters of

two and three-phase alloys. Thus, columbium heated at 1000°C in the three-phase field under the conditions denoted by triangles A, B and C in Fig. 12 all yield the same lattice parameter for  $\alpha$ -Cb. As shown by the arrows, this spacing must correspond to the saturation point D of the  $\alpha$ -Cb phase, the composition of which can be derived from the lattice parameter versus composition curve given in Fig. 7.

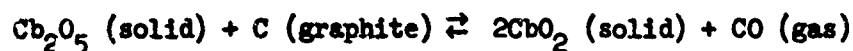
The determination of the upper log p versus  $1/T$  curve for  $\text{CbO}_2$  is of interest. Originally it was decided to confirm the position of the  $\text{CbO}$  line obtained by x-ray, micrographic and chemical analyses by a different and independent technique which would make use of changes in the optical emissivity of the wire surface as the oxide formed. In this technique, the wire was heated in the bell-jar apparatus to a temperature at which an  $\alpha$ -Cb solid solution is formed and then cooled in stages with the dynamic leak maintaining the pressure constant. A curve was then plotted of surface brightness temperature (i.e. uncorrected pyrometer reading) versus watts input to the wire, a break in the curve showing when the emissivity of the sample increased on formation of the oxide. The break was then retraced to establish its validity, a typical curve being shown in Fig. 13 for Cb in  $10^{-3}$  torr  $\text{O}_2$ , the numbers indicating the random order in which the readings were taken. Also included are sketches showing the appearance of the scale on the wire at the different temperatures.

It was rather surprising to find that the above technique did not reproduce the  $\text{CbO}$  log p versus  $1/T$  plot illustrated in Fig. 12, but yielded instead, the upper curve, which x-ray examination of the wire showed to be

associated with the formation of  $\text{CbO}_2$ . No discontinuities whatever could be found in the watts input versus brightness curves corresponding to  $\text{CbO}$ . The reasons for this are probably not far to seek. As shown by the macro-photographs of  $\text{Cb}$  wire after various stages of oxidation (Fig. 14),  $\text{CbO}_2$  forms a highly emissive black layer on the surface of the wire, whereas that of  $\text{CbO}$  is indistinguishable from metallic  $\text{Cb}$ . Thus, the published value of  $\epsilon_{0.65\mu} = 0.70$  refers in all probability to the oxide  $\text{CbO}_2$  (and possibly to  $\text{Cb}_2\text{O}_5$  as well), whereas the emissivity  $\epsilon_{0.65\mu} = 0.374$  probably applies equally to  $\text{Cb}$  and to  $\text{CbO}$ .

### 3.8 Interpretation of the Log p Versus 1/T Curves

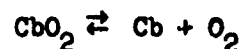
Worrell<sup>(18)</sup> has recently determined the free energy of formation  $\Delta F$  of  $\text{CbO}_2$  by measuring the carbon monoxide equilibrium pressure in the reaction



using solid pellets of  $\text{CbO}_2 + \text{Cb}_2\text{O}_5 + \text{C}$  in a  $\text{CO}$  atmosphere at 1050 to 1250°K. The value obtained for  $\Delta F$  may be expressed in the form:

$$\Delta F = -185,600 + 38.9T, \text{ cal/mole.}$$

From this, the dissociation pressure of  $\text{CbO}_2$  in the reaction



may be calculated using the expression

$$\begin{aligned} \ln p_{O_2} &= \Delta F/RT \\ &= \frac{-40,340}{T} + 8.46 \end{aligned}$$

where the oxygen pressure  $p_{O_2}$  is in units of atmospheres. This leads to an oxygen partial pressure of approximately  $2.8 \times 10^{-16}$  torr at  $1500^\circ\text{C}$ .

In the case of the decomposition reaction



the oxygen equilibrium pressure would be even lower than this.

We note from Fig. 12 that the oxygen pressure involved in the decomposition of CbO to Cb + O at  $1500^\circ\text{C}$  is around  $10^{-4}$  torr, which is about 12-14 orders of magnitude higher than obtained by thermodynamic calculation. A similar experimental result was obtained by Pensler. (19) However, we can easily reconcile the experimental findings with the results of theory.

The thermodynamic calculation means that only at oxygen pressures substantially below  $10^{-16}$  torr and  $T \approx 1500^\circ\text{C}$  is it possible to remove gaseous oxygen from the interstitial  $\alpha\text{-Cb-O}$  primary solid solution, and the computed pressure corresponds to the pressure of oxygen, at equilibrium, when the primary  $\alpha\text{-Cb}$  solid solution is saturated and the monoxide phase CbO is about to form. Such a process should be reversible, in that if oxygen is absorbed by the metal at temperature when the pressure is maintained at the equilibrium value, the same oxygen should be capable of being pumped out of the metal on reducing the pressure.

An experiment was carried out to test this very point, which is crucial to our understanding of the oxidation and de-oxidation mechanism of columbium. Using the Sieverts apparatus, which was now available, an 11 mil diameter Cb wire was converted to a saturated  $\alpha$ -Cb solid solution containing about 6.0 atomic percent  $O_2$  at  $1770^\circ C$ . The wire was quenched to retain the oxygen in solid solution and the vessel containing the sample evacuated down to  $10^{-7}$  Torr where it was closed off. The sample was then reheated in the vacuum to  $2200^\circ C$  in order to draw-off the oxygen and quenched to prevent re-absorption. By cryogenic pumping, using a stainless steel side-tube dipped in liquid helium, it was possible to obtain a gas-sample for analysis in a mass spectrometer. The small amounts of gas obtained by this method were found to consist essentially of CO, hydrocarbons and traces of water, but no free oxygen was present. However, the wire was found to be substantially thinner as a result of this treatment, and the walls of the container were coated with a thin film, presumably consisting of columbium oxide.

The above experiments would seem to indicate that we do not have a true static equilibrium between  $\alpha$ -Cb and oxygen, but rather that a dynamic equilibrium exists between  $\alpha$ -Cb and columbium oxide vapor, the pressure of the vapor adjusting itself to equal that of the oxygen which essentially controls the rate of vapor formation. Thus, as long as the oxygen pressure is above  $10^{-16}$  Torr, oxidation of columbium will occur, the oxide being in the vapor state if the temperature is high enough, and columbium being continuously carried away without any oxide being

apparent either on the surface or inside the metal. Under these conditions, the amount of oxygen retained in solid solution will seem to be a function of the oxygen pressure, but it will, in reality be a function of the oxide vapor pressure. Which oxide it is will depend on the temperature.

In order to test these ideas, experiments were carried out heating fully degassed Cb wires at various temperatures in the Sieverts apparatus, metering-in different amounts of oxygen to form solid solutions, and also heating various solid-solution compositions in the fully evacuated Sieverts apparatus. Both types of experiments led to the same results.

It was found that up to 1775°C, the maximum amount of oxygen which could be retained in solid solution in Cb was 6.0 atomic percent, the partial pressure of the oxide vapor being given by Fig. 12 and being of the order of  $5 \times 10^{-4}$  torr. Above 1775°C a "catastrophic" increase occurs in the rate of evaporation of the oxides from the wire which drastically reduces its oxygen content and leads to a rapid darkening of the chamber walls as the oxides deposit. From weight loss measurements and the known amounts of oxygen fed into the system, it would seem that mixtures of  $\text{CbO} + \text{CbO}_2$  vapor are evolved at temperatures immediately above 1775°C, whereas at 2200°C, the oxide is almost entirely  $\text{Cb}_2\text{O}_5$ . At this latter temperature, the oxygen content of the wire is about 0.1 atomic percent.

The above experiments are incorporated into a pseudo-phase diagram shown in Fig. 15. This shows that a columbium wire heated at 2200°C in the Sieverts apparatus to which enough oxygen had been metered

to form an alloy of effective composition  $Cb_3O$ , only retained 0.1 atomic percent  $O_2$  in solid solution, the rest having evaporated to the walls as  $Cb_2O_5$ . Similarly, a degassed Cb wire heated at  $2100^\circ C$  in the Sieverts apparatus to which 8.0 atomic percent  $O_2$  was added, only retained the same amount of oxygen in solution. The experiment was repeated (a), with 5 atomic percent  $O_2$  in the wire, (b) with degassed Cb and 5 atomic percent  $O_2$  in the vessel. In either case, heating to  $1850^\circ C$  resulted in an "equilibrium" solid solution alloy containing 1.5 at. percent  $O_2$ . At  $1775^\circ C$  the maximum amount of oxygen which could be retained was 6.0 at. percent.

It is quite clear from these experiments that the degassing of columbium at  $2200^\circ C$  in vacuum is not brought about by the removal of oxygen, as such, from the lattice, for this would require pressures below  $10^{-16}$  torr. Rather, the degassing is brought about by the formation at the wire surface of columbium oxides which then volatilize away as vapors. Thus, with solid columbium, there is no way of removing all traces of oxygen from the metal using conventional vacuums of  $10^{-6}$  -  $10^{-7}$  torr, the nearest approach being by actual melting, as in a zone-refining process, and using vac-ion pumps. Similar conclusions have been reached by Gebhardt, Fromm and Jakob. (8)

Because the degassing of columbium is essentially produced by the surface formation and evaporation of columbium oxide, it would be anticipated that the process would be extremely sensitive to the pressure of the surrounding atmosphere. Thus, in the above series of experiments, to produce an alloy at  $2200^\circ C$  of effective composition  $Cb_3O$ , enough oxygen

was bled into the Sieverts apparatus to raise the pressure from less than  $10^{-7}$  to approximately 5.0 torr. After formation of  $\text{Cb}_2\text{O}_5$  vapor, which deposited on the walls, the final pressure in the apparatus had fallen to  $7.0 \times 10^{-4}$  torr (mainly residual argon) and only 0.1 atomic percent  $\text{O}_2$  remained in solid solution. On the other hand, as mentioned in Section 3.6 (page 23), a sample of columbium wire heated for 10 minutes at  $2200^\circ\text{C}$  in a predominantly helium atmosphere consisting of 0.5 torr  $\text{O}_2$  and 760 torr He was found to be single-phase  $\alpha\text{-Cb}$  solid solution containing 8.2 atomic percent oxygen. From this, it would seem that the controlling factor is not so much the oxygen partial pressure, but the total pressure of the atmosphere in which the wire is heated which controls both the rate of oxide evaporation and the amount of oxygen which can be retained in solid solution. Thus the partial Cb-O diagram shown in Fig. 15 must be modified to suit the prevailing pressure conditions.

### 3.9 The System Cb-Hf

The columbium-hafnium phase diagram, as determined by Taylor and Doyle,<sup>(20)</sup> is shown in Fig. 16. It will be seen from the diagram that columbium and hafnium form a continuous series of body centered cubic solid solutions above  $1950^\circ\text{C}$ , the solid-solubility of hafnium in columbium falling below this temperature until only about 34 atomic percent Hf remains in solution at  $1000^\circ\text{C}$ .

### 3.9.1 Lattice Parameters of Cb-Hf Binary Alloys

The lattice parameters of body-centered cubic columbium-rich Cb-Hf alloys, obtained by Taylor and Doyle<sup>(20)</sup> are summarized in Fig. 17.

It will be noted that the lattice parameter for "pure columbium" (from Union Carbide Co.) is plotted at  $a = 3.3024 \text{ \AA}$  and that after an initial drop, the parameter increases almost linearly with hafnium content until the solid solubility limit is reached. We now know that the originally published lattice parameter of columbium is too high as a result of the high oxygen content of the metal, the value for degassed columbium being  $a = 3.2986 \pm 0.0001 \text{ \AA}$ . The high result presumably arises from the use of filings which have a high surface area to volume ratio which makes them susceptible to oxygen pickup, and the use of a stress-relieving treatment of 10 minutes at  $1350^{\circ}\text{C}$  in a pressure of about  $10^{-5} - 10^{-6}$  torr  $\text{O}_2$  and 760 torr He, such temperature and pressure conditions being more conducive to oxygen pickup rather than to degassing. In the present investigation, degassing conditions were, of course, much superior in that the samples were in the form of thin wires which could be electrically heated in a vacuum of  $< 10^{-7}$  torr at temperatures of  $2200^{\circ}\text{C}$  and above.

The Cb-Hf lattice parameter curve is based on chemically analyzed samples. As a result, it could be used as a calibration standard to determine the compositions of the Cb-Hf wires prior to treatment with oxygen (or nitrogen) in the Sieverts apparatus.

### 3.10 Lattice Parameters and Phases in Cb-Hf-O Alloys

A series of Cb-Hf binary alloys in the form of 11 mil diameter wire and containing 2.8, 4.8, 8.2, 9.6, 13.4, 13.6, and 22.3 atomic percent Hf, balance Cb, were treated in the Sieverts apparatus with high purity Baker oxygen at temperatures ranging from 1000 to 2200°C. The phases observed and the lattice parameters of  $\alpha$ -Cb primary solid solution alloys containing oxygen are given in Table 3.

Based on the x-ray and micrographic results it was possible to draw partial phase diagrams of the Cb-Hf-O system corresponding to 1000 and 1500°C. These are illustrated in Figs. 18 and 19. It will be seen that the  $\alpha$ -Cb primary solid solution is quite extensive. At 1500°C, the amount of oxygen in solid solution in Cb is 4.75 atomic percent, but this increases to approximately 9.0 atomic percent at 2.0 atomic percent Hf, further additions of Hf causing the amount of dissolved oxygen to fall drastically until about only 0.2 atomic percent of oxygen is retained in solid solution at 12 atomic percent Hf.

The oxygen is taken into interstitial solid solution in alloys along the Cb-O edge of the ternary system. According to Stringer and Rosenfeld,<sup>(21)</sup> the oxygen atoms prefer the octahedral to the tetrahedral sites of the body centered cubic columbium lattice, the oxygen atom no longer being spherical but lenticular or toroidal in shape. On the other hand, along the Cb-Hf edge of the system, the hafnium atoms replace those of columbium substitutionally in forming the primary solid solution.

Both the addition of interstitial oxygen and substitutional hafnium in the respective binary systems produce an increase in the lattice parameter of the columbium matrix. It would therefore be anticipated that the joint addition of oxygen and hafnium would produce a corresponding increase in the columbium unit cell size, but this is not the case. As may be seen from the isoparametric contours drawn across the  $\alpha$ -Cb phase field in Fig. 18, there is a valley running through the Cb-corner of the system where the lattice parameter is virtually that of pure Cb, namely  $a = 3.2986 \text{ \AA}$ .

The nature of this valley can best be seen by plotting the lattice parameters at various oxygen levels as a function of the hafnium content. This is shown in Fig. 20. With zero oxygen in solution, the lattice parameters of the  $\alpha$ -Cb phase rise continuously with Hf content, but those corresponding to 1.0, 2.0, 4.0, and 6.0 atomic percent  $O_2$  first drop linearly with increasing Hf, reaching a sharply defined minimum value which is little different from that of the lattice parameter for pure Cb, and then rise again in an almost linear fashion.

The positions of these minima are extremely interesting. The minimum for 1.0 atomic percent  $O_2$  is seen to occur at 0.5 atomic percent Hf; that for 2 atomic percent  $O_2$  occurs at 1.0 atomic percent Hf, and so on. In other words, the minima, or the valley in the isoparametric surface of the  $\alpha$ -Cb single phase field, occur at an O:Hf atomic ratio of 2:1. As a result, the valley runs across the  $\alpha$ -Cb single phase field from the Cb-corner and in a direction where it forms a continuous straight line with the tie-line joining the  $\alpha$ -Cb phase boundary composition with  $HfO_2$ .

Table 3  
Summary of Results on Cb-Hf-O Alloys

Composition At %		Time	Temp. °C	Oxygen Added Atomic Percent	Phases Present	α-Cb Lattice Parameter Å
Cb	Hf					
100	--	--	(extrapolated O <sub>2</sub> free spacing)			3.2986
100	--	1 hr	1500	4.0	α-Cb	3.313(5)
100	--	1 hr	1500	8.0	α-Cb + CbO	3.317(5)
100	--	3 hr	1000	4.0	α-Cb + CbO	3.309(2)
97.2	2.8	10 min	2200	degassed	α-Cb	3.304(6)
97.2	2.8	1 hr	1500	2.0	α-Cb	3.303(5)
97.2	2.8	1 hr	1500	4.0	α-Cb	3.301(1)
97.2	2.8	1 hr	1500	4.65	α-Cb	3.300(3)
97.2	2.8	1 hr	1500	5.20	α-Cb	3.300(4)
97.2	2.8	2 hr	1500	6.0	α-Cb	3.304(6)
97.2	2.8	1 hr	1500	8.0	α-Cb + HfO <sub>2</sub>	3.300(8)
97.2	2.8	1 hr	1500	10.0	α-Cb + CbO + HfO <sub>2</sub>	3.316(0)
97.2	2.8	3 hr	1000	6.0	α-Cb + HfO <sub>2</sub>	3.304(8)
97.2	2.8	3 hr	1000	8.0	α-Cb + CbO + HfO <sub>2</sub>	3.311(4)

Table 3 (cont'd)

Composition At %		Time	Temp. °C	Oxygen Added Atomic Percent	Phases Present	α-Cb Lattice Parameter Å
Cb	Hf					
95.2	4.8	10 min	2200	degassed	α-Cb	3.308(7)
95.2	4.8	1 hr	1500	0.5	α-Cb	3.308(4)
95.2	4.8	1 hr	1500	4.0	α-Cb + trace HfO <sub>2</sub>	3.304(6)
95.2	4.8	1 hr	1500	6.0	α-Cb + HfO <sub>2</sub>	3.302(5)
95.2	4.8	2 hr	1500	8.0	α-Cb + HfO <sub>2</sub>	3.300(8)
95.2	4.8	3 hr	1000	2.5	α-Cb + HfO <sub>2</sub>	3.305(0)
95.2	4.8	3 hr	1000	4.0	α-Cb + HfO <sub>2</sub>	3.303(3)
91.8	8.2	10 min	2200	degassed	α-Cb	3.316(0)
91.8	8.2	2 hr	1500	1.0	α-Cb + HfO <sub>2</sub>	3.309(3)
91.8	8.2	1 hr	1500	8.0	α-Cb + HfO <sub>2</sub>	3.305(0)
		etched from 10.2 to 7.2 mils			α-Cb + HfO <sub>2</sub>	3.305(0)
91.8	8.2	3 hr	1000	0.5	α-Cb + HfO <sub>2</sub>	3.314(7)

Table 3 (cont'd)

Composition At %		Time	Temp. °C	Oxygen Added Atomic Percent	Phases Present	α-Cb Lattice Parameter Å
Cb	Hf					
90.4	9.6	10 min	2200	degassed	α-Cb	3.319(0)
90.4	9.6	1 hr	1500	2.0	α-Cb + HfO <sub>2</sub>	3.313(7)
90.4	9.6	1 hr	1500	4.0	α-Cb + HfO <sub>2</sub>	3.308(8)
86.6	13.4	10 min	2200	degassed	α-Cb	3.326(5)
86.6	13.4	1 hr	1500	0.5	α-Cb + HfO <sub>2</sub>	3.325(3)
86.4	13.6	10 min	2200	degassed	α-Cb	3.327(4)
86.4	13.6	1 hr	1500	4.0	α-Cb + HfO <sub>2</sub>	3.314(3)
86.4	13.6	1 hr	1500	8.0	α-Cb + HfO <sub>2</sub>	3.313(9)
77.7	22.3	10 min	2200	degassed	α-Cb	3.346(6)

A possible interpretation of this result may be as follows. The oxygen ions tend to occupy the octahedral sites of the body centered cubic matrix, thus lying at the mid-points of the cell edges, whereas the hafnium atoms go into the cube corners, replacing columbium. A form of "clustering" may now occur in which randomly dispersed "molecules" of  $\text{HfO}_2$  form within the Cb lattice, an ion of Hf being flanked on either side by an oxygen ion. In forming such a molecule, each oxygen would gain two electrons from the Hf, and increase their effective ionic radius, but in losing its four valence electrons to them, the hafnium would decrease in size. The net effect would be a cancellation of charges and sizes which would tend to leave the lattice as a whole with a parameter very little different from that of pure Cb. A study of Fig. 20 shows that, in reality, the valley is not quite level but rises slightly with Hf content.

The state of affairs described above would apply only to  $\alpha$ -Cb alloys lying along the line Cb- $\text{HfO}_2$ . Any oxygen in excess of the 2:1 ratio would, of course, be distributed at random throughout the remaining octahedral sites in the lattice. Such alloys would be expected to behave very much like Cb-O binary alloys and become extremely brittle at the higher oxygen levels. This is indeed the case. On the other hand,  $\alpha$ -Cb alloys lying on the other side of the Cb- $\text{HfO}_2$  line and containing Hf in excess of that required to form  $\text{HfO}_2$  molecules; would be expected to be ductile, and this is what is actually found. Furthermore, in going from the "more metallic" Hf-rich  $\alpha$ -phase alloys to the "less metallic"

O-rich alloys on crossing the Cb-HfO<sub>2</sub> line, a sharp increase in electrical resistivity would be anticipated due to electron scattering produced by the excess interstitial oxygen. This expectation is fully borne out by the results presented in Fig. 21 which shows the electrical resistance at 1500°C of a 2.8 Hf 97.2 Cb wire to which varying atomic percentages of O<sub>2</sub> have been added at temperature in the Sieverts apparatus. As may be seen, on exceeding the critical oxygen content for stoichiometric HfO<sub>2</sub> molecule formation, there is an extremely sharp rise in the electrical resistance.

#### 4. Nitriding of Cb and Cb-Hf Alloys

##### 4.1 General Introduction -- Previous Work

The adsorption of nitrogen by columbium under various conditions of temperature and pressure has been studied by a number of authors. A comprehensive investigation of the system by direct synthesis of Cb and N using oxygen-free preparations and up to 1500°C was carried out by Brauer and Jander<sup>(22)</sup> and Brauer and Esselborn,<sup>(23)</sup> while the synthesis of δ-CbN under a nitrogen pressure of up to 60 atmospheres was studied by Brauer and Kirner.<sup>(24)</sup> The system was also studied by Schönberg<sup>(25)</sup> who nitrated columbium in ammonia at temperatures between 700° and 1100°C, while the structures of the various nitrides were studied by Terao<sup>(26)</sup> using electron diffraction and x-ray techniques. The results of Brauer et al. and Schönberg differ to some extent, presumably due to the methods of preparation, a summary of the phase structures found being given in

Table 4 and schematically represented in Fig. 22. Also included in Fig. 22 are the results obtained by Elliott and Komjathy<sup>(27)</sup> for Cb-N phases at 1450°C. Below about 1300°C, the "CbN" phase changes from face centered cubic to hexagonal.

As would be expected, the amount of nitrogen taken into solid solution in body centered cubic  $\alpha$ -Cb is a function of the temperature and the pressure. According to Brauer, Cb takes less than 4.75 at. % N into solid solution, whereas at 1 atmosphere  $N_2$  pressure, Elliott and Komjathy show it to take about 1.5 at. % N at 1000°C, 3 at. % N at 1500°C, and about 14 at. % N at 2400°C. However, as found by Dürschnabel and Herz<sup>(28)</sup> quenching Cb wire of diameter 0.8 mm (32 mils) from temperatures ranging from 1560 to 1960°C and nitrogen pressures ranging from  $1 \times 10^{-3}$  to  $1 \times 10^{-2}$  torr (25 seconds to 500°C, or 7 seconds in argon) did not retain more than about 1.3 at. %  $N_2$  in solid solution.

The solid-solubility of nitrogen in columbium has also been investigated as a function of pressure and temperature using a Sieverts type of apparatus by both Cost and Wert<sup>(29)</sup> and Gebhardt, Fromm and Jakob.<sup>(30)</sup> This technique does not require cooling the sample down before measuring the nitrogen content and is therefore free from the problem of nitrogen loss caused by nitride precipitation. The solid solubility results of Cost and Wert indicate about 10 at. percent nitrogen in solid solution at 2000°C and  $3.0 \times 10^{-1}$  torr and Gebhardt obtains 10 at. percent, while Elliott obtains about 6.5 at. percent referred to 1 atmosphere pressure (see Ref. (30), Fig. 8).

Table 4  
Phases in the System Cb-N

Phase	Crystal Structure	Homogeneity range. Atomic percent Nitrogen	Lattice Parameters $\text{\AA}$
<u>Brauer et al.</u>			
Cb	b.c.c.	0 - < 2.0	$a=3.301(4) - 3.302(6)$
Cb <sub>2</sub> N	h.c.p.	28.5 - 32.4	$a=3.062, c=4.966, c/a=1.622$ to $a=3.054, c=5.005, c/a=1.639$ (from xX)
CbN	Tet. deformed NaCl	42.8 - 44.1	$a=4.394, c=4.321, c/a=0.983$ to $a=4.396, c=4.339, c/a=0.987$ (from xX)
CbN III	f.c.c. NaCl	45.4 - 48.5	$a=4.386$ to $a=4.389$ (from xX)
CbN II	h.c.p.	48.7	$a=2.93, a=5.45, c/a=1.87$
CbN I	hexagonal	50.0	$a=2.956, c=11.274, c/a=3.82$
<u>Schönberg</u>			
Cb	b.c.c.	0 < 2.0	--
$\beta$	h.c.p.	As for Cb <sub>2</sub> N above	--
$\gamma$	Hexagonal WC-type	44.4 - 47.4	$a=2.950, c=2.772, c/a=0.940$ to $a=2.958, c=2.779, c/a=0.939$
$\theta$	h.c.p.	Same as CbN II above	$a=2.968, c=5.535, c/a=1.865$
$\epsilon$	Hexagonal	Same as CbN I above	$a=2.952, c=11.25, c/a=3.811$

#### 4.2 Lattice Parameters of the $\alpha$ -Cb(N) Primary Solid Solution

According to Brauer and Jander<sup>(22)</sup> the room temperature lattice parameter of Cb after annealing in a high vacuum at 1000°C for 1 hour is 3.301(4) whereas a two phase  $\alpha$ -Cb + Cb<sub>2</sub>N alloy containing 4.7 atomic percent N<sub>2</sub> had a somewhat higher parameter  $a = 3.302(6) \text{ \AA}$  (from xX), the actual amount of nitrogen retained in solution at room temperature being doubtful and at most 2 at. percent. Similar results were obtained by Schönberg using columbium powder nitrated in ammonia at temperatures between 700° and 1100°C. On the other hand, based on rapidly cooled wire of diameter 30 mils, Dürrschnabel and Hörz<sup>(28)</sup> obtained  $a = 3.300(0) \text{ \AA}$  for Cb wire degassed for 13 minutes at about 2240°C and  $5 \times 10^{-6}$  torr and  $a = 3.304(1) \text{ \AA}$  for Cb containing 1 at. percent nitrogen in solution. However, the rate of cooling was not particularly fast (25 seconds to reach 500°C in  $1 \times 10^{-2}$  torr N<sub>2</sub>, or 7 seconds in argon) and ample time would be available for the formation of a nitride precipitate.

Some preliminary nitriding experiments were carried out during the present investigation using the same bell-jar apparatus and dynamic-leak method as for the oxidizing experiments described in Section 3.3.1 (page 17), a nitrogen purification train being inserted between the nitrogen cylinder and the bell jar to remove any traces of oxygen from the gas (Fig. 5). The train consisted of a resistance furnace fitted with an Inconel tube packed with fine copper turnings heated to about 300°C over which nitrogen was stored at 10 pounds pressure. This reduced oxygen pickup considerably.

A summary of the x-ray and microscopical findings for 11 mil Cb wire heated for various times and pressures in the nitrogen purified as above is given in Table 5, where corrections are applied to the observed lattice parameters of the  $\alpha$ -Cb-N solid solution to allow for the oxygen content of the wire.

A plot of corrected lattice parameters versus analyzed nitrogen content for radiation-quenched Cb-N wires is presented in Fig. 23. The number of experimental points is small and the relationship between composition and lattice parameter is assumed to be linear, as it is in the Cb-O system. With these limitations in mind, it would seem from the x-ray data that the maximum amount of nitrogen that can be retained in columbium on quenching from 1680°C after equilibrating in an atmosphere of  $5 \times 10^{-4}$  torr  $N_2$  is 1.05 atomic percent, the corresponding room temperature lattice parameter being  $a = 3.3060 \text{ \AA}$ .

The lattice parameter change produced by the nitrogen interstitially dissolved in columbium is relatively large, the value of  $a$  increasing from the extrapolated value of  $3.2986 \text{ \AA}$  for pure columbium to  $a = 3.3060 \text{ \AA}$  at 1.05 at. percent nitrogen. As shown in Fig. 24, the rate of increase in lattice parameter with nitrogen content (curve a) is appreciably higher than for the corresponding  $\alpha$ -Cb-O solid solution (curve c). Also plotted in Fig. 24 are the parameter data of Dürschnabel and Hörz (curve b), which indicates a lower rate of parameter increase than our own. This is due, in all probability, to a higher initial Cb parameter resulting from incomplete de-oxidation, and to too low an  $\alpha$ -Cb-N parameter resulting from

Table 5

Summary of X-Ray and Microscopical Results  
 Obtained with Nitrided 11 mil Diameter Cb Wire, Radiation Quenched

Pressure Torr N <sub>2</sub>	Heat Treatment	Analysis		X-Rays	Micros	a R	a R Corrected for O <sub>2</sub>
		At % O	At % N				
5 x 10 <sup>-5</sup>	360 min 1680°C	~0.10	0.60	Single phase b.c.c.	Single phase	3.3039	3.3031
5 x 10 <sup>-4</sup>	30 min 1680°C	0.105	0.65	Single phase b.c.c.	Single phase	3.3046	3.3040
1 x 10 <sup>-4</sup>	60 min 1680°C	0.012	1.23	Single phase b.c.c.	Trace of Cb <sub>2</sub> N	3.3064	3.3060
5 x 10 <sup>-4</sup>	5 min 1680°C	0.047	1.16	Single phase b.c.c.	Trace of Cb <sub>2</sub> N	3.3063	3.3061
5 x 10 <sup>-4</sup>	10 min 1680°C	0.087	1.75	2 phase α-Cb + Cb <sub>2</sub> N	α-Cb + Cb <sub>2</sub> N	--	--
5 x 10 <sup>-3</sup>	5 min 1680°C	0.093	5.10	2 phase α-Cb + Cb <sub>2</sub> N	α-Cb + Cb <sub>2</sub> N	3.306(4)	3.306(0)
5 x 10 <sup>-6</sup>	40 min 1000°C	--	--	2 phase α-Cb + Cb <sub>2</sub> N	--	--	--
1 x 10 <sup>-3</sup>	10 min 1680°C	--	--	2 phase α-Cb + Cb <sub>2</sub> N	--	--	--
5 x 10 <sup>-2</sup>	60 min 2055°C	--	--	Single phase b.c.c.	--	--	--
5 x 10 <sup>-1</sup>	4 min 2200°C	--	--	Single phase b.c.c.	--	--	--
1.0	20 min 2050°C	--	--	2 phase α-Cb + Cb <sub>2</sub> N	--	--	--
1.0	1 min 2250°C	--	--	2 phase α-Cb + Cb <sub>2</sub> N	--	--	--

the loss of nitrogen as precipitated nitride on account of the relatively slow cooling rate of their 30 mil diameter wire specimens.

Photomicrographs of columbium 11 mil diameter wires nitrized in the bell-jar using the dynamic leak method show good penetration toward the center, the distribution of the nitride phase  $\text{Cb}_2\text{N}$  apparently being somewhat more uniform at the higher nitrogen concentrations. This point is borne out by Figs. 25 and 26 which show longitudinal and transverse sections of a wire nitrized for 10 minutes at  $1680^\circ\text{C}$  and  $5 \times 10^{-4}$  torr, and containing 1.75 at. percent nitrogen, 0.09 at. percent oxygen, and Figs. 27 and 28 which show longitudinal and transverse sections of a columbium wire nitrized for 10 minutes at  $1680^\circ\text{C}$  and  $5 \times 10^{-3}$  torr, the analyzed nitrogen and oxygen contents being 5.10 and 0.09 atomic percent, respectively. In both cases, nitride has formed both within the grains and at the grain boundaries. This behavior is quite unlike that of the Cb-O alloys where the oxide tends to form on the outside of the wire.

#### 4.3 Determination of Nitrogen Solubility by the Dynamic Leak and Sieverts Methods

Originally the solubility of nitrogen in columbium as a function of pressure and temperature was determined by the dynamic leak method, analyzing the samples for nitrogen and oxygen after quenching to room temperature. By this means, the solid-solubility limit of nitrogen could be determined isobarically or isothermally, both methods leading to the same results.

In the isobaric approach, the pressure was held constant while the wire sample adsorbed nitrogen. By reducing the heating current and slowly cooling the wire under isobaric conditions a point is reached at which  $\text{Cb}_2\text{N}$  begins to form both on the surface of the wire and its interior. This point, which corresponds to the solid solubility limit of nitrogen in the primary  $\alpha\text{-Cb}$  phase, may readily be established by observing the power input to the wire on a sensitive wattmeter while simultaneously noting the brightness temperature of the wire as indicated by an optical pyrometer. Due to the combined effects of resistivity increases on forming  $\text{Cb}_2\text{N}$  and the emissivity change from 0.374 for Cb to 0.23 for  $\text{Cb}_2\text{N}$ ,<sup>(13)</sup> the onset of nitride formation reveals itself by a sharp break in the curve relating watts input to the wire with the observed temperature as shown in Fig. 29.

Once the discontinuity has been located, it may be repeatedly traversed backwards and forwards to establish the equilibrium temperature at the preset pressure. At this point, the wire is radiation quenched from the  $\alpha\text{-Cb}$  phase limit and its nitrogen content determined by chemical analysis. A determination of nitrogen content may also be made by the lattice parameter technique once a lattice parameter versus nitrogen content curve has been established, provided no nitride precipitation occurs during the quenching process.

The alternative technique, which is somewhat more difficult to employ, but which yields almost identical results, is to maintain the wire temperature constant and gradually increase the dynamic pressure of the nitrogen until the solid-solubility limit is reached and  $\text{Cb}_2\text{N}$  commences

to form. This point is marked by a sharp break in the watts input versus nitrogen pressure curve, and also by a marked instability in the readings of the pressure gauges.

The above techniques were superseded by the Sieverts method briefly mentioned in Section 3.3 (page 16), and in which ultra-pure Baker nitrogen was used. The great advantage to be gained by employing this alternative approach is that no chemical analysis of the nitrided sample is required, it being possible to compute directly from the initial weight of the wire and from the initial and final nitrogen pressures, the precise amount of nitrogen adsorbed at temperature. Moreover, since the total volume of the Sieverts apparatus is only 1.8 liters (including McLeod gauge) as against about 44.5 liters for the bell-jar apparatus, the Sieverts apparatus can be completely baked out by heating to 300-400°C overnight under a vacuum of  $10^{-7}$  torr. Such a procedure is impossible with the bell jar. Furthermore, by using Granville-Phillips bakeable valves, "Conflat" all-metal joints and gold-wire gasket seals, the leak rate of the Sieverts equipment could be reduced to negligible proportions. This was not the case with the bell-jar apparatus which was fitted with conventional synthetic rubber O-ring seals and gaskets. However, it is interesting to note that the final results obtained by both the dynamic leak and Sieverts methods were surprisingly similar.

The Sieverts apparatus may be employed in two different ways to determine the pressure-temperature-composition relationship. The first of these is a constant temperature method in which a series of small

additions of known amounts of nitrogen is made to the degassed specimen which is held at a given temperature in the system, the entire apparatus being held at a pressure of  $10^{-7}$  torr approximately. After each nitrogen addition, the pressure in the system is followed as it decreases with time until it finally becomes constant. At this stage, the nitrogen is in thermodynamic equilibrium with the solid wire specimen. After noting the equilibrium pressure and the composition of the specimen a new increment of nitrogen is introduced into the system and the procedure repeated.

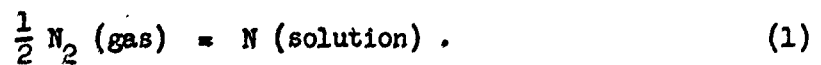
An alternative to this first method was also employed, in that after equilibrium was obtained at  $1500^{\circ}\text{C}$ , the temperature was raised in stages to  $1750$ ,  $2000$ , and  $2200^{\circ}\text{C}$  respectively, and the equilibrium pressures noted at these temperatures. The wire was quenched from  $2200^{\circ}\text{C}$  and a small increment of nitrogen introduced into the system, after which the equilibrium pressures were again measured at  $1500$ ,  $1750$ ,  $2000$  and  $2200^{\circ}\text{C}$ . In practice, this technique proved the more convenient.

It is, in essence, a constant composition method, for if we take into account the mass of the wire and the small volume of the Sieverts apparatus, it is found that relatively trivial changes in the amount of adsorbed nitrogen will produce quite large changes in the pressure of the surrounding nitrogen atmosphere. However, a small correction must be applied for the highest temperatures. This is done by noting the equilibrium pressure, quenching the wire, and measuring the final pressure when the apparatus has cooled to room temperature since all composition calculations must be referred to nitrogen at standard temperature and pressure.

In using the above method, the first nitride to form is  $\text{Cb}_2\text{N}$ . The composition and pressure at which the  $\text{Cb}_2\text{N}$  forms immediately yields the terminal solid solubility limit of the  $\alpha\text{-Cb}$  solid solution and the decomposition pressure of  $\text{Cb}_2\text{N}$  for the constant temperature at which the measurements were made. Any further additions of nitrogen at this equilibrium temperature merely results in the formation of more  $\text{Cb}_2\text{N}$ , the pressure remaining constant at the equilibrium value.

#### 4.4 Discussion of the Nitriding Results

As distinct from the dynamic equilibrium in the Cb-O system where  $\alpha\text{-Cb}$  with oxygen in solution was in contact with oxide vapor, in the case of the Cb-N system the adsorption of nitrogen takes place at temperatures and pressures at which only nitrogen gas and  $\alpha\text{-Cb}$  solid-solution co-exist. Thus, the process is strictly reversible; if the temperature is raised above the equilibrium value the adsorbed nitrogen is released as nitrogen gas, while if the pressure is raised more nitrogen is adsorbed. It is assumed that the nitrogen gas-phase consists of diatomic molecules which split-up into atoms at the metal surface before going into solid solution. We may therefore write



Thus, according to Sieverts Law, the equilibrium concentration  $x$  of nitrogen in solid solution at the temperature  $T$  should be expressible by an equation of the form:

$$x = \text{constant } (p_{N_2})^{1/2} \exp (Q/RT) \quad (2)$$

where  $x$  is in atomic percent,  $p_{N_2}$  is the nitrogen pressure and  $Q$  is the heat of solution of nitrogen in columbium in calories per gram atom.

Cost and Wert<sup>(29)</sup> using a Sieverts apparatus obtained

$$x = 6.2 \times 10^{-4} (p_{N_2})^{1/2} \exp (46,000/RT) \quad (3)$$

where  $p_{N_2}$  is in torr.

A plot of  $\log p_{N_2}$  versus  $\log x$  as abscissa for constant  $T$  should yield a straight line with a slope of 2. Our own results, obtained with the Sieverts apparatus, are plotted in this manner in Fig. 30 for the temperature range 1500-2200°C. It will be seen that the results plot as perfectly straight lines with a slope of 2 as required by theory.

A critical examination of the  $\log p_{N_2}$  versus  $\log x$  plots of Cost and Wert which cover a similar pressure range, namely  $10^{-6}$  to  $10^1$  torr approximately, shows that average lines of slope 2 were drawn through the experimental points. Actually, the curve for 1525° has a slope of 1.57 if drawn accurately through the points, while the curves for 1760 and 2255° show quite distinct breaks, the upper portions of the curves at high pressure ends of the range having slopes of 1.62 and 1.42 respectively. Similarly, the curves obtained by Gebhardt, Fromm and Jakob<sup>(25)</sup> have slopes of 2 for temperatures ranging from 1600° to 2000°, but the curve for 2100° has a slope of only 1.8. It is possible that the departure from

the theoretical slope is associated with the pickup of oxygen in the higher temperature and pressure ranges, or failure to obtain true equilibrium on account of the size of the specimens.

The isothermal plots of  $\log p_{N_2}$  versus  $\log x$  presented in Fig. 30 may be converted to constant composition curves as shown in Fig. 31 in which  $\log p_{N_2}$  is plotted as a function of  $10^4/T(^{\circ}K)$ . These lines terminate at the solid-solubility limit of the  $\alpha$ -Cb-N primary solid solution and mark out the line which gives the decomposition pressure of  $Cb_2N$  as a function of  $1/T$ .

Using the p-T-x data in Figs. 30 and 31, the solid-solubility limit of nitrogen as a function of  $1/T$  can be drawn as shown in Fig. 32. As shown by the Figure, the present set of results is remarkably close to those published by Cost and Wert and by Gebhardt, Fromm and Jakob, for temperatures above  $1500^{\circ}C$ , thus confirming the thermodynamic data incorporated in equation (3) (page 51).

#### 4.5 Nitrogen Retained on Quenching

Figures 30-33 illustrate the amount of nitrogen which can be held in interstitial solid solution within the body-centered cubic  $\alpha$ -Cb matrix at a particular temperature and surrounding nitrogen-gas pressure. The question which now arises is how much of this nitrogen can be retained in solution on quenching. As mentioned above, Dürschnabel and Hörz<sup>(28)</sup> quenched Cb wire of diameter 0.8 mm (32 mils) from temperatures ranging from  $1560$  to  $1960^{\circ}C$  and nitrogen pressures ranging from  $1 \times 10^{-3}$  to

$1 \times 10^{-2}$  torr and did not retain more than 1.3 at. %  $N_2$  in solid solution.

(No proof was offered that the quenched alloys were single phase  $\alpha$ -Cb.)

Our own investigations with the dynamic leak method seemed to indicate that the maximum amount of nitrogen which can be retained in solid solution on quenching 11 mil Cb from  $1680^\circ\text{C}$  after equilibrating in an atmosphere of  $5 \times 10^{-4}$  torr  $N_2$  is 1.05 atomic percent.

When the Sieverts apparatus became available, some additional quenching experiments were carried out. Using ultra-high purity Baker nitrogen, a 14.3 mil diameter Cb wire was doped with 9.48 atomic percent  $N_2$  at  $2200^\circ\text{C}$  in an equilibrium pressure of 1 torr  $N_2$  and then quenched. The x-ray diffraction pattern of the wire showed it to be two-phase,  $\alpha$ -Cb +  $\text{Cb}_2\text{N}$ . The lattice parameter of the  $\alpha$ -Cb solid solution was  $a = 3.304(2) \text{ \AA}$ , corresponding to a retained nitrogen content of 0.77 atomic percent, based on the calibration curve shown in Fig. 23. Similar lattice parameter results were obtained for the same batch of wire containing 2.04 atomic percent  $N_2$  and quenched from  $2200^\circ\text{C}$  at the equilibrium pressure of  $4.6 \times 10^{-2}$  torr, the lattice parameter now being  $a = 3.303(7) \text{ \AA}$  corresponding to about 0.72 atomic percent  $N_2$  retained in solid solution.

It would seem that the extremely rapid rate of nitride formation prevents the  $\alpha$ -Cb solid solution from retaining more than about 1.0 atomic percent  $N_2$  in the lattice, the amount retained being extremely sensitive to the rate of quench, being lower for the thicker wires and lower gas pressures.

On being precipitated during a quench, the rapidly forming  $\text{Cb}_2\text{N}$  phase produces an extremely fine Widmannstätten structure. At the higher nitrogen levels, precipitation is general throughout the grains and along the grain boundaries as shown in Fig. 33 for Cb + 9.48 atomic percent  $\text{N}_2$ , quenched from  $2200^\circ\text{C}$ . At low nitrogen contents, precipitation of  $\text{Cb}_2\text{N}$  in wire quenched from  $2200^\circ\text{C}$  is confined mainly to the grain and sub-grain boundaries as shown in Fig. 34 for Cb + 2.04 atomic percent  $\text{N}_2$ .

#### 4.6 The System Columbium-Hafnium

This constituent binary system of the ternary system Cb-Hf-N has already been dealt with in Section 3.9 (page 32), and the lattice parameters in Section 3.9.1 (page 32).

#### 4.7 The System Hafnium-Nitrogen

The only information on this system is that it forms the nitride HfN. This compound has a metallic character, melts at  $3310^\circ\text{C}$  and has a face-centered cubic structure of the  $\text{B1-NaCl}$  type with  $a = 4.52 \pm 2 \text{ \AA}$ .<sup>(31)</sup> It is probable, however, that Hf takes some nitrogen into solid solution.

#### 4.8 The System Columbium-Hafnium-Nitrogen

Since the amount of nitrogen which can be retained in solid solution in the  $\alpha$ -Cb phase is conditioned by the pressure of the nitrogen atmosphere and the decomposition pressures of the  $\text{Cb}_2\text{N}$  and HfN phases, it is possible only to draw a pseudo-equilibrium diagram of the Cb-Hf-N system for any particular temperature isothermal.

When nitrogen is added to pure columbium in the Sieverts apparatus, the pressure falls to the decomposition pressure of the  $\text{Cb}_2\text{N}$  phase corresponding to the temperature, should the nitride begin to form. This pressure is given by the  $\log p_{\text{N}_2}$  versus  $1/T$  plot in Fig. 31, shown as the heavy line. Thus for temperatures within the range 1400 to 2300°C, the decomposition pressure of  $\text{Cb}_2\text{N}$  varies from  $10^{-5}$  to  $10^1$  torr and lies within the range of measurements of the McLeod gauge employed with the Sieverts apparatus. Thus the solid-solubility limit of nitrogen in  $\alpha\text{-Cb}$  can be determined from a measure of the nitrogen pressure.

However, this no longer becomes possible when doping Cb-Hf alloys with nitrogen because if  $\text{HfN}$  forms, the decomposition pressure falls far below that of the range of the McLeod gauge and cannot be determined. All that can be done is to compute the total nitrogen content of the ternary alloy so formed, and use x-ray diffraction and micrographic techniques to establish the identities and quantities of the phases present.

Figure 35 illustrates the case for an alloy of atomic composition 90.4 Cb 9.6 Hf to which 15 atomic percent of nitrogen has been added in the Sieverts apparatus (the effective atomic percentages of Cb and Hf will be correspondingly reduced by the nitrogen addition, but their ratio will remain 90.4/9.6). At time  $t = 0$  and 1500° the pressure in the Sieverts apparatus is 2.5 torr and it falls to  $10^{-4}$  torr after about 58 minutes, after which it remains constant. Thus virtually all the nitrogen has been adsorbed by the alloy, and its average nitrogen content is established. The residual pressure of  $10^{-4}$  torr can easily be accounted

for by the 60 ppm of argon which is the chief impurity in Baker nitrogen. By quenching the wire and pumping the system down to  $10^{-7}$  torr, re-isolating it and reheating the wire to  $1500^{\circ}\text{C}$ , it is found that there is no appreciable increase in pressure, which remains below the range of the McLeod gauge, and hence no free nitrogen gas evolved by the wire.

After the above experiment, the wire was again quenched and examined by x-ray and micrographic methods. The Debye-Scherrer pattern showed it to consist of the three phases  $\alpha\text{-Cb} + \text{Cb}_2\text{N} + \text{HfN}$ , although this would by no means be obvious from the microstructure shown in Fig. 36. From experience with the Cb-N binary system, it is probable that the grain boundary phase consists of  $\text{Cb}_2\text{N}$ .

Binary Cb-Hf alloys in the form of wire and respectively containing 2.8, 4.8, 9.6, and 22.3 atomic percent Hf were degassed at  $2200^{\circ}\text{C}$  in the Sieverts apparatus and then doped at  $1500^{\circ}\text{C}$  with varying amounts of nitrogen ranging up to 25 atomic percent of the final alloy composition and then quenched on attaining equilibrium. The x-ray and micrographic findings are summarized in Table 6 and incorporated in the pseudo-equilibrium diagram in Fig. 37, due allowance being made for the shifts in composition produced by adding the nitrogen.

It will be noted that the  $\alpha\text{-Cb}$  phase Cb-Hf alloys all have a nitrogen solubility limit of less than 0.5 atomic percent at  $1500^{\circ}\text{C}$ , the lack of a Widmannstätten structure in the microstructures and the sharpness of the Debye-Scherrer pattern of the second phase indicating that the alloys were definitely two-phase at temperature. The second phase,

Table 6

Summary of Results on Cb-Hf-N Alloys Nitrided at 1500°C and Quenched

Initial Composition At %	At % N Added	Heat Treatment	Results	
			X-Rays	Micrcs.
Cb 97.2 Hf 2.8.	0	degassed 10 min 2200°C	single phase $\alpha$ -Cb, a = 3.3046 Å	$\alpha$ -Cb + trace HfN
	0.55	200 min 1500°C	$\alpha$ -Cb,	
Cb 95.2 Hf 4.8	0	degassed 10 min 2200°C	$\alpha$ -Cb,	$\alpha$ -Cb + HfN
	1.79	30 min 1500°C	$\alpha$ -Cb + HfN,	
	6.32	16 hrs 1500°C	$\alpha$ -Cb + Cb <sub>2</sub> N + HfN,	$\alpha$ -Cb + HfN + Cb <sub>2</sub> N
			a = 3.3087 Å	
Cb 90.4 Hf 9.6	0	degassed 10 min 2200°C	$\alpha$ -Cb,	$\alpha$ -Cb + HfN
	1.04	60 min 1500°C	$\alpha$ -Cb + HfN,	
	6.37	4 hrs 1500°C	$\alpha$ -Cb + HfN,	$\alpha$ -Cb + HfN
	14.5	3 hrs 1500°C	$\alpha$ -Cb + Cb <sub>2</sub> N + HfN,	$\alpha$ -Cb + HfN + Cb <sub>2</sub> N
	25.0	23 hrs 1500°C	Cb <sub>2</sub> N	Cb <sub>2</sub> N
			a = 3.3190 Å	
Cb 77.7 Hf 22.3	0	degassed 10 min 2200°C	$\alpha$ -Cb,	$\alpha$ -Cb + trace HfN
	1.0	3 hrs 1500°C	$\alpha$ -Cb,	
	15.0	3 hrs 1500°C	$\alpha$ -Cb + HfN,	c-Cb + HfN
	24.0	2 hrs 1500°C	$\alpha$ -Cb + HfN + Cb <sub>2</sub> N,	$\alpha$ -Cb + HfN + Cb <sub>2</sub> N
		a = 3.3466 Å		
		a = 3.348(7) Å		
		a = 3.305(9) Å		
		a = 3.304(1) Å		

in this case, is not  $\text{Cb}_2\text{N}$  as would be expected, but face-centered cubic HfN.

The HfN phase is probably close to the stoichiometric composition, through this point should be explored further, but the  $\text{Cb}_2\text{N}$  phase is found to extend some distance into the system as shown in Fig. 37. The  $\alpha\text{-Cb}$  and  $\text{Cb}_2\text{N}$  apices of the ternary triangle  $\alpha\text{-Cb} - \text{Cb}_2\text{N} - \text{HfN}$  have been fixed on the basis of the lattice parameters of the  $\alpha\text{-Cb}$  and  $\text{Cb}_2\text{N}$  phases.

On account of the extremely low decomposition pressure ( $< 10^{-6}$  torr) of the HfN phase, it is probable that the  $\alpha\text{-Cb}/\alpha\text{-Cb} - \text{HfN}$  phase boundary is not very sensitive to changes in nitrogen pressure, so that the  $\alpha\text{-Cb}$  apex of the triangle  $\alpha\text{-Cb} + \text{Cb}_2\text{N} + \text{HfN}$  is fixed. On the other hand, the  $\alpha\text{-Cb}/\alpha\text{-Cb} + \text{Cb}_2\text{N}$  boundary will be sensitive both to pressure and temperature, and, at  $1500^\circ\text{C}$ , will lie at about 2.5 atomic percent  $\text{N}_2$  at  $6 \times 10^{-5}$  torr, and at about 10.0 atomic percent  $\text{N}_2$  at  $3.0 \times 10^{-1}$  torr. It is also highly probable that the boundary of the  $\text{Cb}_2\text{N}$  phase-field is both pressure and temperature sensitive.

## 5. Columbium-Rich Columbium-Hafnium-Carbon Alloys

### 5.1 General Introduction -- Previous Work

In the determination of the solid-solubility limits of carbon in the body-centered cubic Cb-rich Cb-Hf primary solid solution, it is necessary for identification purposes to know which carbide-phases are in equilibrium with the Cb-Hf solid solution. Possible carbides in equilibrium with Cb-rich Cb-Hf alloys are  $\text{Cb}_2\text{C}$ ,  $\text{CbC}$ ,  $\text{HfC}$  and mixed carbides such as  $(\text{Cb,Hf})\text{C}$ .

## 5.2 The Cb-Hf System

This system, which consists of an unbroken series of body centered cubic solid solutions above 1950°C has been dealt with in Section 3.6.

## 5.3 The System Cb-C

Although a number of investigations have been carried out on the carbides formed in this system,<sup>(32)</sup> the only comprehensive study to be made is that by Brauer, Renner and Wernet<sup>(33)</sup> using x-ray, microscopic and pycnometric techniques on alloys made by direct synthesis and by carburizing in methane. In all, four single-phase fields are of interest in the system, namely  $\alpha$ -Cb, hexagonal close-packed  $Cb_2C$ , cubic NaCl-type CbC, and carbon, the extents of the phases at 1600-1700°C being shown in Fig. 38. According to the microstructures,<sup>(33)</sup> the Cb phase retains, at most, 0.02 at. percent C in solid solution with negligible change in the lattice parameter of the matrix. The crystal structures of the carbides  $Cb_2C$  and CbC have also been studied in the form of thin films by Terao<sup>(34)</sup> using electron diffraction methods.

## 5.4 The System Hf-C

According to Hansen,<sup>(35)</sup> only the intermediate phase HfC is formed in the system. The melting point of HfC is  $3890 \pm 150^\circ C$ . The crystal structure is of the face-centered cubic B1-NaCl type with a lattice parameter  $a = 4.6365 \text{ \AA}$ . As is the case with TiC and ZrC which have the

same type of structure, the HfC phase will, in all probability, have a certain homogeneity range and this will certainly influence the value obtained for the lattice parameter.

#### 5.5 The System Cb-Hf-C

Nothing has been published on this system.

#### 5.6 The System Cb-C -- Present Investigation

Two methods of approach were employed in attempting to obtain the solid-solubility limit of carbon in columbium. These entailed the use of (a) solid specimens containing respectively 0.5, 1.0 and 5.0 atomic percent carbon prepared by melting together powdered columbium with a master alloy of stoichiometric composition  $\text{Cb}_2\text{C}$ , and (b) using zone-refined columbium wires which were given a thin coating of Aquadag and heated in the bell-jar apparatus for various times and temperatures in a vacuum of  $10^{-6}$  -  $10^{-7}$  torr.

In the case of the solid samples, which weighed approximately 7-8 grams, the alloys were homogenized in the tungsten tube furnace for 24 hours at  $1600^\circ\text{C}$  and quenched on a molybdenum sheet. Typical photomicrographs corresponding to 5.0 and 1.0 atomic percent C are presented in Figs. 39 and 40 and show hexagonal  $\text{Cb}_2\text{C}$  in a matrix of columbium primary solid solution. A photomicrograph of 0.5 at. percent C Cb-C alloy heat-treated and quenched under the same conditions was entirely single phase. Thus it would seem that the solid-solubility limit of

carbon in columbium at 1600°C lies between 0.5 and 1.0 atomic percent carbon (660 ppm and 1300 ppm respectively). Using a point-counting technique, (36,37) the 5 at. percent C alloy yielded  $14.0 \pm 2.2\%$  by volume of  $Cb_2C$  in the Cb matrix, based on a total of 1998 point intersections. This places the solid-solubility limit of carbon in columbium at approximately  $0.55 \pm 0.75$  at. percent C, in agreement with the original micrographic findings. A similar count, with 8176 point intersections on the 1.0 at. percent C alloy yielded a  $Cb_2C$  volume-fraction of  $2.56 \pm 1.0\%$  corresponding to a carbon content at the solid solubility limit of  $0.24 \pm 0.28$  at. percent C. The same 1.0 at. percent C alloy heated for 16 hours at 2180°C in a vacuum of  $5 \times 10^{-7} - 1 \times 10^{-6}$  torr had slightly less  $Cb_2C$ .

In order to avoid the possibility of oxygen pickup when using filed samples, x-ray diffraction studies were made on fully degassed zone-refined Cb-wire which had been coated with a thin layer of Aquadag, as mentioned above, and heated for various times and temperatures in vacuum. On account of the varying thickness of the Aquadag layer, there was a tendency to large variations in the surface brightness, which made accurate temperature determinations almost impossible, while the occasional formation of hot-spots caused the wire to fail. Nevertheless, carbide formation occurred as shown in Fig. 41 for the typical case of a wire heated to a nominal 1700°C and held for 16 hours in a vacuum of  $1 \times 10^{-6}$  torr and radiation quenched. X-ray diffraction patterns taken from the wires in the region where the temperature measurement was made showed a

small but significant increase in lattice parameter of the Cb primary solid-solution and also the presence of appreciable amounts of hexagonal  $\text{Cb}_2\text{C}$  both within the grain boundaries and within the grains themselves. Thus the behavior of columbium with respect to carbon is very similar to its behavior with respect to nitrogen, and very different from that with oxygen, where the oxide tends to form almost entirely on the surface.

Lattice parameter determinations made on wire carburized at  $1700^\circ\text{C}$  yielded a value of  $a = 3.3010 \text{ \AA}$  as against a parameter value for zone-refined oxygen-free columbium of  $a = 3.2986 \text{ \AA}$ . Based on the micrographic work on the lump samples, the lattice parameter of the carburized wire corresponds to an approximate carbon content of 0.55 at. percent, it being assumed that as a result of the prior degassing treatment almost all the oxygen and nitrogen has been removed and that any residues would be carried off as a gaseous reaction product with some of the carbon in the wire.

Comparing the rates of lattice parameter change per unit atomic percent increase in carbon, nitrogen and oxygen, we obtain for  $(da/a)/\text{unit}$  increase the values 0.00132, 0.00224 and 0.00118 respectively. Thus based on these initial results it would seem that nitrogen is the most effective of the three elements in increasing the columbium spacing.

#### 5.6.1 Discussion of the Results

The present work on the Cb-C system places the solid-solubility of carbon in columbium close to 0.55 atomic percent C for alloys

quenched from 1600° and 2180°C. This value is much higher than the value of 0.02 atomic percent attributed to Brauer et al.<sup>(32)</sup> However, a careful study of Brauer's paper<sup>(33)</sup> indicates that the solubility limit was based on the planimetry of the Cb<sub>2</sub>C phase in an alloy of composition CbC<sub>0.05</sub> (4.76 at. percent C) which yielded a phase boundary composition of CbC<sub>0.026</sub> or 2.52 atomic percent C. This was erroneously reported as 0.02 atomic percent, and subsequently published as such in "Hansen". As may be seen from the present investigation, a value of 2.52 atomic percent C is much too high, while 0.02 is much too low. Our own work, with alloys at 0.5 and 1.0 atomic percent C effectively traps the boundary composition at 0.55 atomic percent. This value was fully confirmed by the subsequent work on the ternary system Cb-Hf-C.

#### 5.6.2 The System Cb-Hf-C -- Present Investigation

As a prelude to studying the solid-solubility of C in the  $\alpha$ -Cb-Hf solid solution, a number of ternary alloys were made to establish the identities of the carbide phases present in the system as an aid to interpreting the x-ray diffraction patterns and photomicrographs of multiphase low-carbon alloys. The ternary Cb-Hf-C alloys high in carbon were made from mixtures of Kennametal columbium powder, filed Hf crystal bar from the Foote Mineral Co., and Specpure carbon powder, the mixtures being compressed into 1/2-inch diameter slugs and then alloyed by solid state diffusion in vacuo for 24 hours at 2500°C. However, the diffraction patterns were diffuse indicating incomplete homogenization and an attempt

was made to improve matters by melting the samples in the argon arc furnace followed by a second anneal of 2 days at 2000°C. The patterns were considerably improved by this procedure but a small amount of residual diffuseness remained. The following compositions were investigated: CbC,  $Cb_2HfC_3$ ,  $CbHf_2C_3$ , HfC;  $Cb_2C$ ,  $Cb_4Hf_2C_3$ ,  $Cb_3Hf_3C_3$  and  $Cb_2Hf_4C_3$ . These alloys were quite brittle and could easily be powdered in a tungsten carbide mortar for subsequent x-ray diffraction analysis.

In addition to the above, four low-carbon alloys of nominal atomic compositions 94 Cb 5 Hf 1C, 89 Cb 10 Hf 1 C, 84 Cb 15 Hf 1 C, and 79 Cb 20 Hf 1 C, were made by melting suitable mixtures of CbC, Cb and Hf powders in the argon arc furnace. These alloys were subsequently levitation melted at  $10^{-5}$  -  $10^{-6}$  torr and vacuum cast into cylindrical rods of approximate size 1-1/2" long x 3/16" in diameter, after which they were homogenized by heating for 1 day at 2000°C and vacuum quenched.

After this heat treatment, the ends of the rods were subjected to micrographic examination and were found to be two-phase, thus showing that the solid-solubility limit of carbon in Cb-Hf alloys is less than 1.0 atomic percent at 2000°C. This falls in line with the solid-solubility limit of carbon in the binary system Cb-C. It was expected that the second phase would be  $Cb_2C$ , but subsequent x-ray analysis showed it to be an extension of the CbC phase, as will be described below.

Of the four 3/16" diameter ternary alloy rods containing 1.0 atomic percent carbon, only those containing 5.0 and 10.0 atomic percent Hf could be drawn down successfully to wire of 11-12 mil diameter; the two

ternary alloys with a higher Hf content, namely those with 15 and 20 atomic percent respectively, cracked during the swaging operation from 1/8" diameter rod to 1/16" diameter wire and any attempts to reduce the diameter still further by drawing had to be abandoned. As a result, only the first two wires could be heat treated in the Sieverts apparatus, while the cracked rods were heat treated in the tungsten tube furnace.

The results of the x-ray and micrographic investigations of the samples after various heat treatments are presented in Table 7 and the tentative Cb-Hf-C phase diagram based on the data is given in Fig. 42. It will be noted that only three single-phase fields are of interest, namely (Cb,Hf)C, Cb<sub>2</sub>C and  $\alpha$ -Cb. These will be described below.

### 5.6.3 The (Cb,Hf)C Phase-Field

The present investigation indicates that at 2000°C, the phase-field based on the cubic B1-type CbC structure extends as a wide band across the Cb-Hf-C composition triangle as a continuous series of solid solutions and links up with face-centered cubic B1-type HfC. As shown in Fig. 43, the lattice parameter of CbC increases almost linearly from the published values of 4.46(5) Å for CbC to 4.636(5) Å for HfC. Additions of Cb and Hf to make the metal content of (Cb,Hf)C alloys greater than 50 atomic percent leads to parameter changes which are tentatively indicated by the isoparametric contours interpolated across the (Cb,Hf)C phase-field as shown in Fig. 42. In the portion of the phase field richest in Cb, increases in the metal content actually leads to a marked

Table 7

Summary of Results on Cb-Hf-C Alloys

Composition At %		Heat Treatment	Phases Present		Lattice Parameter $\bar{a}$
Cb	Hf C		X-Rays	Micro	
94	5 1.0	L.A. 1 day 2000°C R.Q. + 10 min 2200°C Q + 2200°C sc → 1500°C 16 hr Q	α-Cb α-Cb	α-Cb + (Cb, Hf)C α-Cb α-Cb + (Cb, Hf)C	3.311(4) 3.310(9)
89	10 1.0	L.A. 1 day 2000°C R.Q. + 10 min 2200°C Q + "Aquadag" coated + 2 hrs 2000°C Q	α-Cb α-Cb + (Cb, Hf)C	α-Cb + (Cb, Hf)C α-Cb + (Cb, Hf)C α-Cb + (Cb, Hf)C	3.324(5) a(b.c.c.) = 3.301(2) a(f.c.c.) = 4.456(5)
84	15 1.0	L.A. 1 day 2000°C R.Q. + 2200°C sc → 1500°C 16 hrs Q		α-Cb + (Cb, Hf)C α-Cb + (Cb, Hf)C	
79	20 1.0	L.A. 1 day 2000°C R.Q. + 2200°C sc → 1500°C 16 hrs Q		α-Cb + (Cb, Hf)C α-Cb + (Cb, Hf)C	
33.33	16.67 50	L.A. 2 days 2000°C R.Q.	(Cb, Hf)C		a(f.c.c.) = 4.570(8)
16.67	33.33 50	L.A. 2 days 2000°C R.Q.	(Cb, Hf)C		a(f.c.c.) = 4.521(0)
22.22	44.45 33.33	L.A. 2 days 2000°C R.Q.	(Cb, Hf)C		a(f.c.c.) = 4.515(9)
33.33	33.33 33.33	L.A. 2 days 2000°C R.Q.	(Cb, Hf)C		a(f.c.c.) = 4.547(0)
44.45	22.22 33.33	L.A. 2 days 2000°C R.Q.	(Cb, Hf)C		a(f.c.c.) = 4.582(0)

L.A. -- Lump Annealed  
R.Q. -- Furnace Quenched Tungsten Tube Furnace  
S.C. -- Slow Cooled

reduction in the lattice parameters. This means that the carbon atoms are not replaced substitutionally by metal atoms in the structure, but rather that lattice vacancies are created by the absence of carbon atoms from their preferred sites.

#### 5.6.4 The $\text{Cb}_2\text{C}$ Phase-Field

Based on the x-ray and micrographic results it would seem that the hexagonal  $\text{Cb}_2\text{C}$  phase is closely confined to the Cb-C edge of the composition triangle as shown in Fig. 42 and takes very little Hf into solid solution.

#### 5.6.5 The $\alpha\text{-Cb}$ Phase-Field

At  $2000^\circ\text{C}$ , body centered cubic  $\alpha\text{-Cb}$  forms a continuous series of substitutional solid solutions with body centered cubic  $\beta\text{-Hf}$ , the  $\alpha\text{-Cb}$  phase thus stretching, in effect, across the entire Cb-Hf edge of the Cb-Hf-C composition triangle. As shown by the photomicrographs of the series of alloys containing 1 atomic percent of carbon, there is a second phase present, the quantity of which is too small to be clearly identified in the x-ray diffraction patterns of the samples.

Figures 44 and 46 show the microstructures of the respective alloys 94 Cb 5 Hf 1 C and 89 Cb 10 Hf 1 C after an equilibrating anneal of 24 hours at  $2000^\circ\text{C}$ . Both alloys reveal the presence of significant amounts of a carbide phase which increases somewhat on re-annealing for 16 hours at  $1500^\circ\text{C}$  after slowly cooling from  $2200^\circ\text{C}$ . As shown by Fig. 45,

wire of composition 94 Cb 5 Hf 1 C becomes single phase on heating for 10 minutes at 2200°C, but this is not the case for alloys of higher Hf content. Based on the amount of carbide observed, the boundary of the  $\alpha$ -Cb phase for the 2000°C isothermal is probably located at less than 0.2 atomic percent C.

The amount of carbide in the samples is too small to yield an x-ray diffraction pattern which would enable its identity to be recognized. Rather than use an elaborate extraction technique or make up a new series of alloys having a higher carbon content, the following method was employed to identify the carbide phase. The wire of initial composition 89 Cb 10 Hf 1 C was given a coating of "Aquadag" and heated in vacuum in the Sieverts apparatus at 2000°C, this temperature being chosen instead of 2200°C to avoid the wire's burning out should hot spots form due to slight irregularities in the coating. After heating for 2 hours, the wire was quenched. Micrographical examination of the wire showed it to have an almost uniform two-phase structure over the whole of its cross section (see Fig. 47), while x-ray diffraction analysis showed the carbide to consist entirely of the face centered cubic (Cb,Hf)C phase and not hexagonal  $\text{Cb}_2\text{C}$  as might have been expected.

It is possible, without chemical analysis of the carburized alloy, to make a rough estimate of its composition and of the compositions of the constituent phases in equilibrium with each other. In the first place, it is known that the  $\alpha$ -Cb matrix must contain about 0.2 to 0.5 atomic percent C. On carburizing, the lattice parameter of the  $\alpha$ -Cb matrix falls

drastically from 3.324(5) Å to 3.301(2) Å. This means that almost all the Hf has been removed from the  $\alpha$ -Cb-Hf-C solid solution, thereby pushing the composition of the  $\alpha$ -Cb phase almost into the Cb corner of the ternary triangle.

Since carburizing the alloy does not change the Cb/Hf ratio, the addition of carbon to 89 Cb 10 Hf 1 C will push its composition along the line AC to a point B in the composition triangle as shown in Fig. 42. To pin B down, we need to know the direction of the tie line passing through it, joining the  $\alpha$ -Cb phase to the co-existing composition D on the (Cb,Hf)C phase boundary. We know from the lattice parameter of the  $\alpha$ -Cb phase obtained from the diffraction pattern of the carburized wire that the tie-line originates almost at the Cb corner of the diagram. Thus one end of the tie-line is fixed. The same diffraction pattern yields the lattice parameter of the (Cb,Hf)C solid solution. Thus the tie-line must meet the corresponding isoparametric contour at D on the phase boundary of the (Cb,Hf)C phase. If the position of the phase boundary were known, the position of D would be known, thus fixing the tie-line and hence the position of B. This last piece of information can be obtained by the lever principle using the relative amounts of the phases  $\alpha$ -Cb and (Cb,Hf)C as derived from the photomicrograph. Thus, without the chemical analysis of B, a rough estimate of its composition and of the (Cb,Hf)C phase boundary may be derived by a combination of lattice parameter and photomicrographic data once the constituent phases have been identified.

Since the position of the tie line BD effectively originates in the Cb corner of the Cb-Hf-C triangle, all Cb-Hf alloys containing more than about 0.2 atomic percent carbon will have (Cb,Hf)C phase as a second constituent.

Appendix I  
X-Ray Diffraction Techniques

Throughout the investigations into the Cb-Hf-(O,N,C) systems the identification of the phases observed in the microsections was carried out by the now classical Debye-Scherrer x-ray diffraction powder technique. This technique was also used to determine any changes produced in the lattice parameters of the Cb-solid solution by the interstitial incorporation of oxygen, nitrogen or carbon in the structure, and where possible, the solid-solubility limits of these elements were determined with the assistance of the parameter versus composition curves.

In the present investigation, where wire-form specimens of about 11 mil diameter were employed to a large extent, it was found quite adequate to employ a 114.6 mm diameter Debye-Scherrer powder camera using copper K $\alpha$  radiation ( $\lambda\alpha_1 = 1.54051 \text{ \AA}$ ,  $\lambda\alpha_2 = 1.54433 \text{ \AA}$ ) from a high intensity rotating anode x-ray tube.<sup>(38)</sup> Some typical Debye-Scherrer patterns of columbium-base alloys are shown in Fig. 48.

Where specimens were not in the form of a wire, the usual methods of filing or crushing the lump samples, followed by sieving, were employed to produce the necessary powder. This was heat treated to remove cold work in either pure columbium or pure tungsten containers consisting of hollowed-out capped cylinders, about 5/8" in diameter and 5/8" high, with a wall thickness of 1/16", the heat treatment being carried out in a vacuum of about  $10^{-7}$  -  $10^{-6}$  torr in the tungsten tube furnace.

Despite the vacuum employed and the fact that the containers were degassed prior to use, traces of oxygen were invariably picked up by the columbium-rich powders on account of their high surface area/volume ratio.

This difficulty is avoided in the case of wire-form specimens which can be fully degassed and annealed in the bell-jar or Sieverts apparatus, but wire-form specimens present a difficulty of their own, namely the tendency to grain growth which causes the diffraction lines to become spotty. This can make the line-position measurement difficult for accurate lattice parameter determinations, but this drawback can be overcome in most cases by taking diffraction patterns from positions along the wire until a point is reached which yields sharp spots on the equator of the film and by translating the wire specimen parallel to its axis in addition to the usual rotation around it.

The columbium-rich solid solution is body centered cubic and yields excellent diffraction lines at sufficiently high Bragg angles for making good lattice-parameter determinations. In the present instance, provided the diffraction lines were smooth, a precision of about 1 part in 30,000 to 50,000 could be obtained using the well-known plot of measured parameter  $a$  versus the angular function  $\frac{1}{2}(\cos^2 \theta/\theta + \cos^2 \theta/\sin \theta)$ , (39,40) but in the case of spotty lines, the precision fell to about 1 part in 3,000.

The solid-solubility limit of a phase-field may be determined by plotting the lattice parameter of the single phase alloy as a function of atomic or weight percent of one of the constituents and observing

where a discontinuity occurs on entering the two-phase field. The accuracy with which this discontinuity can be determined depends on the slope of the parameter-composition curve. Thus, if the accuracy  $da/a$  to which a parameter  $a$  can be determined is  $1/50,000$ , and  $dc$  is the uncertainty in composition with which the boundary can be located by the x-ray method, it can easily be shown that

$$dc = \frac{a}{50,000 (da/dc)}$$

the final accuracy being set by the chemical analyses used to determine the parameter-composition curve.

Using the data for the Cb-O system obtained by Seybolt, by way of an example,

$$\frac{da}{dc} = \frac{0.0110}{0.736} \text{ R/wt. \% } O_2$$

so that the accuracy of determination of the  $O_2$  solid-solubility limit in columbium will be given by

$$dc = \frac{3.3112}{50,000 \left( \frac{0.011}{0.736} \right)}$$

= 0.004 weight percent.

## Appendix II

### Metallography of Cb-Hf-C Alloys

The specimens were mounted in 1" diameter molds in a polymethyl methacrylate resin ("Kold-Mount" and "Quick-Mount"). It takes this plastic about 30 minutes to harden and no pressure or external heat is needed. A temperature of about 135°C is reached during the polymerization. The 1" diameter mounts were next loaded into a Buehler Automet polishing attachment and ground and polished in the following steps:

- (1) Ground on 600 grit silicon carbide paper, water cooled, 160 rpm, 40 lbs. pressure for 2 minutes.
  - (2) Rough-polished on 6 micron diamond, white duck cloth lapping, oil cooled, 160 rpm, 40 lbs. pressure for 5 minutes.
  - (3) Final-polished on Microcloth in two steps:
    - a. Attack-polished using Linde "B" abrasive (gamma alumina 0.03 micron size) and an etching solution of the following composition:
      - 50 ml Lactic Acid
      - 10 ml HNO<sub>3</sub>
      - 2-10 ml HF, depending on the composition of the alloy.
- 160 rpm, 40 lbs. pressure for 5 minutes and 30 lbs. pressure for 1 minute.

- b. After rinsing all the abrasive off the cloth, the mounts are etch-polished for 1 additional minute at 30 lbs. pressure and 160 rpm.

Next the mounts are removed from the Buehler polishing attachment and etched to bring out the microstructure. If the structure is faintly discernible when the sample is removed from the Automet, the above etching solution will usually work. The sample is cotton-swabbed for 1 to 60 seconds to reveal the microstructure. If no structure is present when the sample is finish-polished or if the above solution does not work, the more severe Dupont columbium-etching reagent is used. Etching is done by immersion for 5 to 30 seconds. The following is the composition of the etching reagent:

50 ml Water

5 ml  $\text{HNO}_3$

14 ml  $\text{H}_2\text{SO}_4$

20 ml HF.

### References

1. A. Calverley, M. Davis, and R. F. Lever, *J. Sci. Instrum.* 34, 142, 1957.
2. R. G. Carlson, Meeting of the Electrochem. Soc., New York, April 1958.
3. A. Taylor and H. B. Ryden, *Journ. Less-Common Metals* 4, 451, 1962.
4. R. T. Bryant, *Journ. Less-Common Metals* 4, 62, 1962.
5. G. Brauer, *Zeits. anorg. und allgem. Chemie* 248, 1, 1941.
6. A. U. Seybolt, *Trans. AIME* 200, 770, 1954.
7. R. P. Elliott, *Trans. ASM* 52, 990, 1960.
8. E. Gebhardt, E. Fromm, and D. Jakob, "Metals for the Space Age," *Plansee Proceedings*, Editor, F. Benesovsky (Springer Verlag), 1965.
9. E. Gebhardt and R. Rothenbacher, *Zeits. für Metallkunde* 54, 443, 1963;  
54, 623, 1963.
10. H. J. Goldschmidt, *J. Inst. Metals* 87, 235, 1959.
11. H. Terao, *Japanese Journ. of Appl. Phys.* 2, 156, 1963.
12. L. V. Whitney, *Phys. Rev.* 43, 458, 1935.
13. J. R. Cost, *Trans. AIME* 224, 634, 1962.
14. C. Y. Ang and C. West, *Trans. AIME* 197, 1032, 1953.
15. M. C. Neubürger, *Zeits. für Kristallogr.* A93, 158, 1936.
16. J. W. Edwards, R. Speiser and H. L. Johnston, *J. Appl. Phys.* 22, 424, 1951.
17. A. Taylor, W. Hickam and N. J. Doyle, *Journ. Less-Common Metals*, Sept. 1965.
18. W. L. Worrell, *J. Phys. Chem.* 68, 952-953, 1964.
19. J. P. Pensler, *Journ. Electrochem. Soc.* 108, 744, 1961.

References (cont'd)

20. A. Taylor and N.J. Doyle, *Journal Less-Common Metals* 7, 37, 1964..
21. J. Stringer and A.R. Rosenfield, *Nature*, 199, 337, 1963.
22. G. Brauer and J. Jander, *Zeits. für anorg. und allg. Chemie*, 270, 160, 1952.
23. G. Brauer and R. Esselborn, *Zeits. für anorg. und allg. Chemie*, 309, 151, 1961.
24. G. Brauer and H. Kirner, *Zeits. für anorg. und allg. Chemie*, 328, 34, 1964.
25. N. Schönberg, *Acta Chem. Scand.*, 8, 208, 1954.
26. N. Terao, *Jap. Journal of Applied Physics*, 4 (5), 353, 1965.
27. R.P. Elliott and S. Komjathy, "Columbian Metallurgy", p. 367. *Met. Soc. Conferences*, vol. 10. Ed. D.C. Douglass and P.W. Kunz (Interscience Publishers) 1961.
28. W. Dürrschnabel and G. Hörz, *Naturwissenschaften*, 22, 687, 1963.
29. J.R. Cost and C.A. Wert, *Acta Met.*, 11, 231, 1963.
30. E. Gebhardt, E. Fromm and D. Jakob, *Zeits. für Metallkunde*, 25, 423, 1964.
31. M. Hansen, "Constitution of Binary Alloys", (McGraw-Hill Book Co., 2nd Ed., 1958), p. 813.
32. M. Hansen, "Constitution of Binary Alloys", (McGraw-Hill Book Co., 2nd Ed., 1958), p. 372.
33. G. Brauer, H. Renner and J. Wernet, *Zeits. anorg. und allg. Chemie*, 27, 249, 1954.

References (cont'd)

34. N. Terao, Jap. Journal of Applied Physics, 3 (2), 104, 1964.
35. M. Hansen, "Constitution of Binary Alloys", (McGraw-Hill Book Co., 2nd Ed., 1958), p. 365.
36. J.E. Hilliard, "Volume Fraction Analysis by Quantitative Metallography", G.E. Co. Report No. 61-RL-2652M, March 1961.
37. T. Gladman and J.H. Woodhead, Journal Iron & Steel Inst., (London), p. 189, February 1960.
38. A. Taylor, Rev. Sci. Instruments, 27, 757, 1956.
39. A. Taylor and H. Sinclair, Proc. Phys. Soc. (London), 57, 126, 1945.
40. J.B. Nelson and D.P. Riley, Proc. Phys. Soc. (London), 57, 160, 1945.

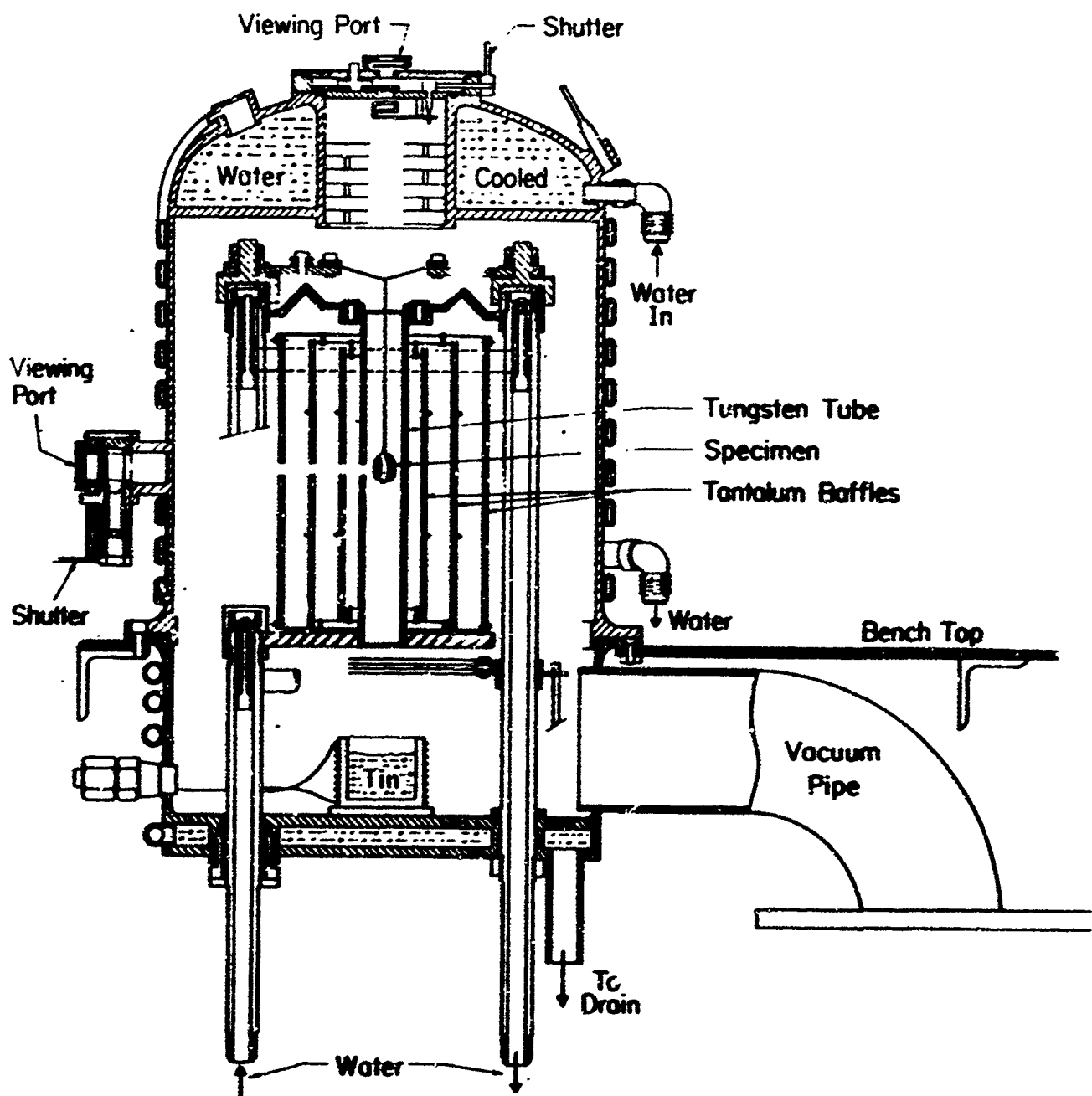


Fig. 1—Tungsten tube high temperature furnace



Fig. 2—Transverse section of Cb wire in copper sheath after swaging. X50

ENG. 4426416

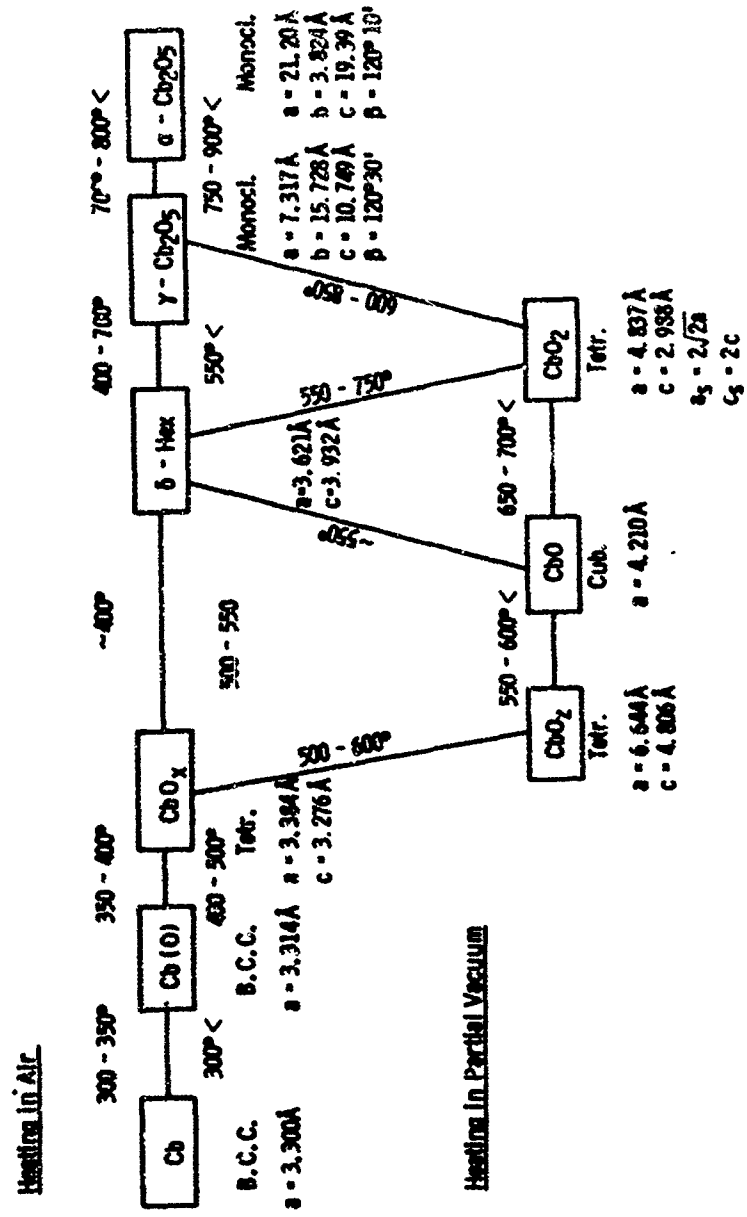


Fig. 3—Structural relationships between the oxides of Columbium (N. Teraz, Jap. Journ. Appl. Physics, 2, 156, 1963)

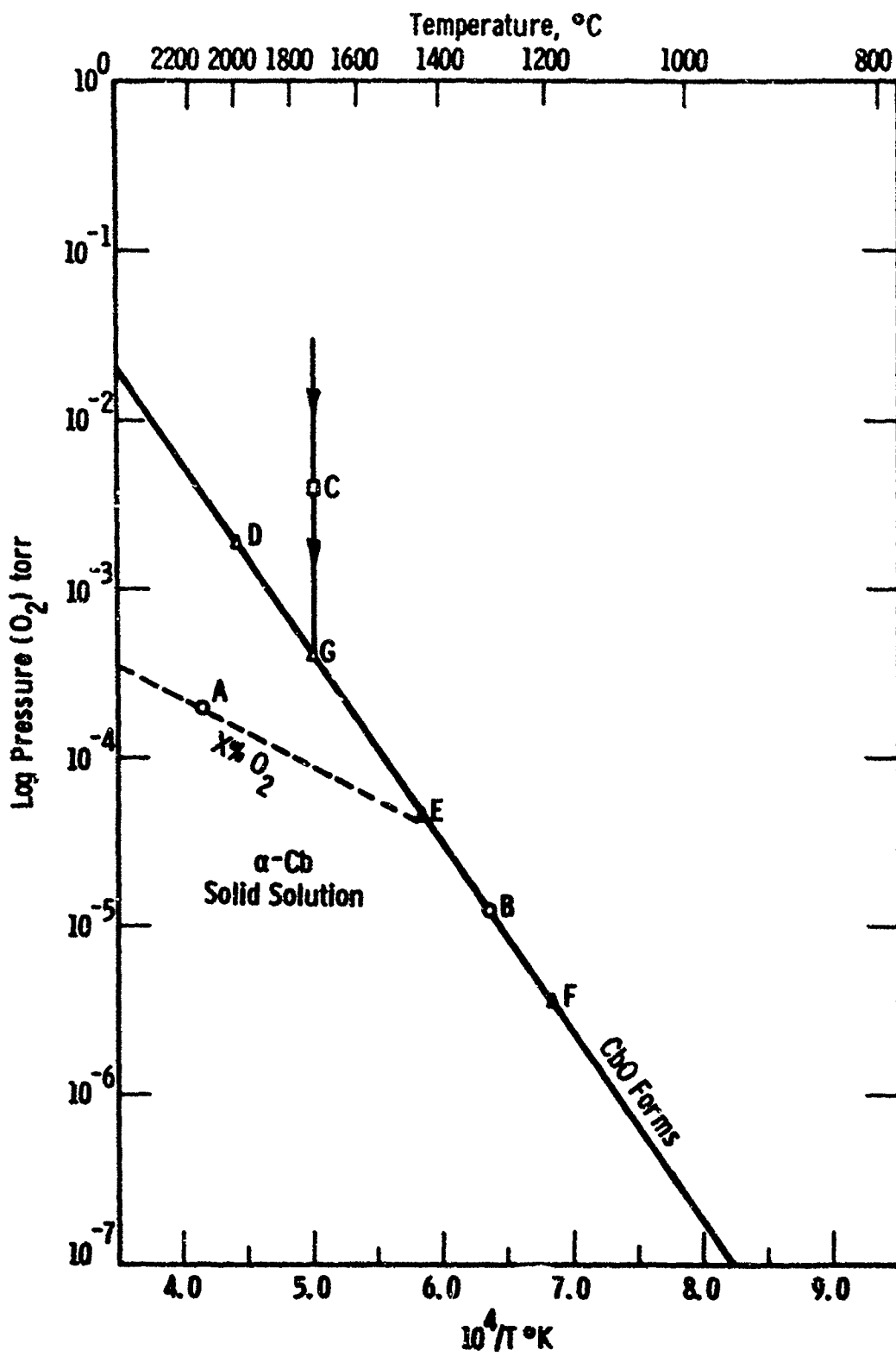


Fig. 4—Hypothetical plot of log P(O<sub>2</sub>) vs 10<sup>4</sup>/T (°K)



Fig. 5 -Vacuum bell - jar and associated equipment for oxidizing Cb-alloy wires

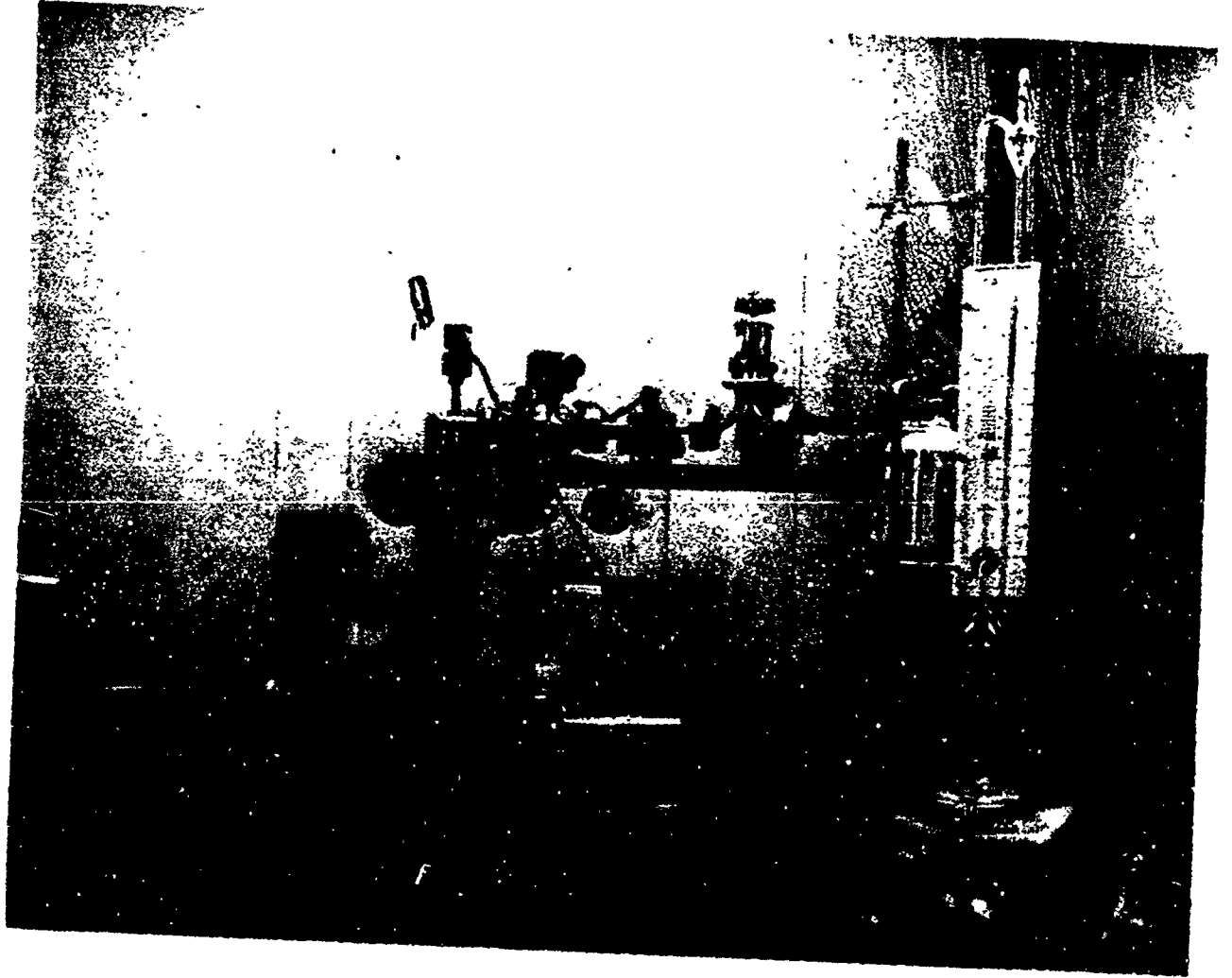


Fig. 6—Sieverts apparatus

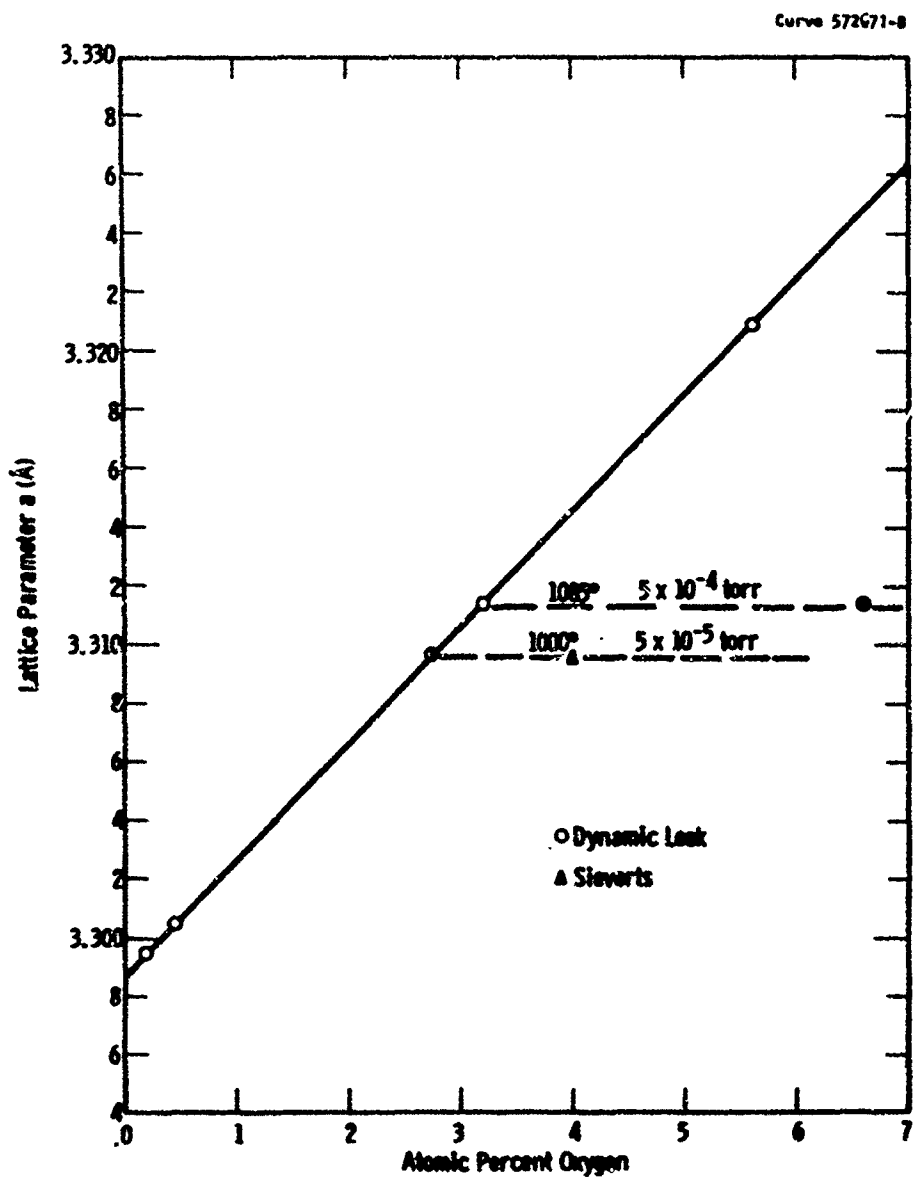


Fig. 7—Lattice parameters vs O<sub>2</sub> content of Cb (O) solid solutions

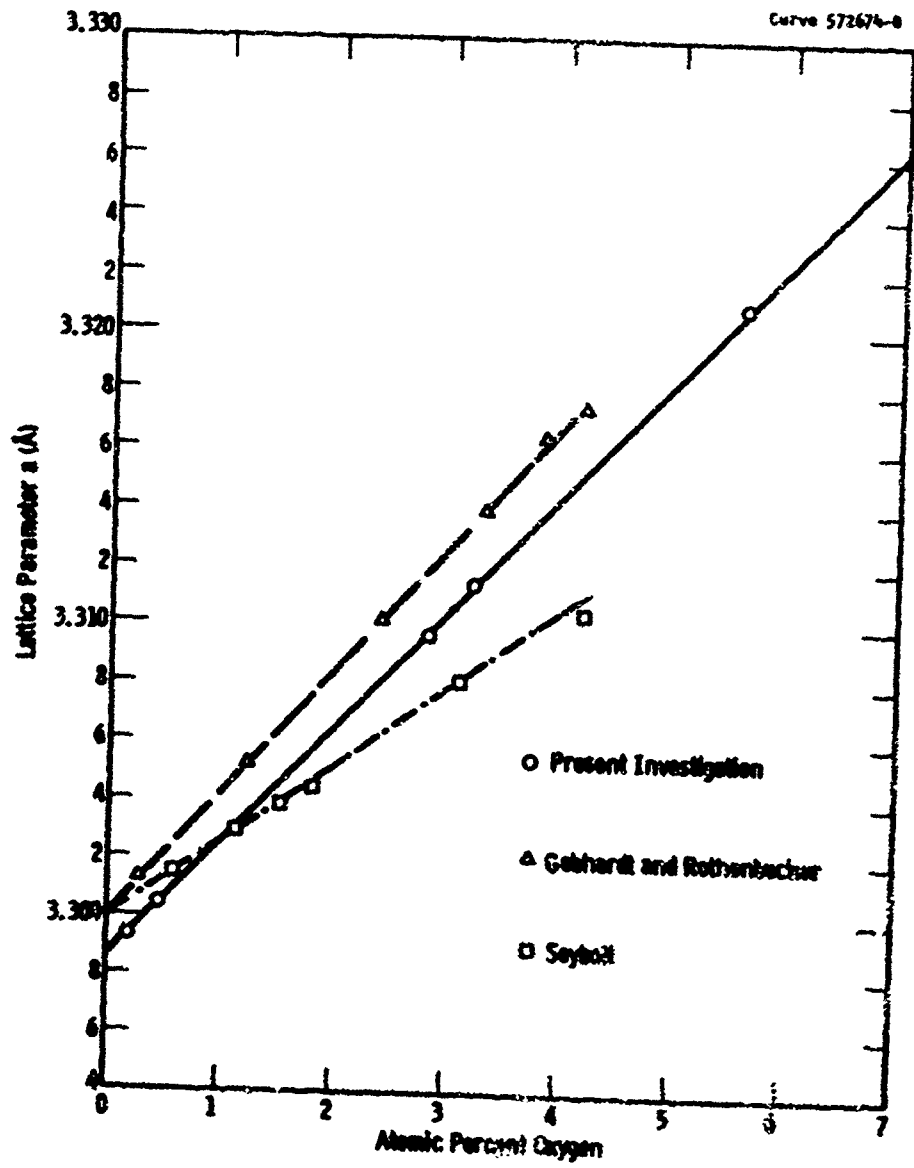


Fig. 8—Comparison of lattice parameter composition curves

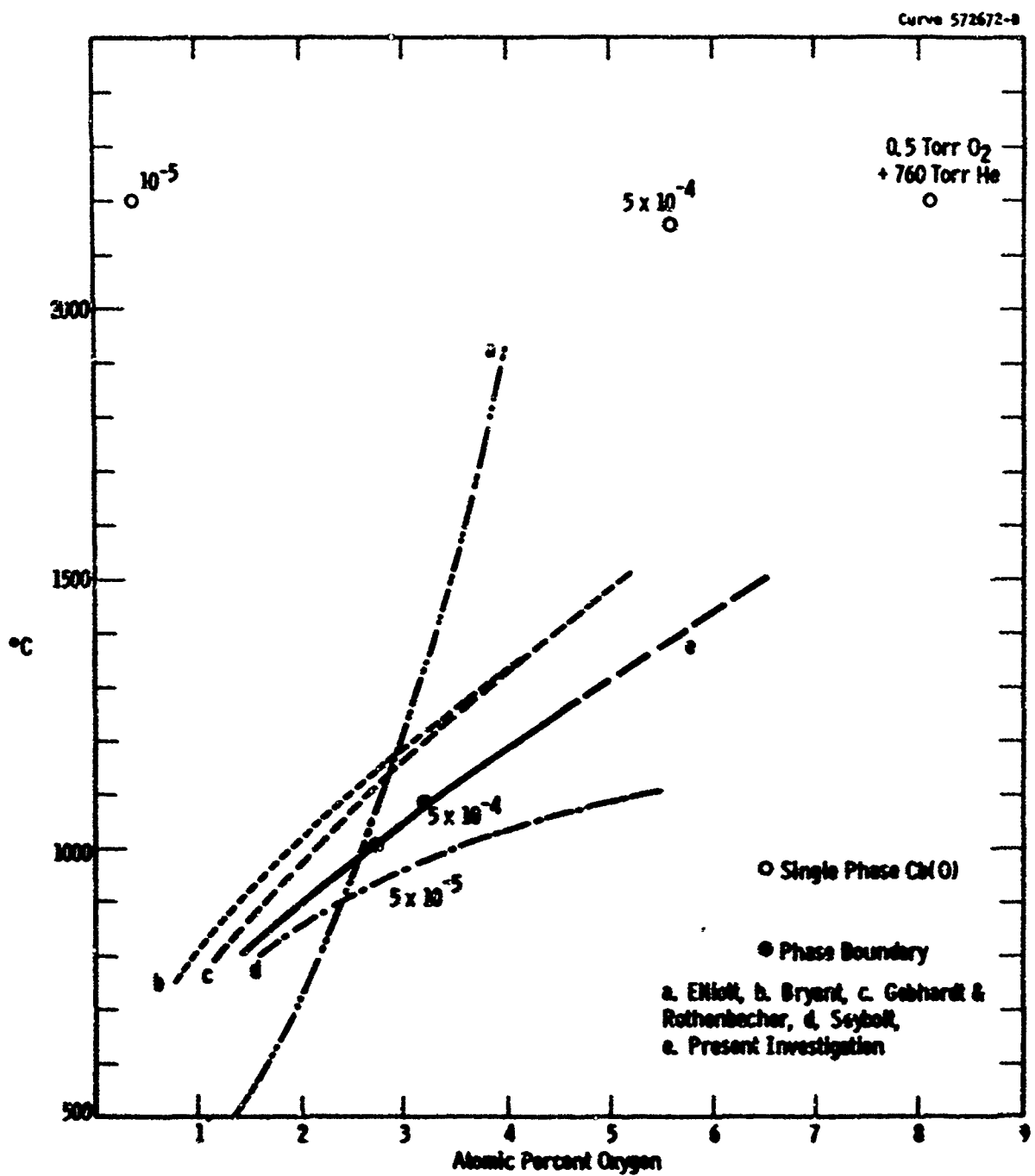
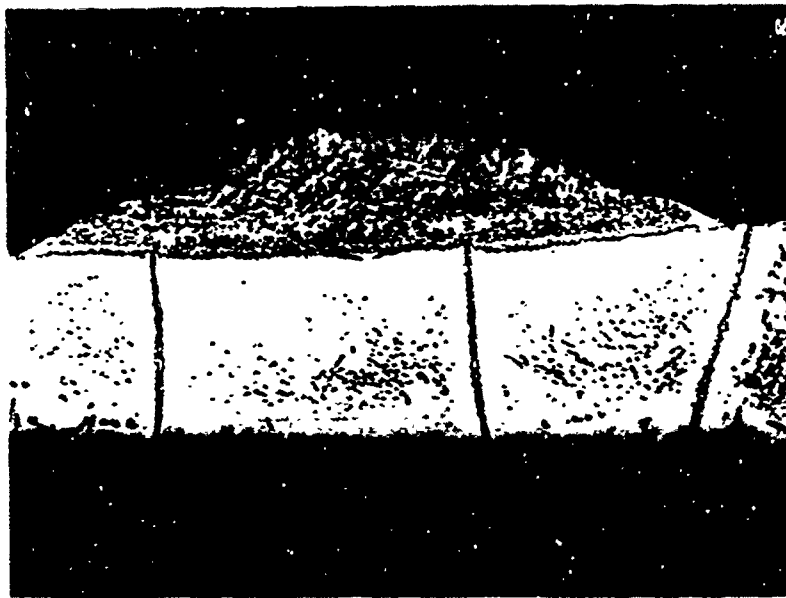
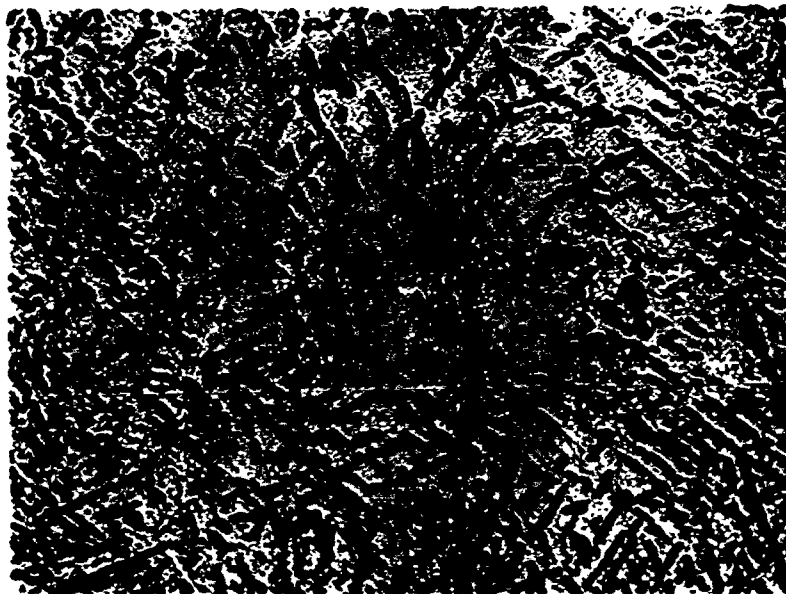


Fig. 9—Solid solubility limit of oxygen in the Cb(O) phase field  
 a. Elliott, b. Bryant, c. Gebhardt & Rotherbecher, d. Seybolt,  
 e. Present Investigation



X 200

Fig. 10 —Longitudinal section of 11 mil diameter Cb wire melted at 1775°C in 0.5 torr O<sub>2</sub> and 760 torr He, showing localized swelling and eutectic structure



X 1000

Fig. 11 —Transverse section of Cb wire shown in Fig. 9, close to swelling

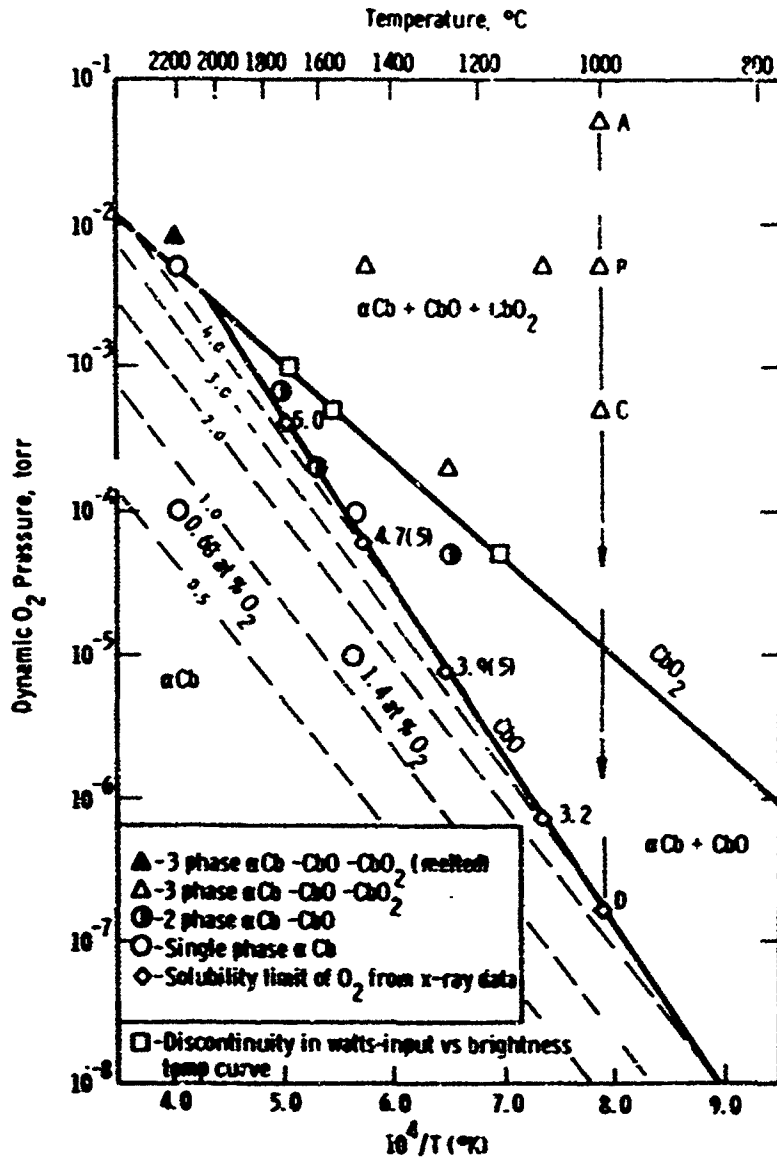


Fig. 12—Vapor pressure curves of columbium oxides

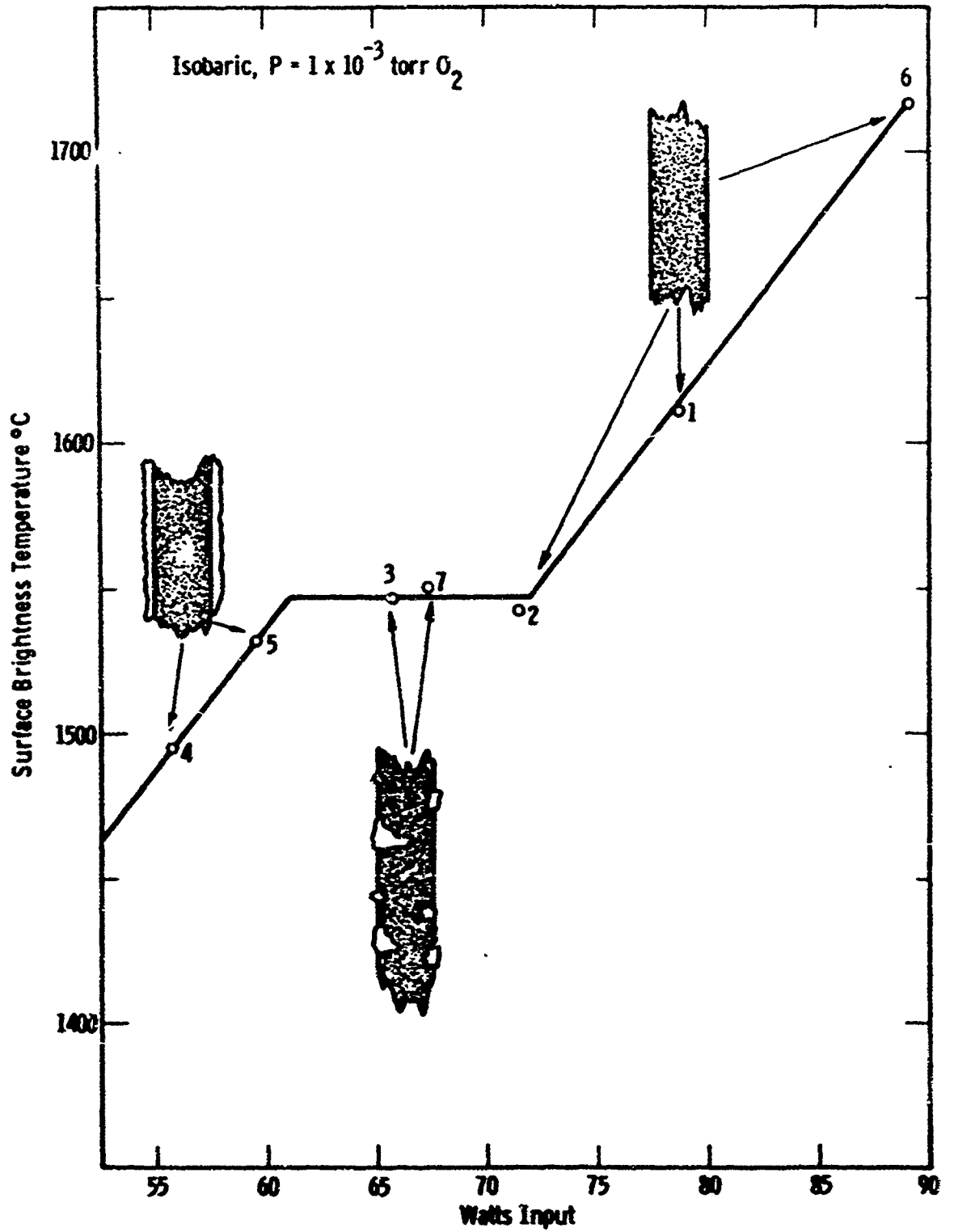
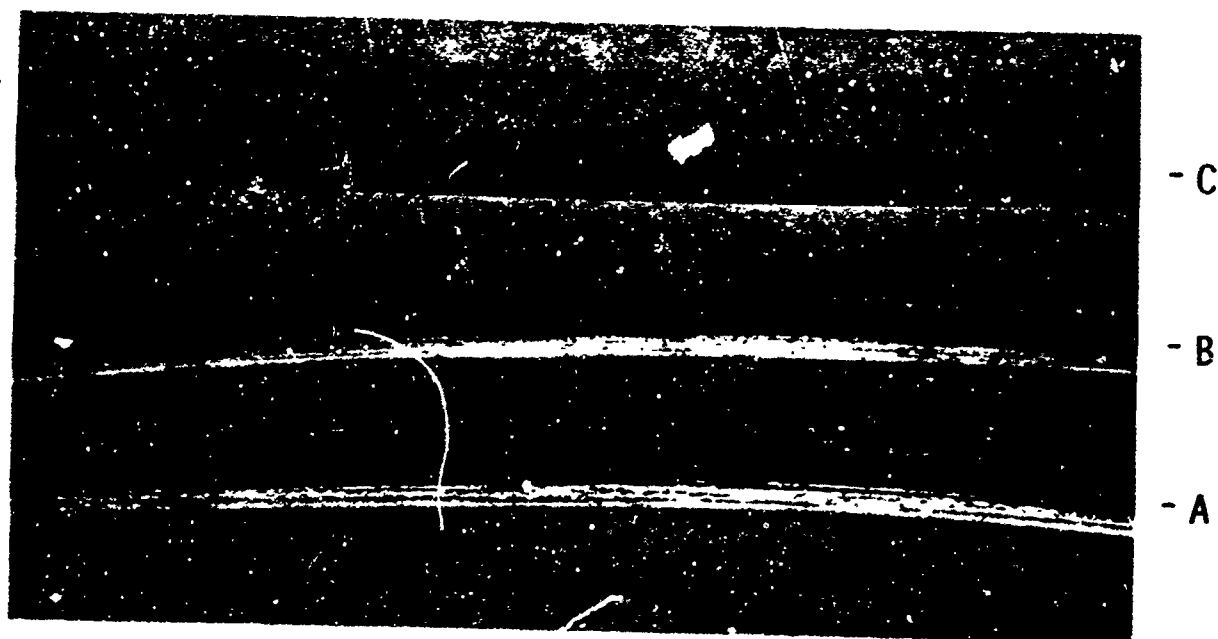


Fig. 13—Typical plot of watts input vs surface brightness temperature for columbium wire oxidized by the dynamic leak method with constant oxygen pressure



20X

Fig. 14—Oxidized specimens of zone-refined Cb wire using the dynamic leak method

- A - Oxidized 2 hrs 1500°C  $1 \times 10^{-5}$  torr  $O_2$  x-ray result, single phase  $Cb(O)$
- B - Oxidized 15 min 1725°C  $7 \times 10^{-4}$  torr  $O_2$   $Cb(O) + CbO$
- C - Oxidized 1 hr 1000°C  $5 \times 10^{-3}$  torr  $O_2$   $CbO_2 + CbO + Cb(O)$

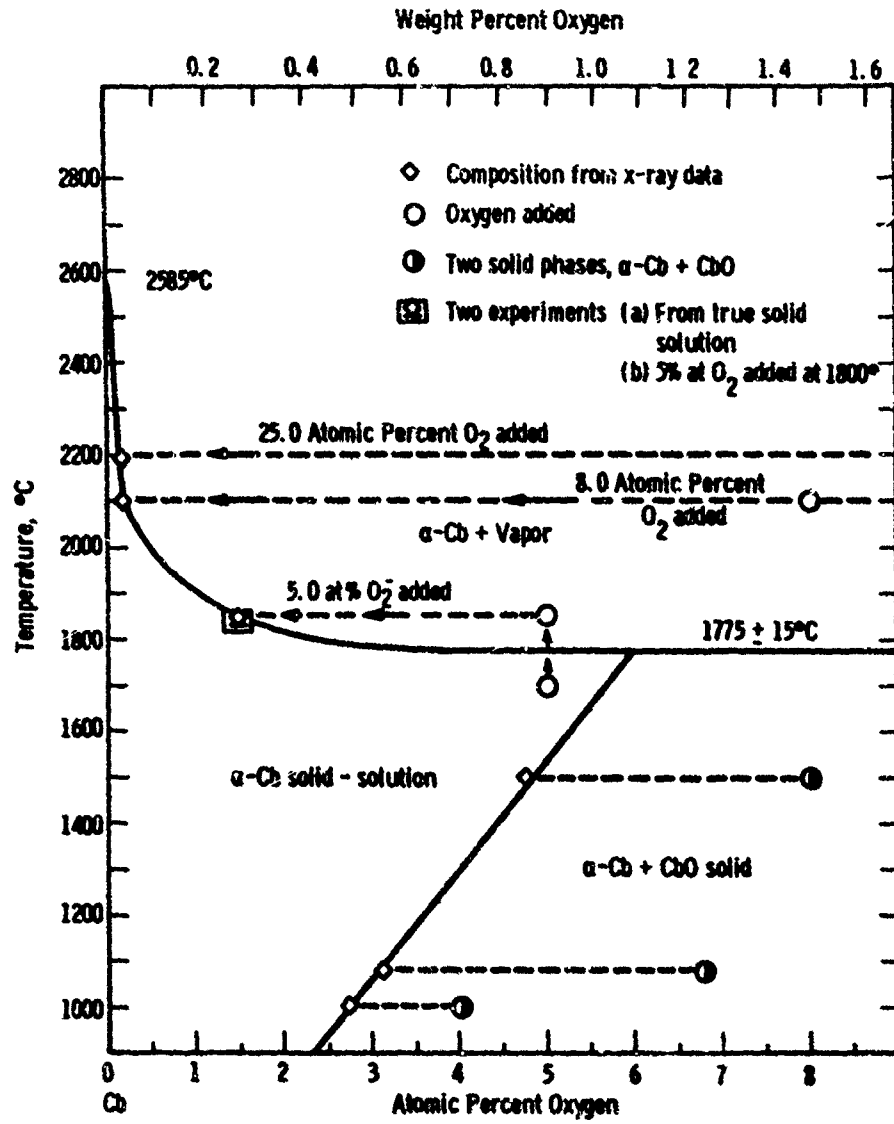


Fig. 15-Partial Cb-O system

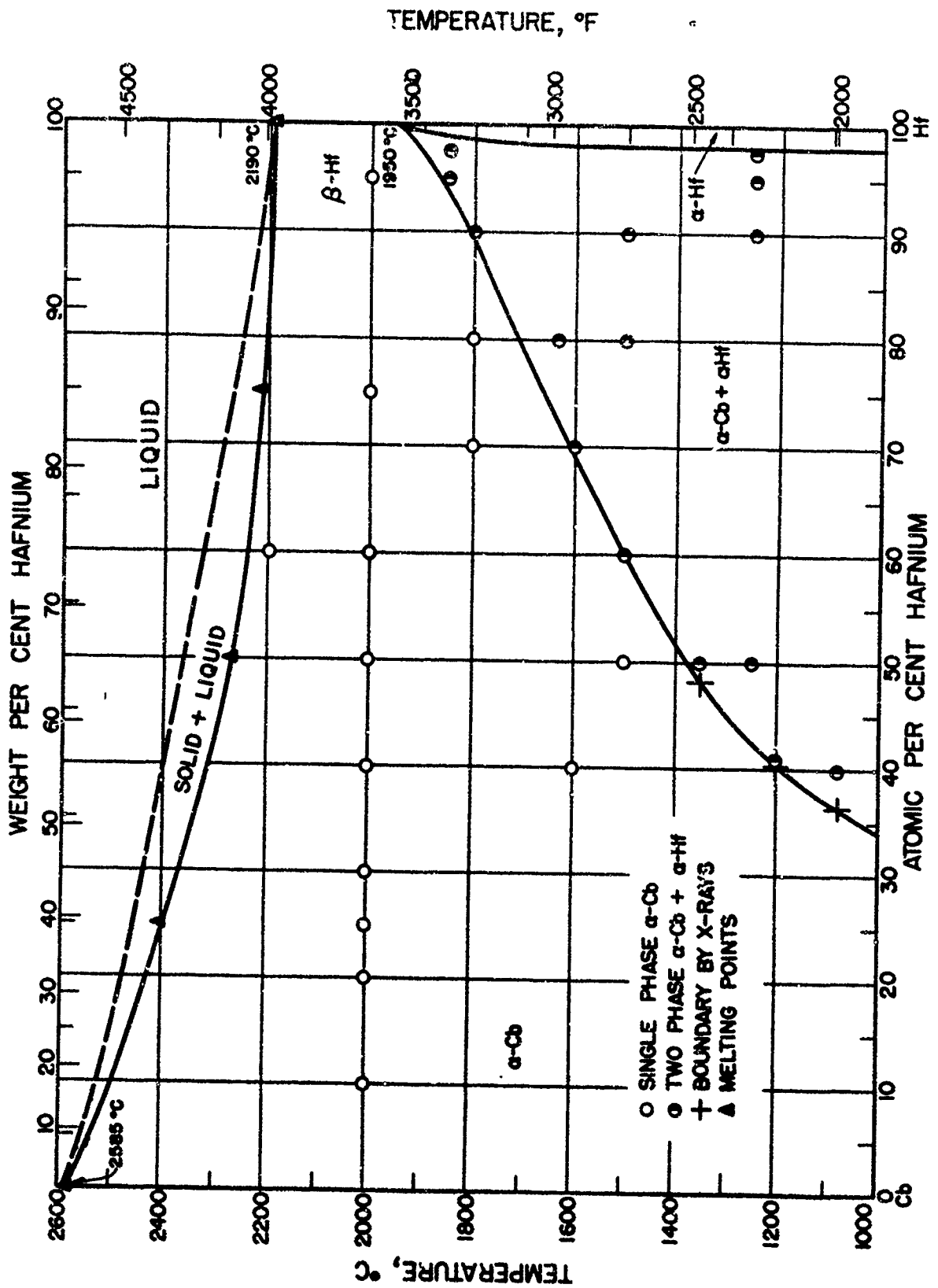


Fig. 16 - Tentative Cb-Hf constitution diagram (Taylor & Doyle (20))

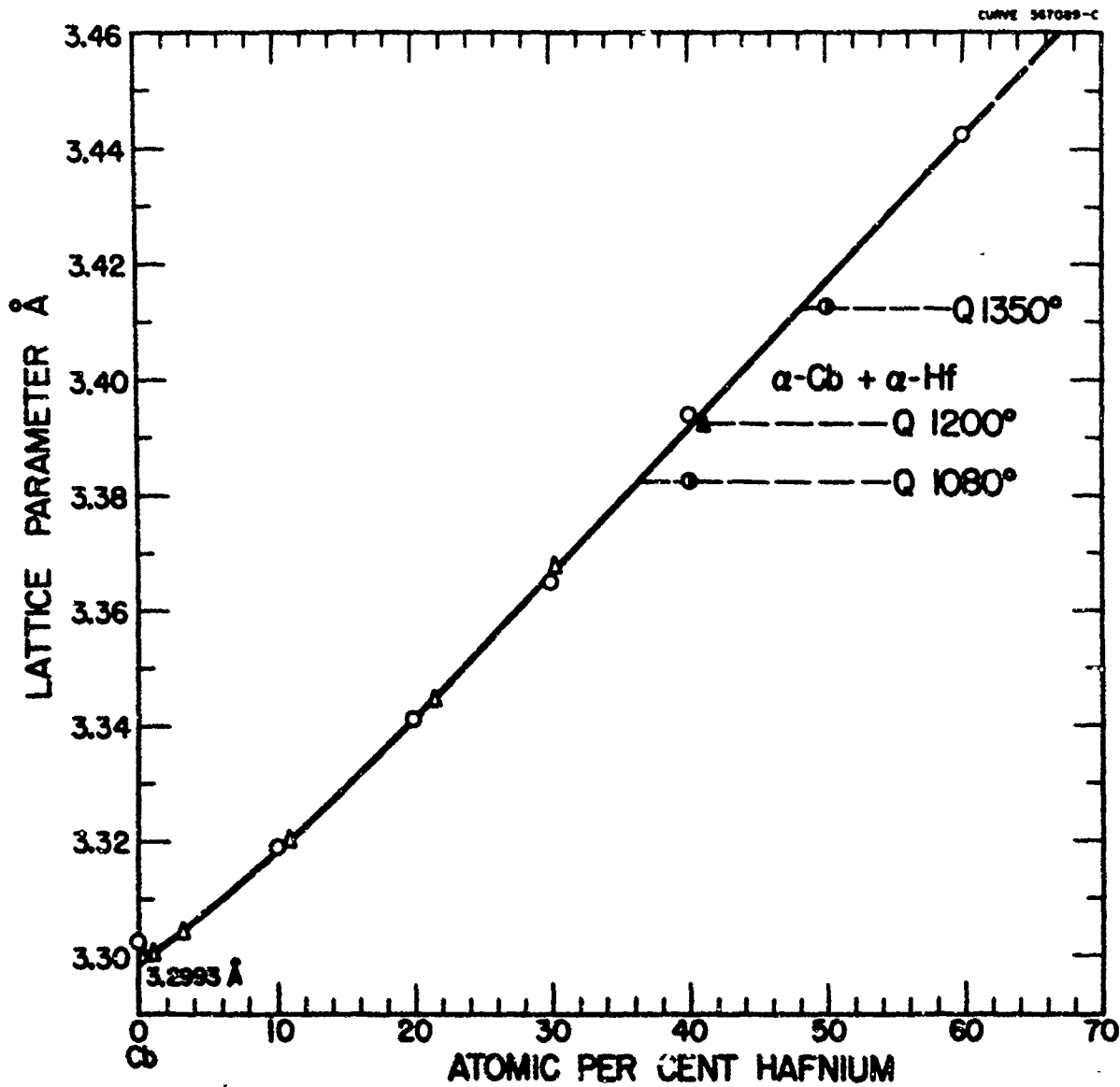


Fig.17 -Lattice parameters of  $\alpha$ -Cb, Cb-Hf alloys  
(Taylor & Doyle<sup>(20)</sup>)

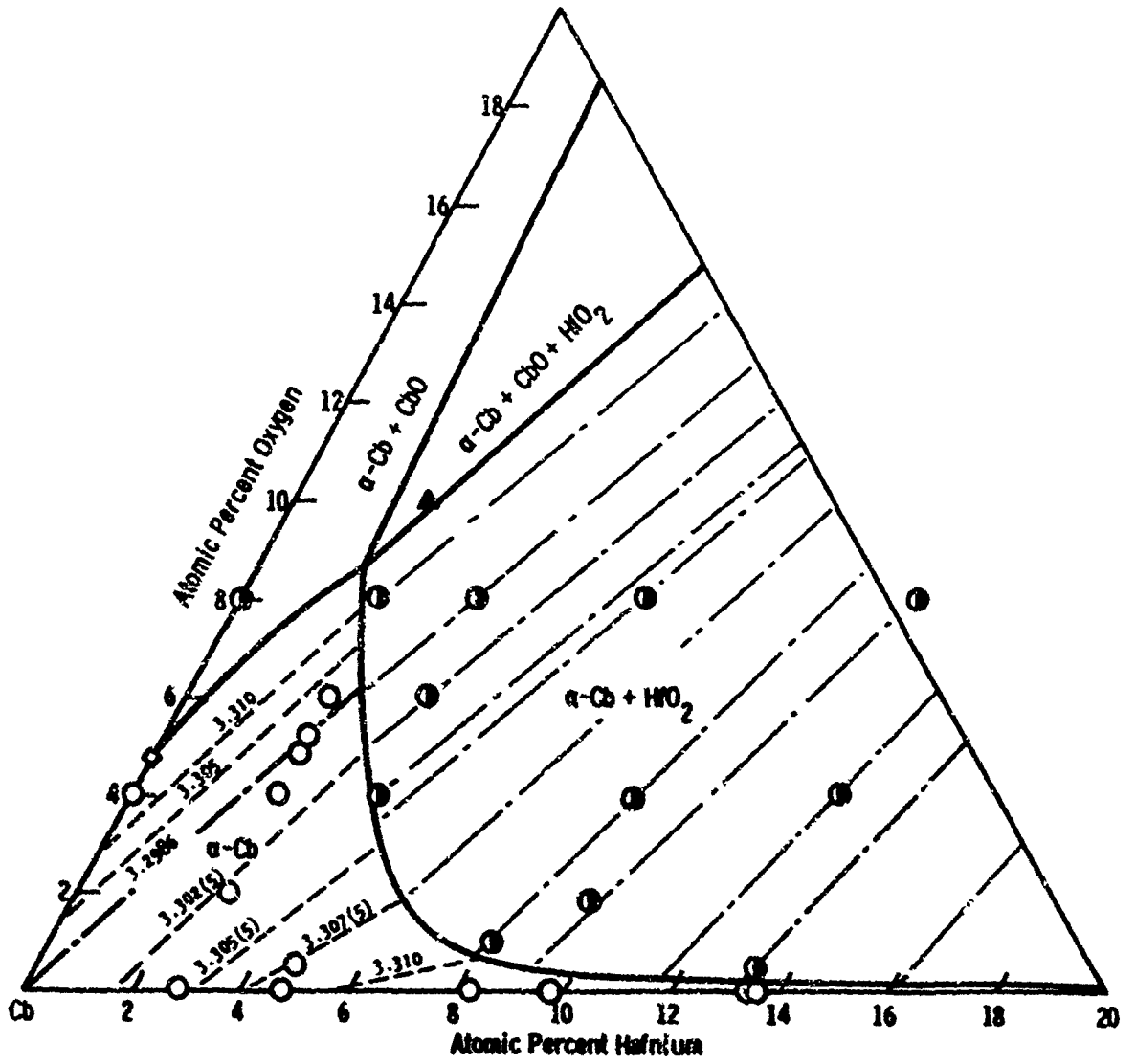


Fig. 18-Cb-14-O 1500°C isothermal

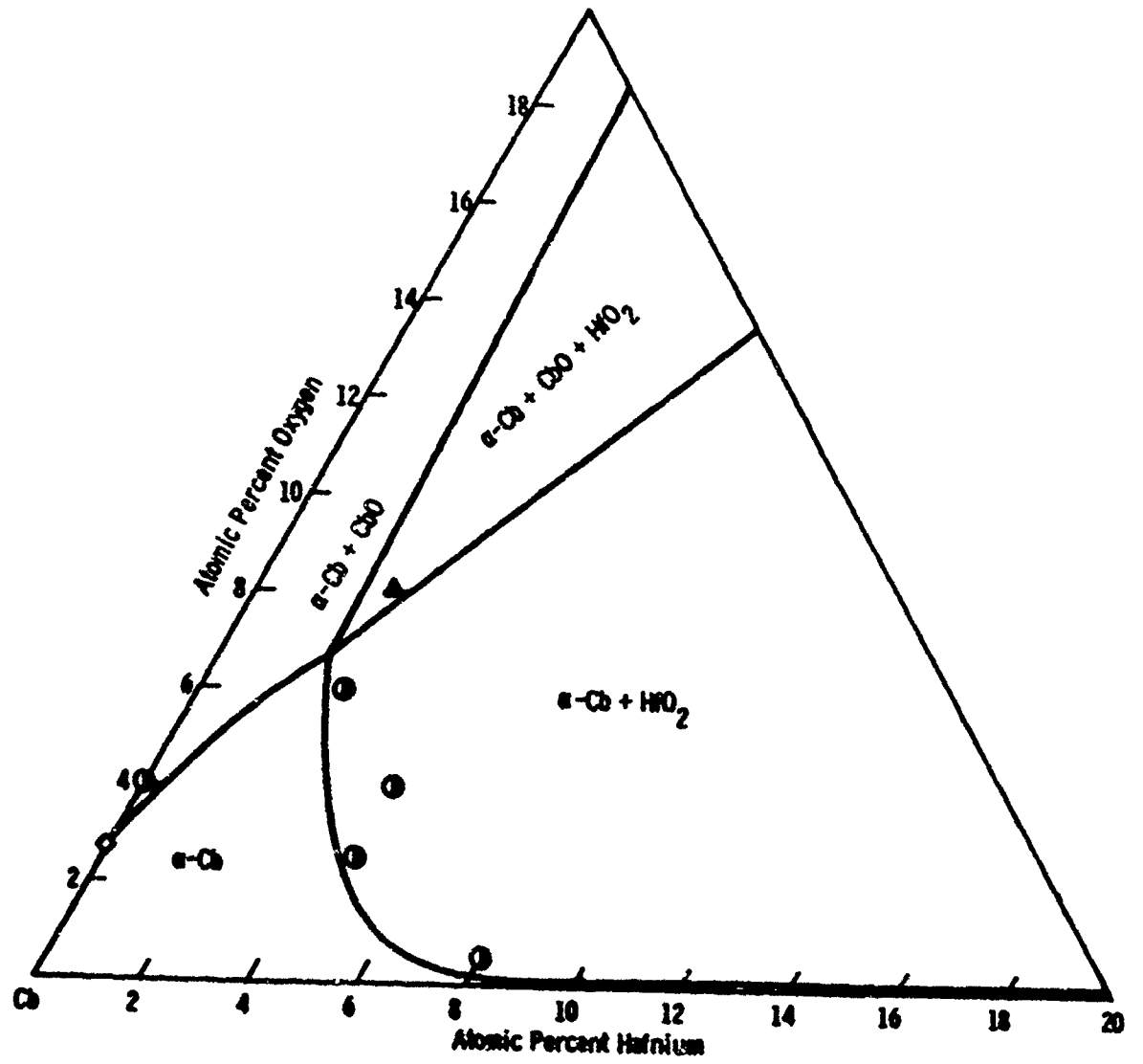


Fig. 19-Cb-Hf-O 1000°C isothermal

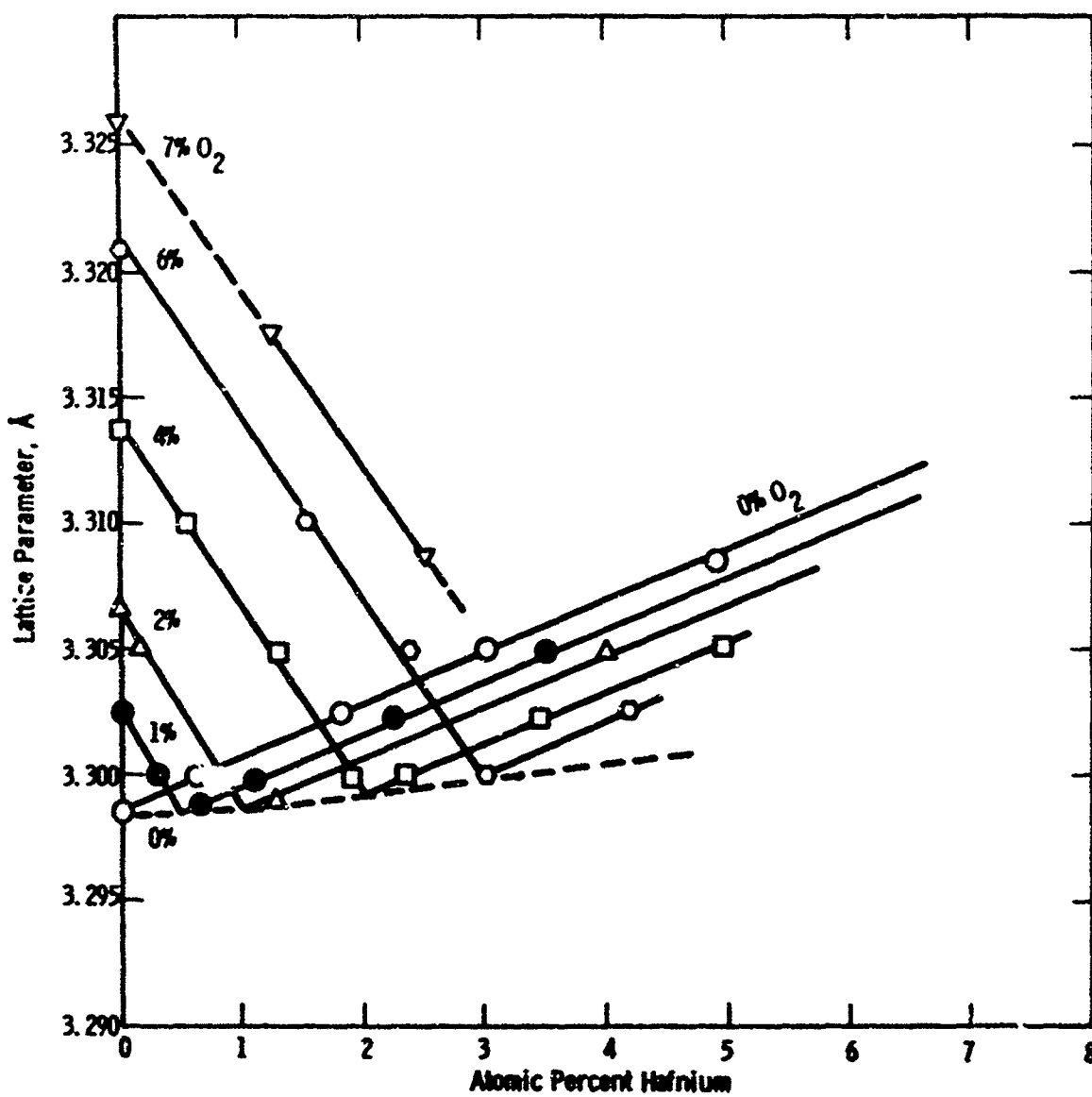


Fig. 20—Room temperature lattice parameters of Co-Hf  $\alpha$ -phase alloys containing 0, 1, 2, 4, 6 and 7 atomic percent oxygen and showing minima at a 2:1 oxygen to hafnium atomic ratio

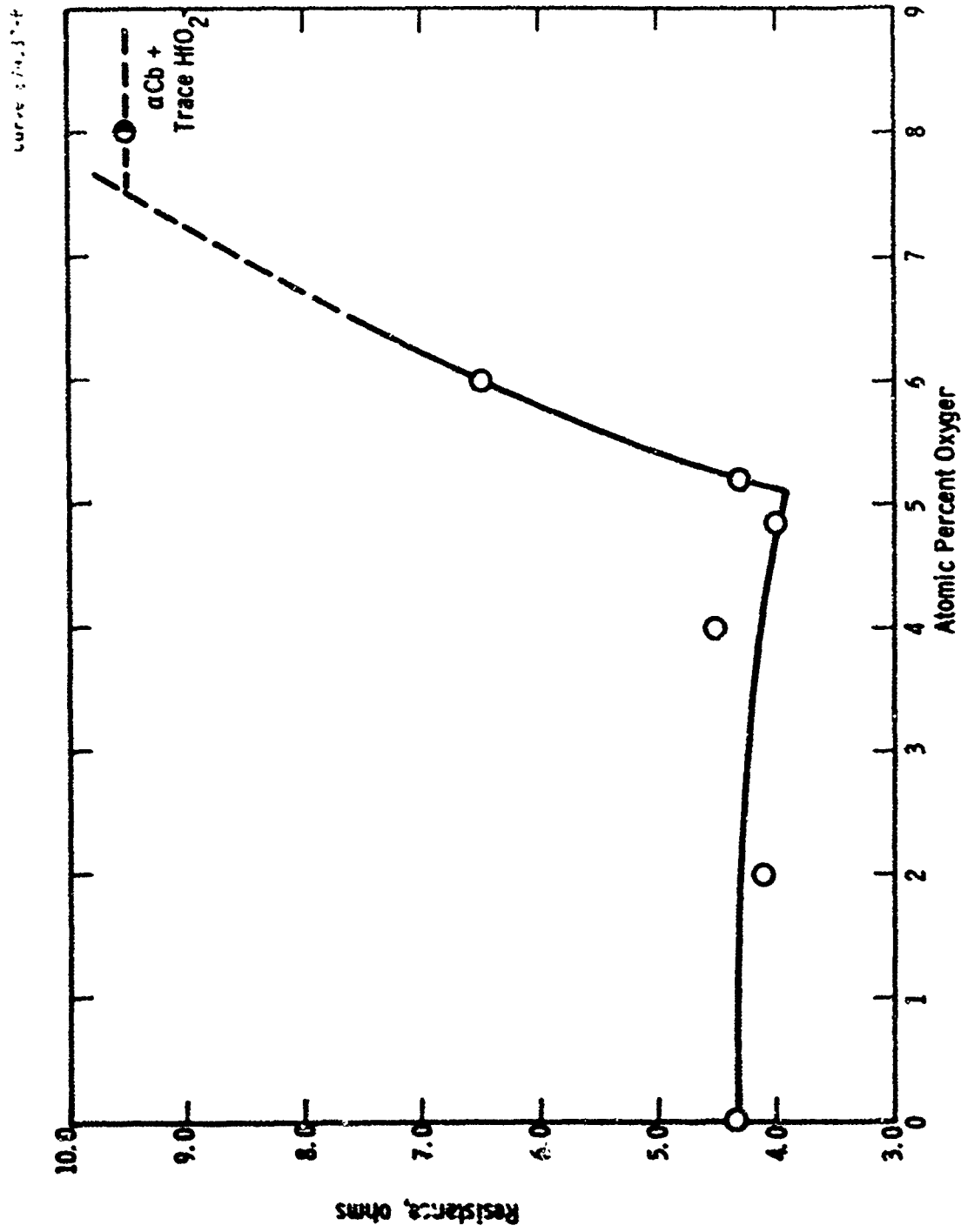
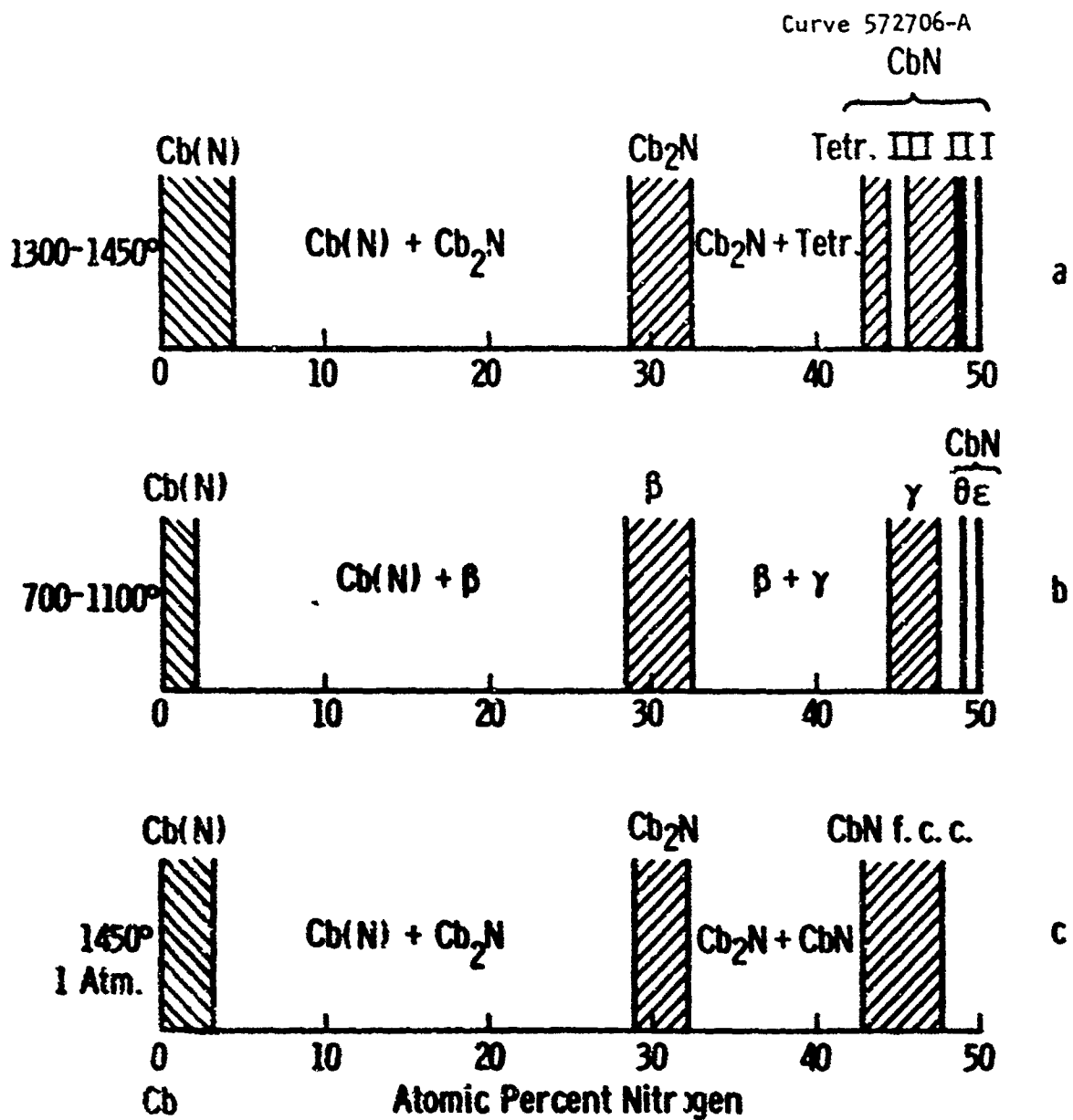


Fig. 21 -- Resistance of Hf/Cb = 2.8/97.2 (atomic) alloy, 10.2 mils diameter, 12' long at 1500°C



a. Brauer et. al b. Schönberg c. Elliott et. al.

Fig. 22—Phases in the CbN system

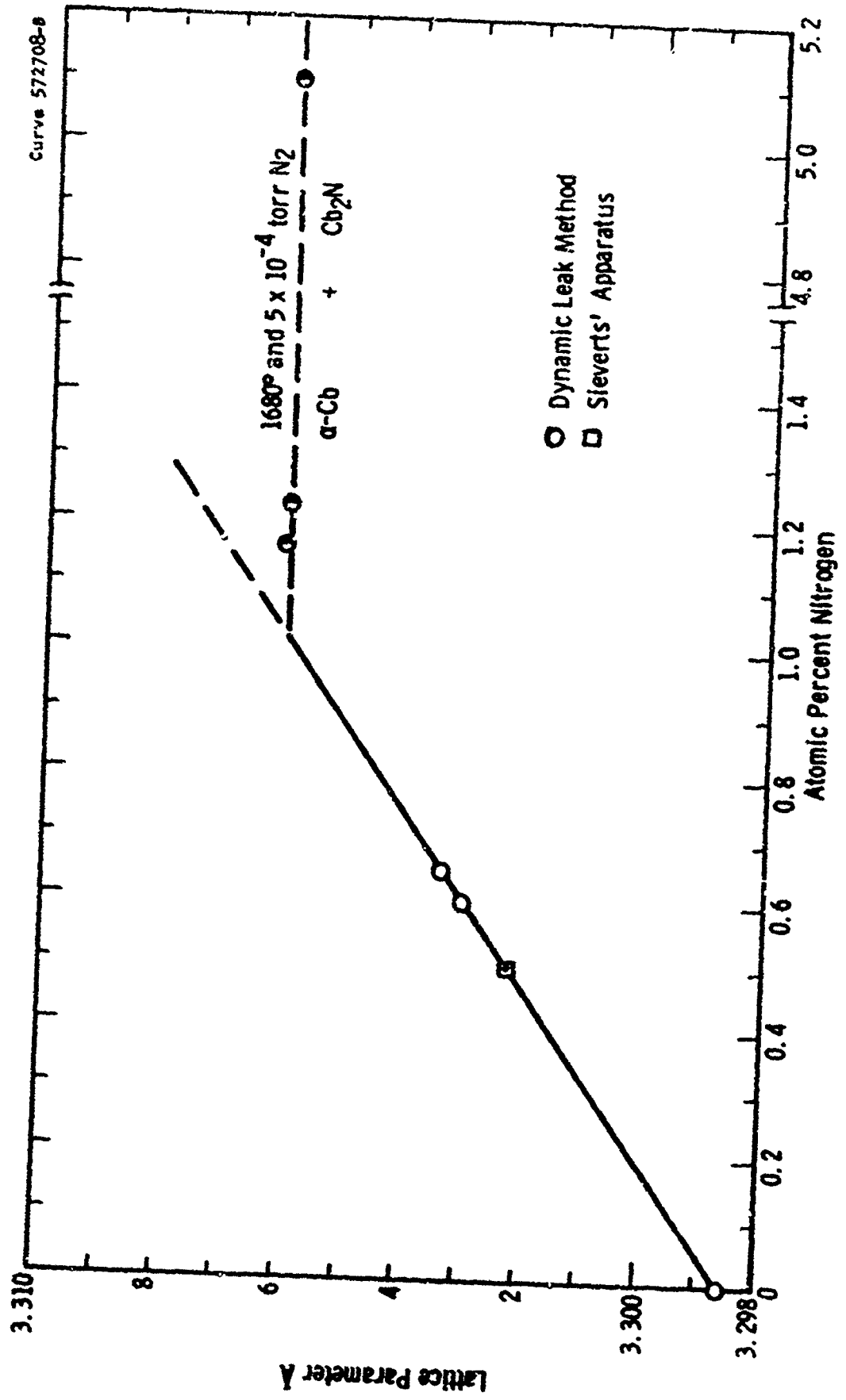


Fig. 23--Lattice parameters of Cb-N alloys

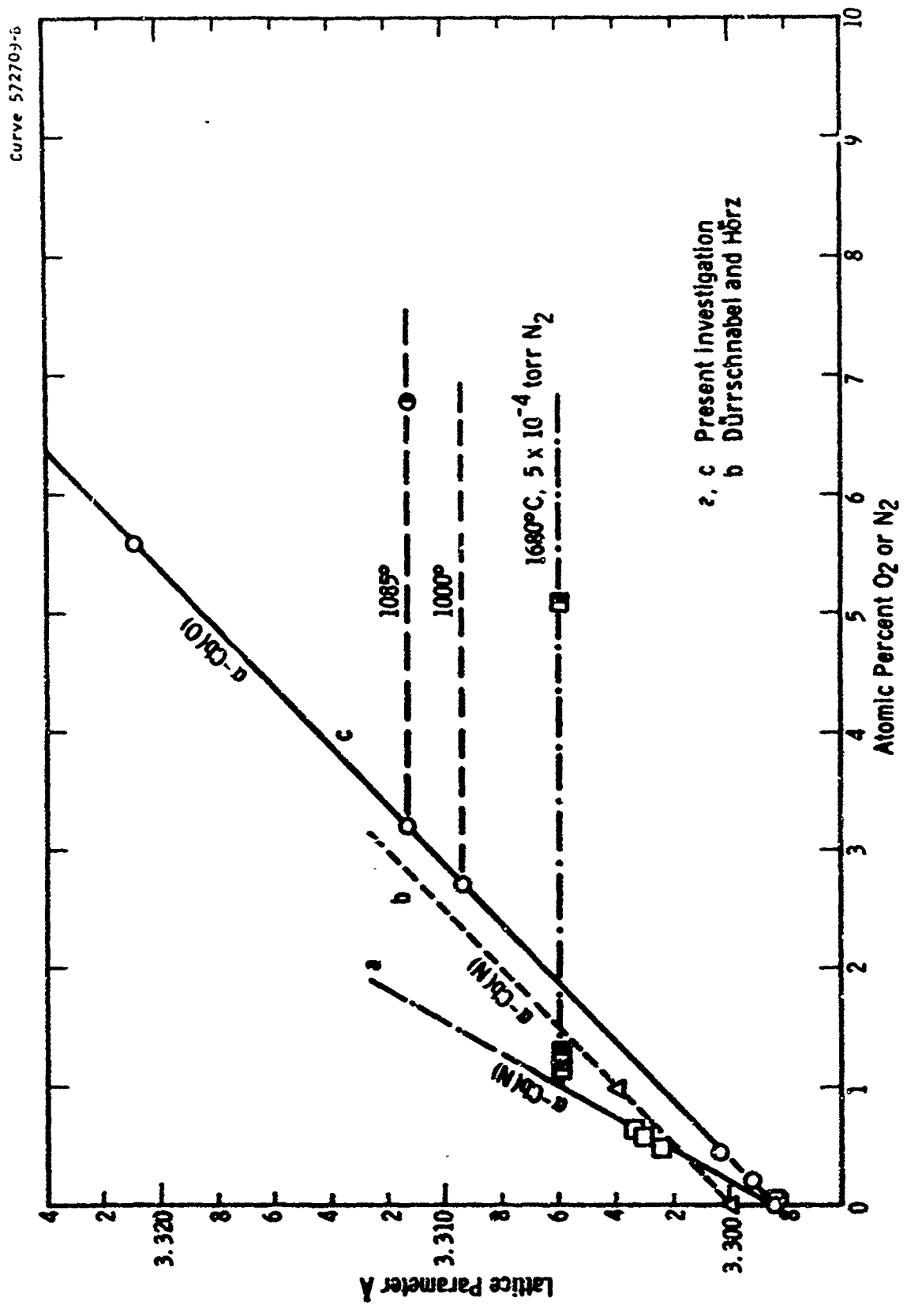


Fig. 24--Lattice parameter of  $\alpha$ -Cb-O and  $\alpha$ -Cb-N interstitial solid solutions

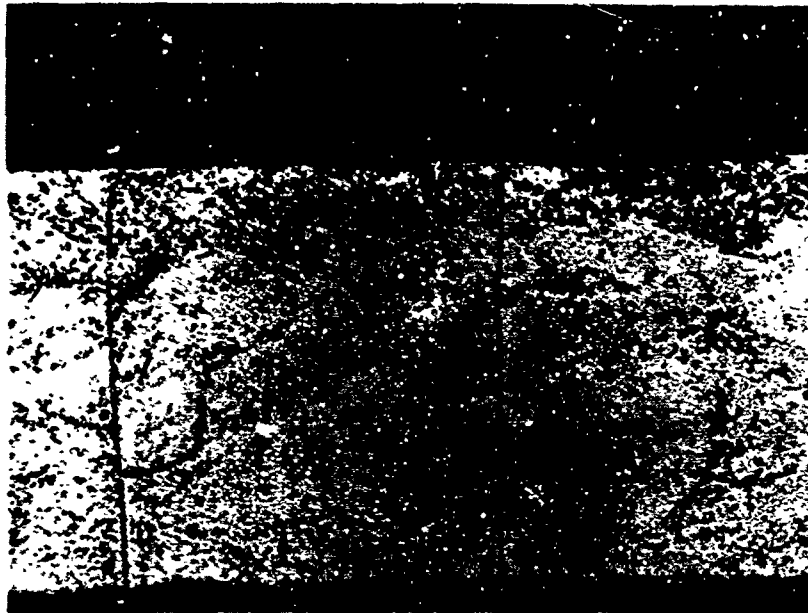


Fig. 25 - Longitudinal section of 11 mil Columbian wire  
nitrided for 10 min at 1680 °C and  $5 \times 10^{-4}$  torr  $N_2$  200X  
1.75 at %  $N_2$  0.09 at %  $O_2$

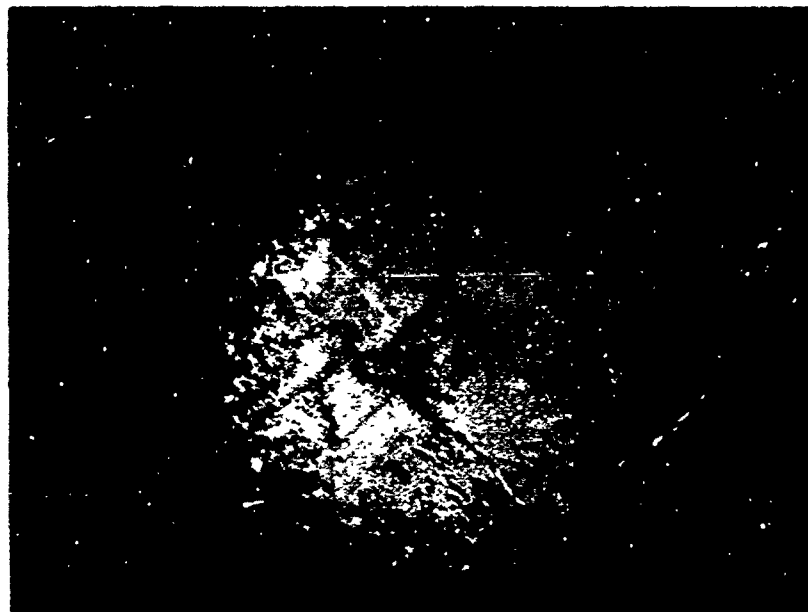


Fig. 26 - Transverse section of 11 mil Columbian wire  
nitrided for 10 min at 1680 °C and  $5 \times 10^{-4}$  torr  $N_2$  200X  
1.75 at %  $N_2$  0.09 at %  $O_2$

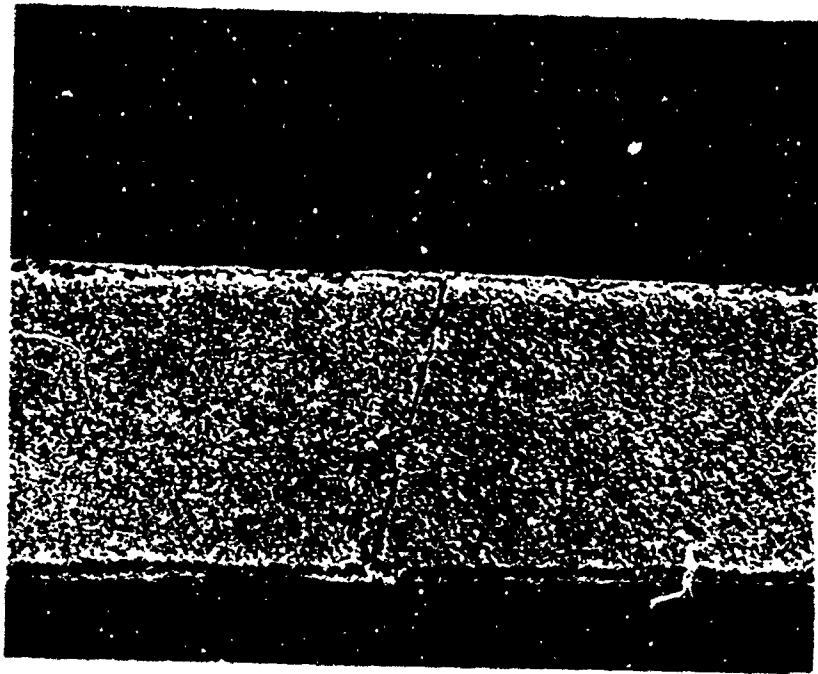


Fig. 27 -Longitudinal section of 11 mil Columbian wire  
nitrided 10 min at 1680 °C and  $5 \times 10^{-3}$  torr  $N_2$  200X  
5.10 at %  $N_2$  0.09 at %  $O_2$

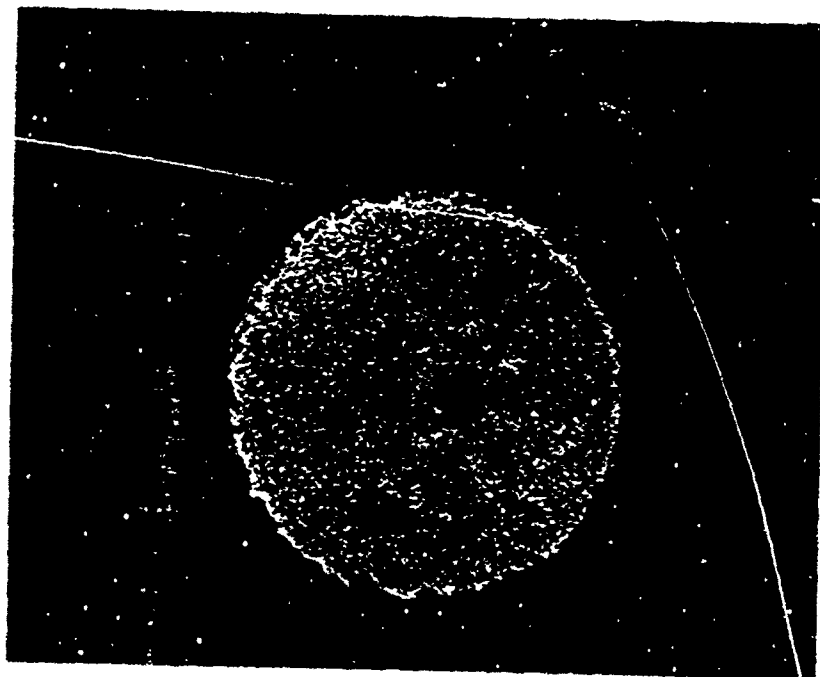


Fig. 28 -Transverse section of 11 mil Columbian wire  
nitrided 10 min at 1680 °C and  $5 \times 10^{-3}$  torr  $N_2$  200X  
5.10 at %  $N_2$  0.09 at %  $O_2$

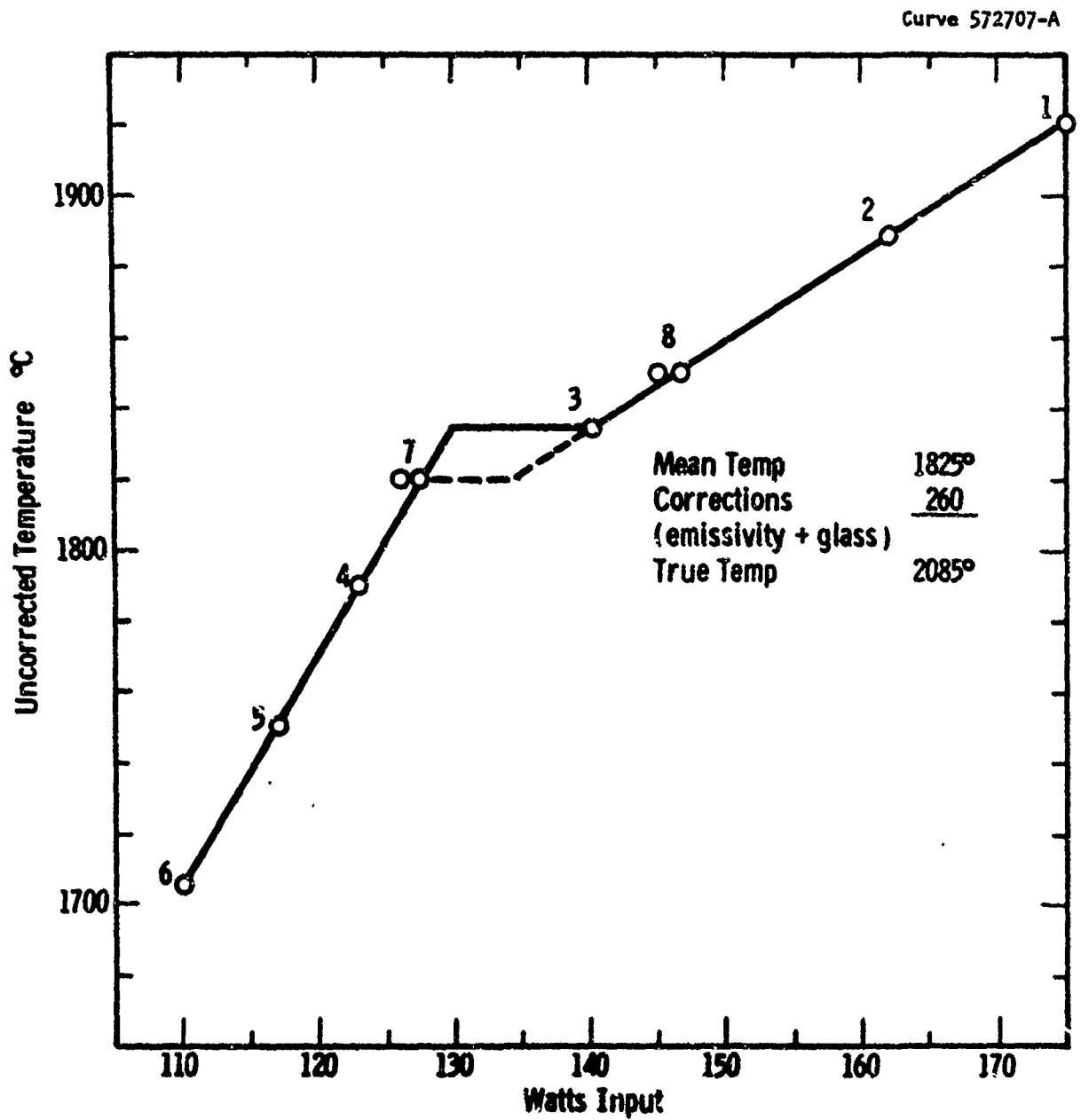


Fig. 29—Temperature vs watts Input during isobaric nitriding of Cb wire at 1.1 Torr  $N_2$

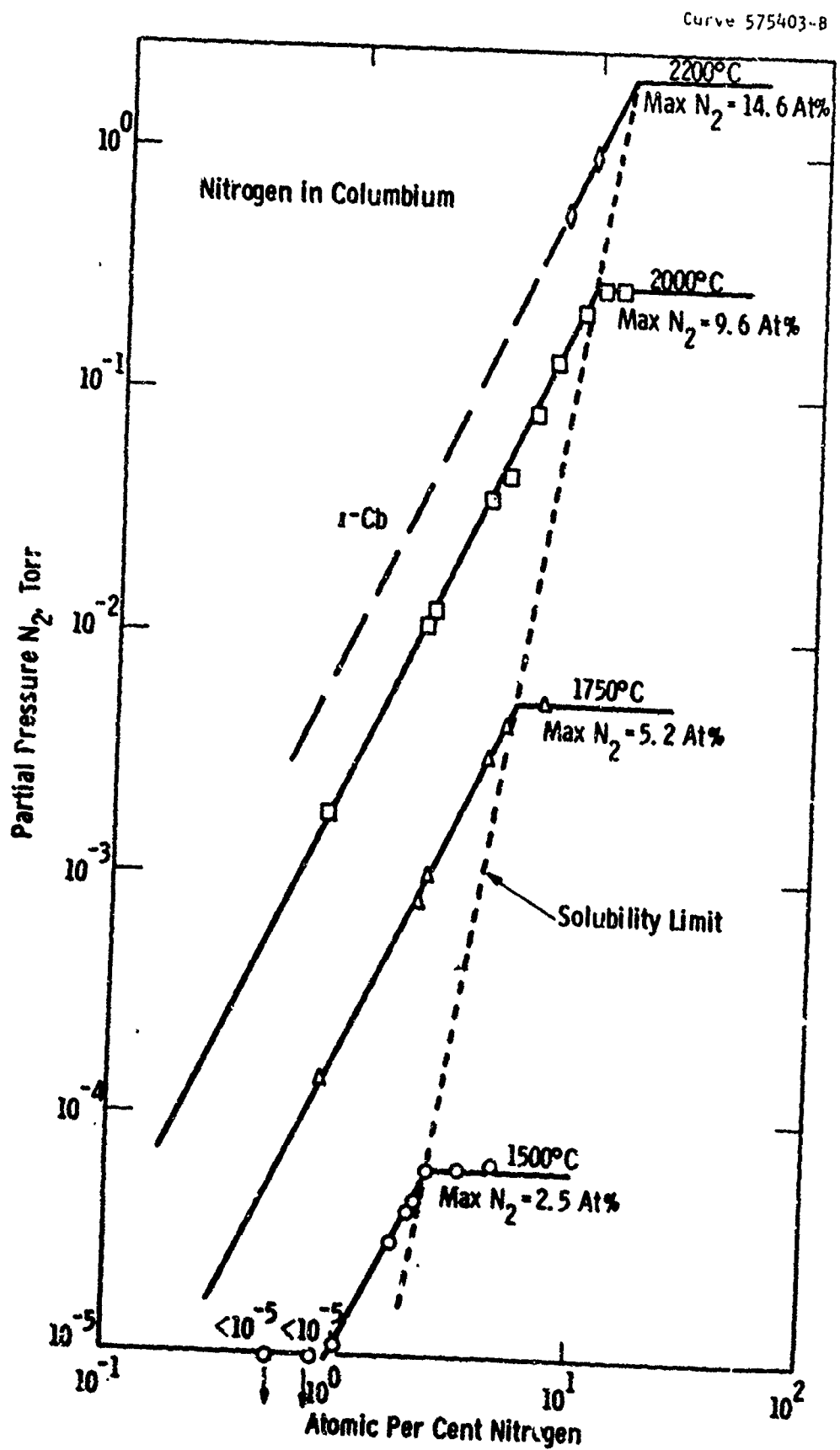


Fig. 30—Isothermal equilibrium for the  $\alpha$ -Cb-N terminal solid-solution

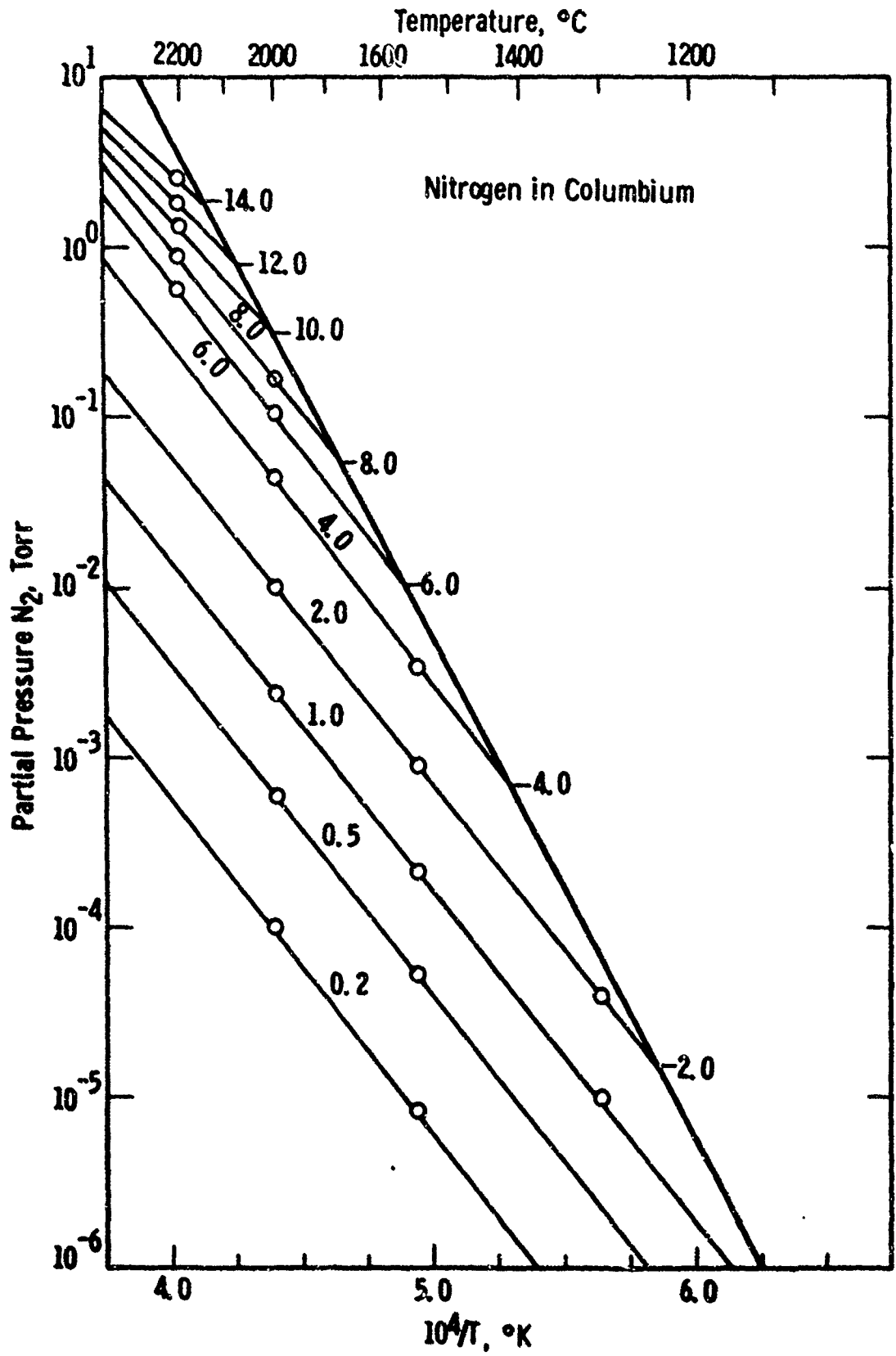


Fig. 31—Constant composition equilibrium for the  $\alpha$ -Cb-N terminal solid-solution

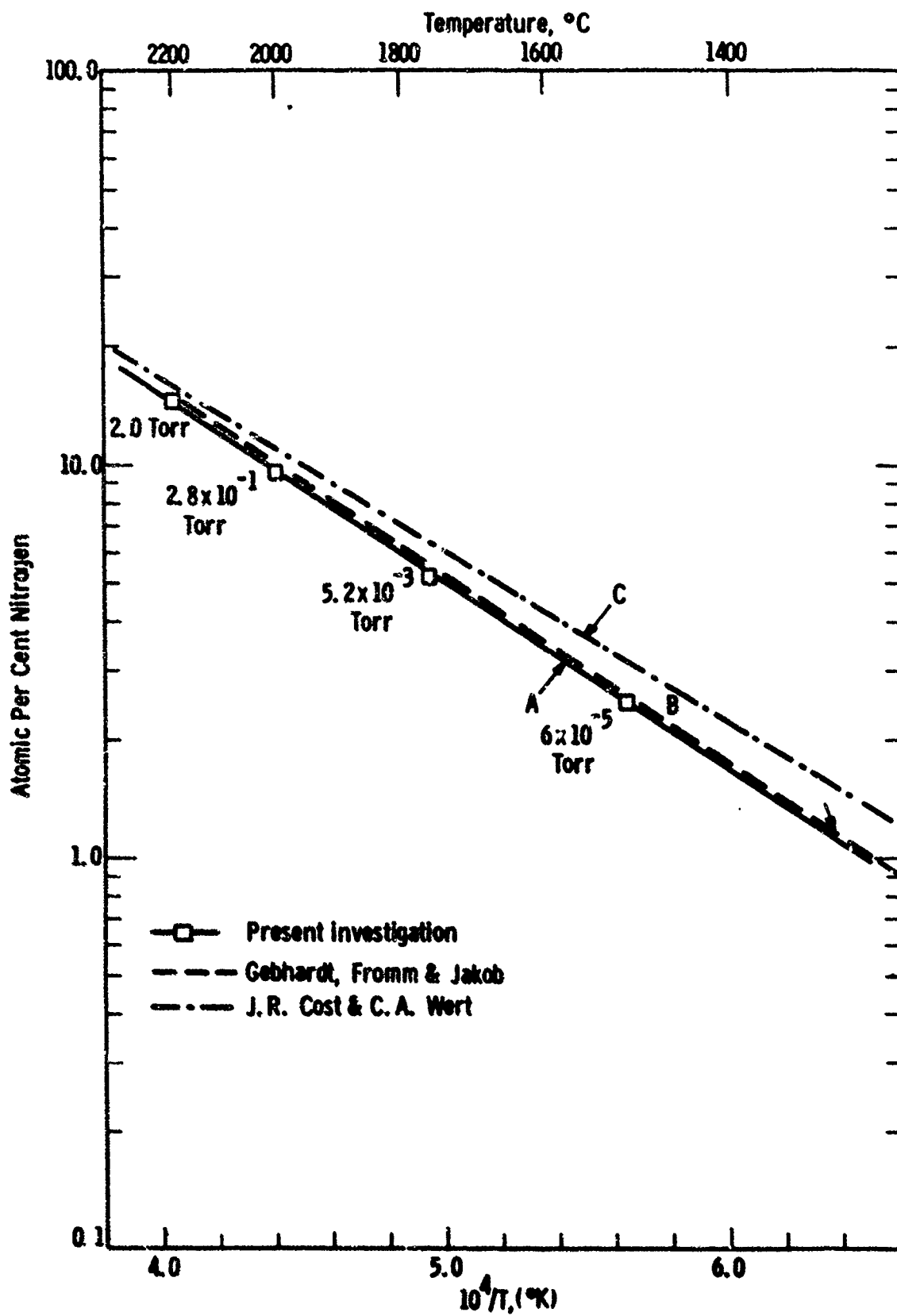


Fig. 32—Maximum solubility of Nitrogen in Columbium

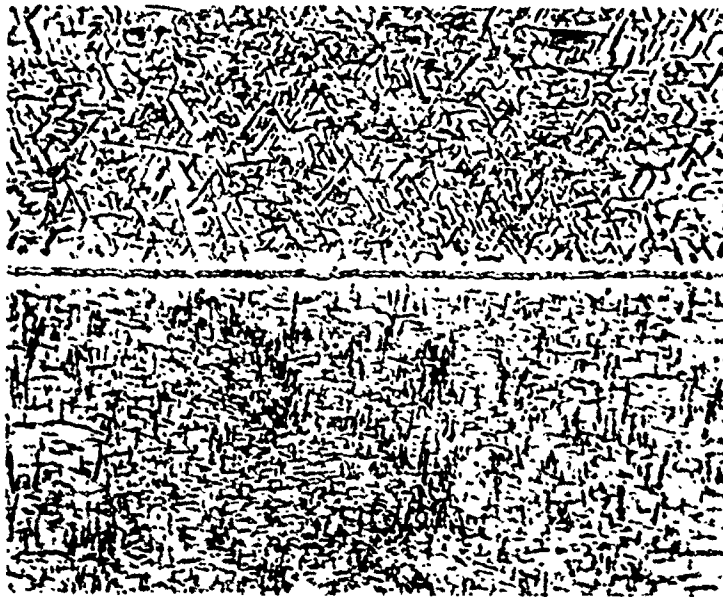


Fig. 33— $\alpha$ -Cb + 9.48 atomic %  $N_2$ , Q 2200° C.  
14.3 Mil wire.  $\alpha$ -Cb + ppt.  $Cb_2N$   
Longitudinal section. X500



Fig. 34— $\alpha$ -Cb + 2.04 atomic %  $N_2$ , Q 2200° C.  
14.3 Mil wire.  $\alpha$ -Cb + ppt.  $Cb_2N$ .  
Transverse section. X500

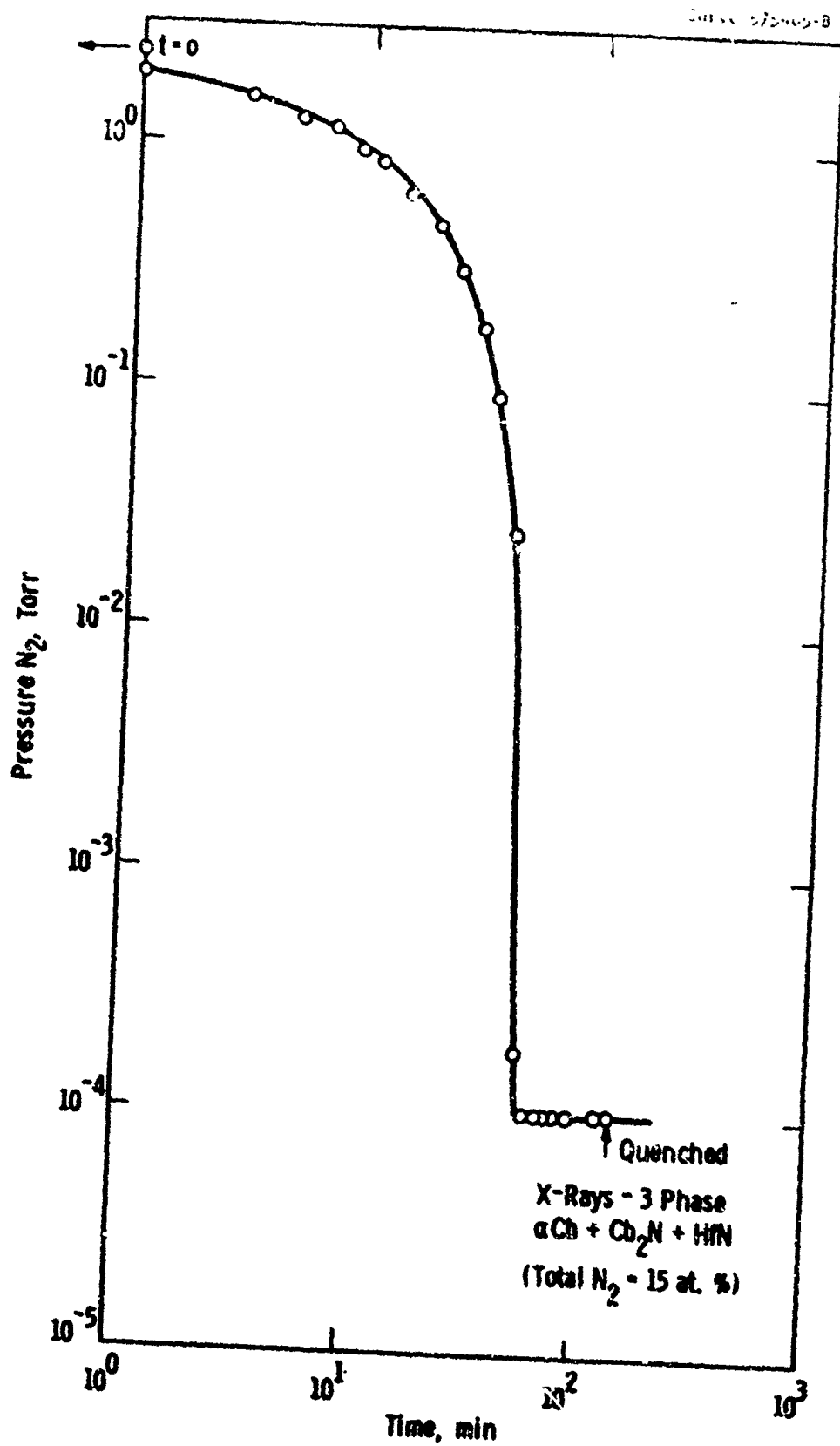
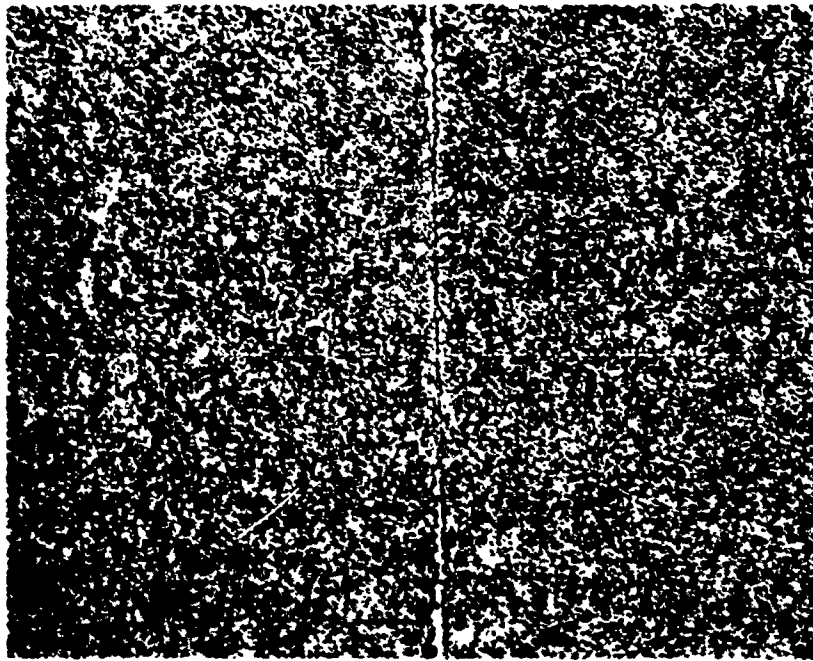


Fig. 35—Variation in N<sub>2</sub> pressure on nitriding  $\text{Cb}_{90.4}\text{Hf}_{9.6}$  wire at 1500°C



X500

Fig. 36—90.4 Cb, 9.6 Hf + 15 atomic % N<sub>2</sub>.  
3 Hours at 1500° C and quenched.  
 $\alpha$ -Cb + Cb<sub>2</sub>N + HfN. 11 Mil wire.

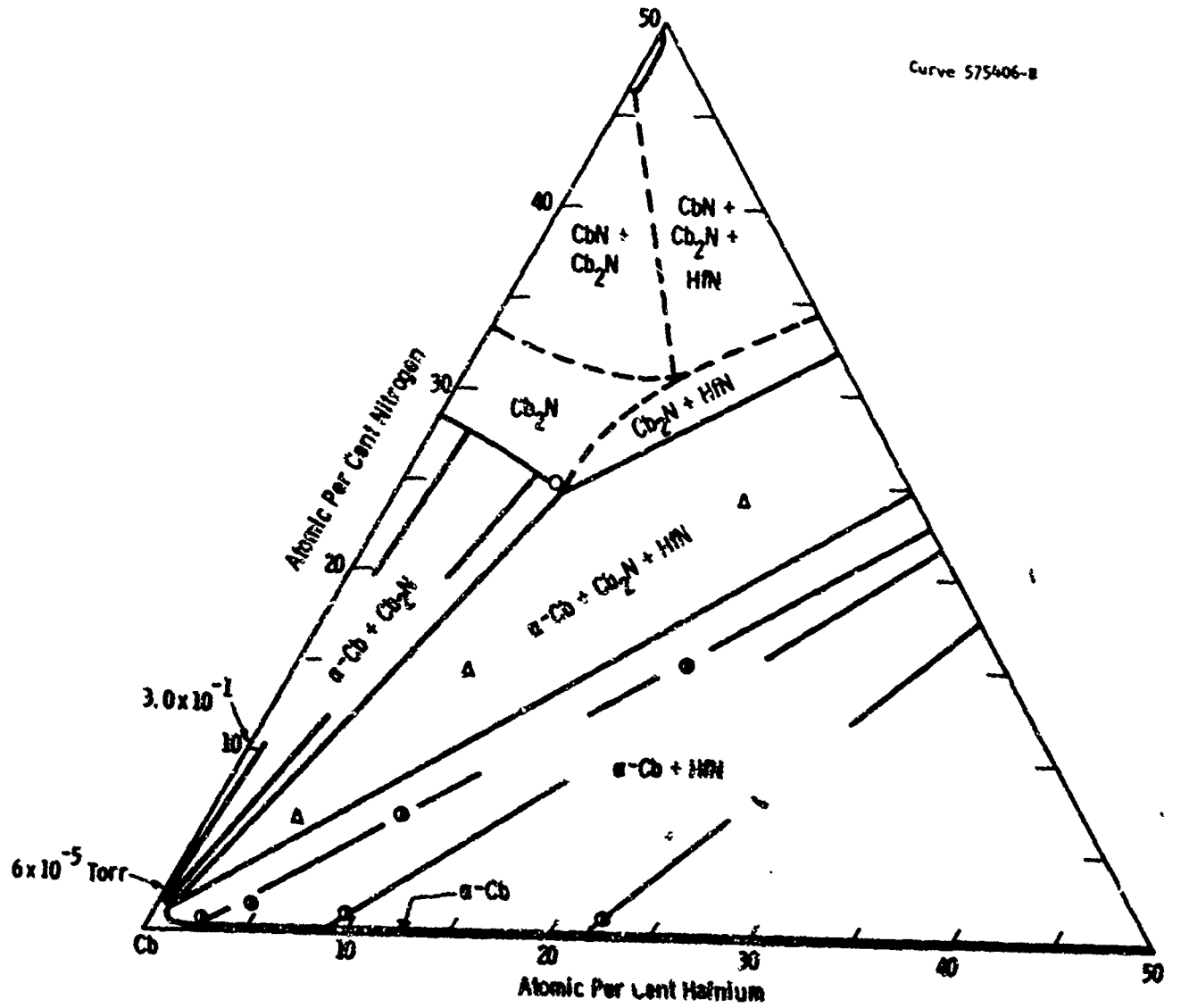


Fig. 37—Tentative Co-Hf-N equilibrium diagram. 1500°C Isothermal

Curve 572742-A

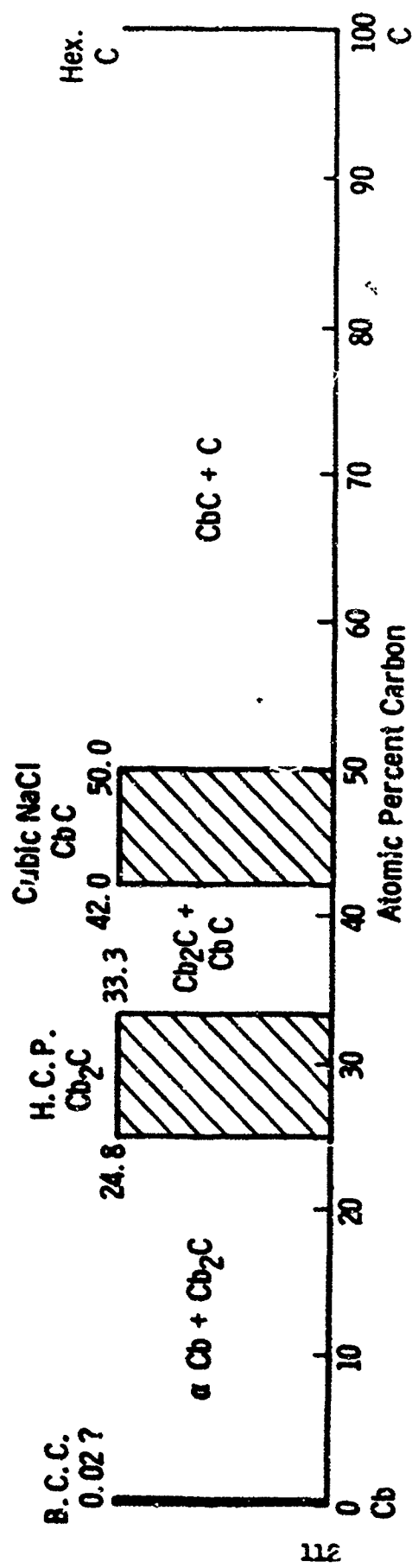


Fig. 38 - Phase-fields in the system Cb-C, (1600-1700°C). (G. Brauer et. al. (33))



Fig. 39 - 5.0 at % C, Cb-C alloy, L. A. 24 hrs 1600°C  
in  $1 \times 10^{-6}$  torr and quenched 200X



Fig. 40 - 1.0 at % C, Cb-C alloy, L. A. 20 hrs 1600°C  
in  $1 \times 10^{-6}$  torr and quenched 200X

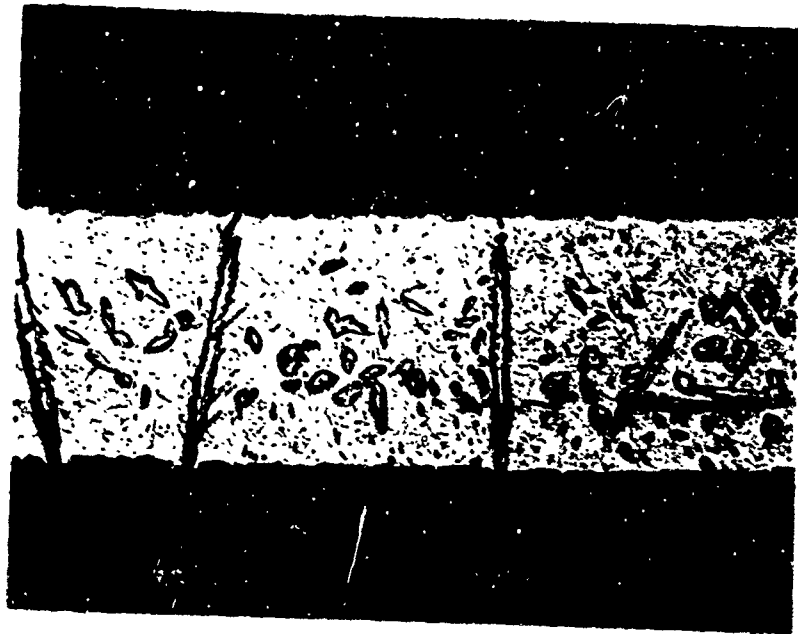


Fig. 41-11 Mil. dia., "Aquadag" coated, zone refined columbium wire after heating for 16 hrs  $\sim 1700^{\circ}\text{C}$  in  $1 \times 10^{-6}$  torr and quenching 200X

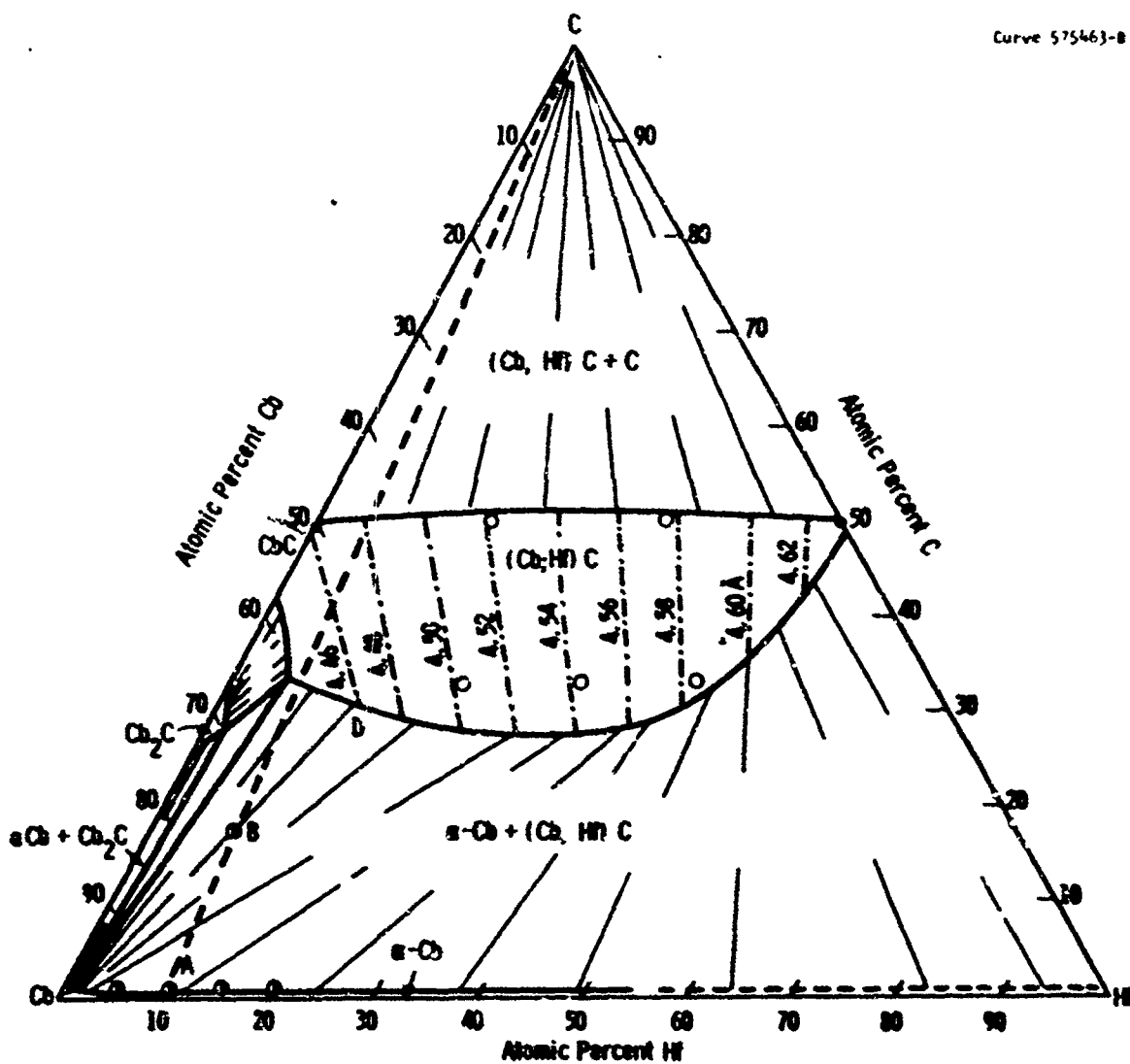


Fig. 42-Tentative Co-Hf-C phase diagram. 2000°C isothermal

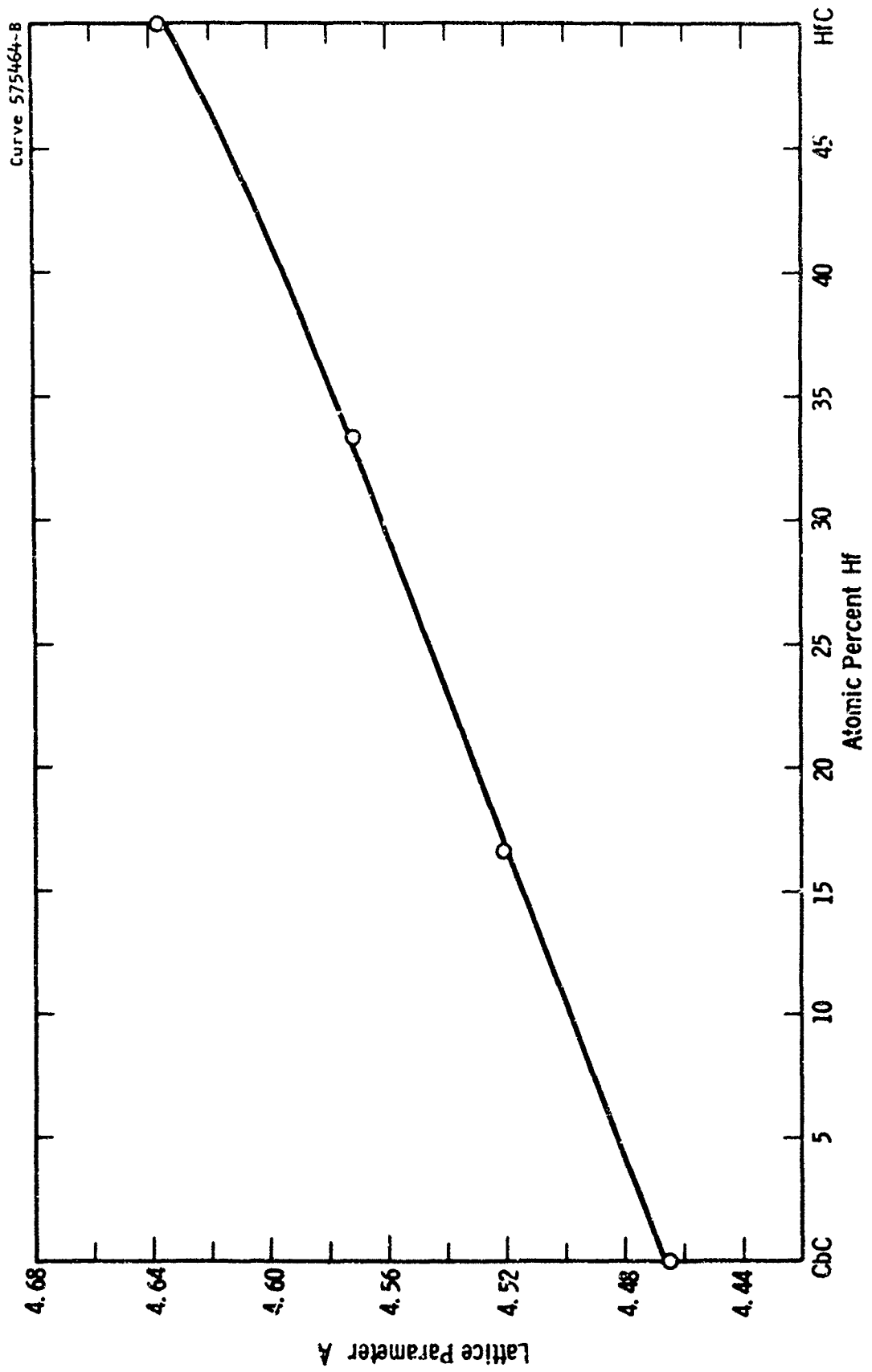


Fig. 43—Lattice parameters of CbC-HfC alloys

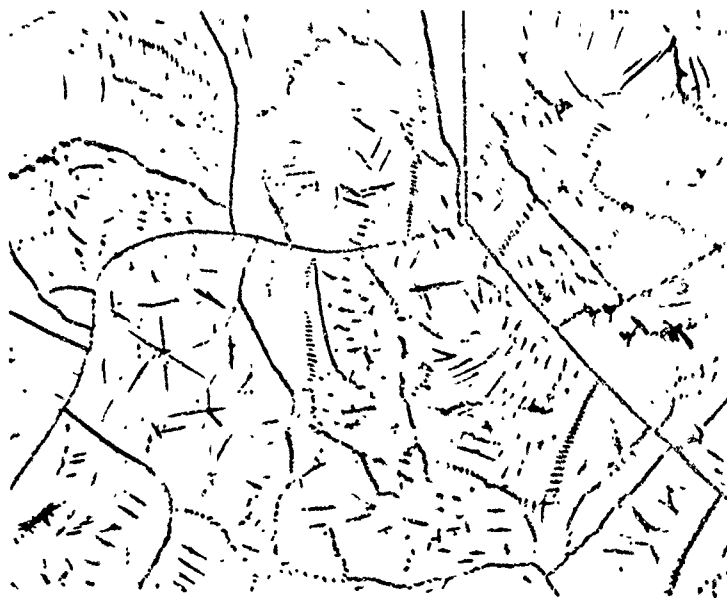


Fig. 44—Photomicrograph of 94Cb 5Hf 1C, 24 hrs at 2000°C and quenched.  $\alpha$ Cb + (Cb, Hf) C 200X

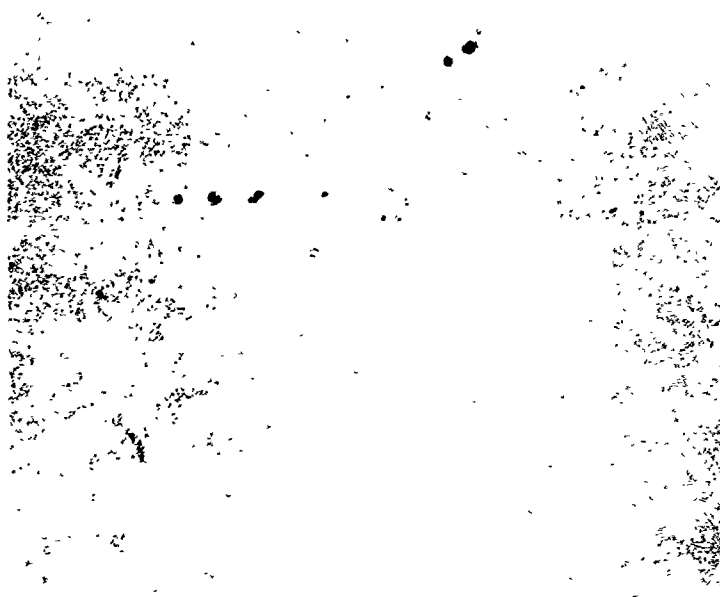


Fig. 45—Photomicrograph of 94Cb 5Hf 1C, 10 min at 2200°C and quenched.  $\alpha$ Cb + (Cb, Hf) C 200X

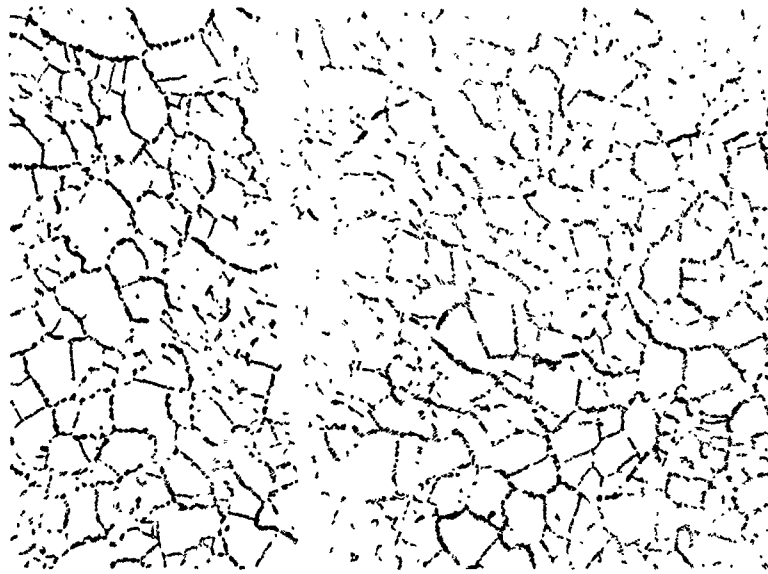


Fig. 46—Photomicrograph of 89Cb 10Hf 1C, 24 hrs at 2000°C and quenched.  $\alpha$ Cb + (Cb, Hf) C 200X



Fig. 47—Photomicrograph of 89Cb 10Hf 1C, after coating with "Aquadag" and annealing 2 hrs at 2000°C and quenching.  $\alpha$ Cb + (Cb, Hf) C 200X

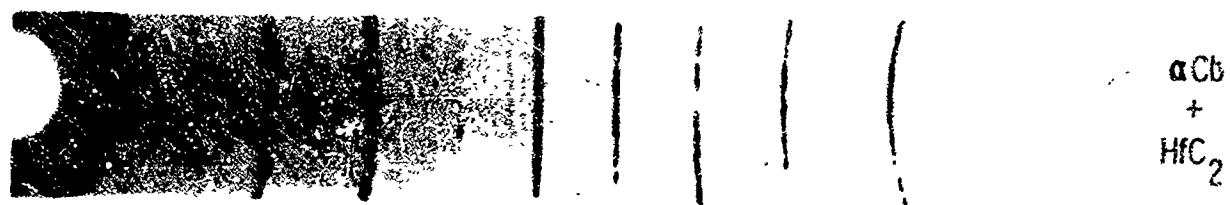
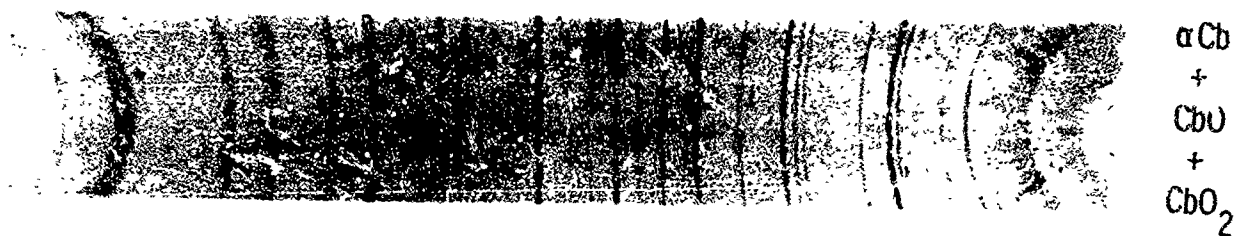
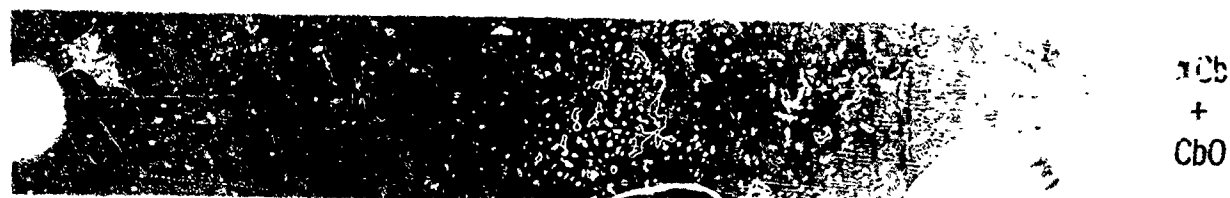
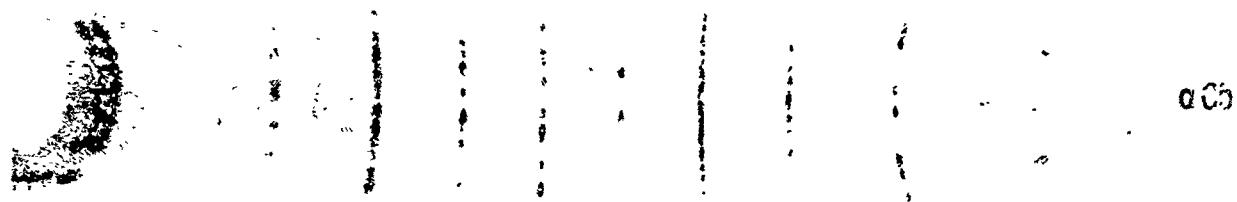


Fig. 48a —Typical Debye-Scherrer patterns of  
Cb-Hf (O, N, C) alloys

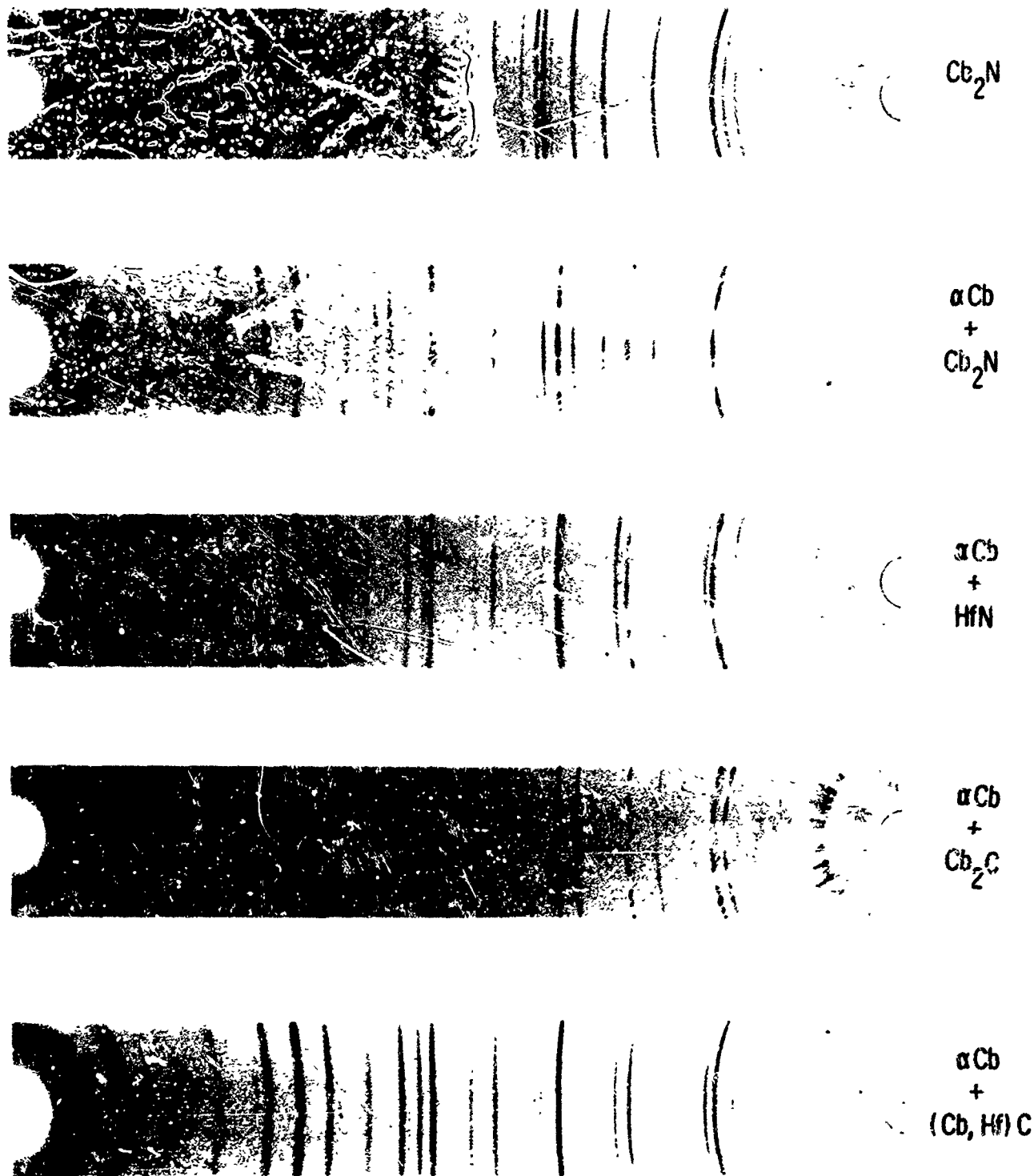


Fig. 48b —Typical Debye-Scherrer patterns of Cb-Hf-(O, N, C) alloys

Unclassified

Security Classification

DOCUMENT CONTROL DATA - R&D		
<i>(Security classification of this body of abstract and tracking annotation must be entered when the overall report is classified)</i>		
1. ORIGINATING ACTIVITY (Corporate or other)	2a. REPORT SECURITY CLASSIFICATION	
Westinghouse Research Laboratories Pittsburgh, Pennsylvania, 15235	Unclassified	
	2b. GROUP	
	None	
3. REPORT TITLE		
I) Research for Solubility of Interstitials in Columbium II. A Study of Columbium-Rich Alloys in the Ternary Systems Cb-Hf-O, Cb-Hf-N, and Cb-Hf-C		
4. DESCRIPTIVE NOTES (Type of report and inclusive dates)		
Summary Technical Report		
5. AUTHOR(S) (Last name, first name, initial)		
Taylor, A.		
6. REPORT DATE	7a. TOTAL NO. OF PAGES	7b. NO. OF REFS
October 1965	131	40
8a. CONTRACT OR GRANT NO.	8b. ORIGINATOR'S REPORT NUMBER(S)	
AF33(657)-11157	AFML-TR-65-48, Part II	
a. PROJECT NO.	9a. OTHER REPORT NO(S) (Any other numbers that may be assigned to this report)	
7351	65-974-900-RL	
c. Task No.		
735101		
d.		
10. AVAILABILITY/LIMITATION NOTES		
This document is subject to special export controls and each transmittal to foreign governments or foreign nationals may be made only with prior approval of the Metals and Ceramics Division (M&C), Air Force Materials Laboratory, Wright-Patterson AFB, Ohio		
11. SUPPLEMENTARY NOTES		12. SPONSORING MILITARY ACTIVITY
		AFML (NAME) Wright-Patterson AFB, Ohio 45433
13. ABSTRACT		
<p>The solubility of oxygen, nitrogen and carbon in columbium-rich columbium-hafnium alloys has been studied by means of x-ray diffraction, micrographic and thermal techniques using both a dynamic leak method and a Sieverts apparatus.</p> <p>At pressures above <math>10^{-4}</math> torr <math>O_2</math>, Cb is in thermodynamic equilibrium with oxide vapor and can take up to 6 at. % <math>O_2</math> into solid solution at 1775°C. Above this temperature oxidation is "catastrophic" and the volatile oxides <math>Cb_2O_3</math>, <math>CbO</math> and <math>Cb_2O_5</math> form on the surface. The "degassing" of Cb at 2200°C and above at <math>10^{-6}</math> torr is, in effect, brought about by the volatilization of the oxide and not by the de-adsorption of gaseous oxygen. The solid solution of the Cb-Hf-O system at 1500°C contains 9.0 at. % <math>O_2</math>, at. % Hf, falling to 4.7 at. % for Cb and 0.2 at. % for an alloy containing 12 at. % Hf, the phase being characterized by the formation of <math>HfO_2</math> "clusters" or "molecules" within the body-centered cubic -Cb matrix.</p> <p>The ternary system Cb-Hf-N shows that although Cb can accommodate 9.48 at. % N interstitially at 2200°C and <math>3 \times 10^{-1}</math> torr <math>N_2</math>, the amount retained on quenching drops to about 1 at. %, the precise amount depending on the quenching rate. The addition of only 2 at. % of Hf immediately reduces the amount of <math>N_2</math> which can be accommodated at high temperatures to less than 0.5 at. %, the -Cb phase being in equilibrium with <math>HfN_3</math>. In the Cb-Hf-C system, the -Cb primary solid solution retains, at most, 0.55 at. % C at 2000°C, the carbide in equilibrium with the -Cb phase being essentially face-centered cubic (Cb-Hf)<math>_3</math>C, and not <math>Cb_2C</math> as might have been expected.</p>		

DD FORM 1473  
1 JAN 64

Unclassified

Security Classification

Security Classification

14. KEY WORDS	LINK A		LINK B		LINK C	
	ROLE	WT	ROLE	WT	ROLE	WT
Alloys (metals), columbium (niobium), hafnium, oxygen, nitrogen, carbon, phases, x-ray diffraction, structure, vacuum.						

INSTRUCTIONS

1. **ORIGINATING ACTIVITY:** Enter the name and address of the contractor, subcontractor, grantee, Department of Defense activity or other organization (corporate author) issuing the report.
- 2a. **REPORT SECURITY CLASSIFICATION:** Enter the overall security classification of the report. Indicate whether "Restricted Data" is included. Marking is to be in accordance with appropriate security regulations.
- 2b. **GROUP:** Automatic downgrading is specified in DoD Directive 5200.10 and Armed Forces Industrial Manual. Enter the group number. Also, when applicable, show that optional markings have been used for Group 3 and Group 4 as authorized.
3. **REPORT TITLE:** Enter the complete report title in all capital letters. Titles in all cases should be unclassified. If a meaningful title cannot be selected without classification, show title classification in all capitals in parentheses immediately following the title.
4. **DESCRIPTIVE NOTES:** If appropriate, enter the type of report, e.g., interim, progress, summary, annual, or final. Give the inclusive dates when a specific reporting period is covered.
5. **AUTHOR(S):** Enter the name(s) of author(s) as shown on or in the report. Enter last name, first name, middle initial. If military, show rank and branch of service. The name of the principal author is an absolute minimum requirement.
6. **REPORT DATE:** Enter the date of the report as day, month, year, or month, year. If more than one date appears on the report, use date of publication.
- 7a. **TOTAL NUMBER OF PAGES:** The total page count should follow normal pagination procedures, i.e., enter the number of pages containing information.
- 7b. **NUMBER OF REFERENCES:** Enter the total number of references cited in the report.
- 8a. **CONTRACT OR GRANT NUMBER:** If appropriate, enter the applicable number of the contract or grant under which the report was written.
- 8b, 8c, & 8d. **PROJECT NUMBER:** Enter the appropriate military department identifier, such as project number, subject number, system number, task number, etc.
- 9a. **ORIGINATOR'S REPORT NUMBER(S):** Enter the official report number by which the document will be identified and controlled by the originating activity. This number must be unique to this report.
- 9b. **OTHER REPORT NUMBER(S):** If the report has been assigned any other report numbers (either by the originator or by the sponsor), also enter this number(s).
10. **AVAILABILITY/LIMITATION NOTICES:** Enter any limitations on further dissemination of the report, other than those

imposed by security classification, using standard statements such as:

- (1) "Qualified requesters may obtain copies of this report from DDC."
- (2) "Foreign announcement and dissemination of this report by DDC is not authorized."
- (3) "U. S. Government agencies may obtain copies of this report directly from DDC. Other qualified DDC users shall request through \_\_\_\_\_."
- (4) "U. S. military agencies may obtain copies of this report directly from DDC. Other qualified users shall request through \_\_\_\_\_."
- (5) "All distribution of this report is controlled. Qualified DDC users shall request through \_\_\_\_\_."

If the report has been furnished to the Office of Technical Services, Department of Commerce, for sale to the public, indicate this fact and enter the price, if known.

11. **SUPPLEMENTARY NOTES:** Use for additional explanatory notes.
12. **SPONSORING MILITARY ACTIVITY:** Enter the name of the departmental project office or laboratory sponsoring (paying for) the research and development. Include address.
13. **ABSTRACT:** Enter an abstract giving a brief and factual summary of the document indicative of the report, even though it may also appear elsewhere in the body of the technical report. If additional space is required, a continuation sheet shall be attached.

It is highly desirable that the abstract of classified reports be unclassified. Each paragraph of the abstract shall end with an indication of the military security classification of the information in the paragraph, represented as (TS), (S), (C), or (U).

There is no limitation on the length of the abstract. However, the suggested length is from 150 to 225 words.

14. **KEY WORDS:** Key words are technically meaningful terms or short phrases that characterize a report and may be used as index entries for cataloging the report. Key words must be selected so that no security classification is required. Identifiers, such as equipment model designation, trade name, military project code name, geographic location, may be used as key words but will be followed by an indication of technical content. The assignment of links, roles, and weights is optional.